Hydrodynamic numerical model of waves and currents at Landeyjahöfn Harbour

Sunna Viðarsdóttir

Faculty of Civil and Environmental Engineering
University of Iceland
2019

Hydrodynamic numerical model of waves and currents at Landeyjahöfn Harbour

Sunna Viðarsdóttir

30 ECTS thesis submitted in partial fulfilment of a
Magister Scientiarum degree in Environmental Engineering

MS Committee
Sigurður Sigurðarson
Hrund Ólöf Andradóttir

Master's Examiner
Helgi G. Gunnarsson

Faculty of Civil and Environmental Engineering
School of Engineering and Natural Sciences
University of Iceland
Reykjavik, May 2019

Hydrodynamic numerical model of waves and currents at Landeyjahöfn Harbour
Hydrodynamic numerical model of Landeyjahöfn Area
30 ECTS thesis submitted in partial fulfilment of a *Magister Scientiarum* degree in Environmental Engineering

Faculty of Civil and Environmental Engineering
School of Engineering and Natural Sciences
University of Iceland
Hjarðarhaga 5
107, Reykjavik
Iceland

Telephone: 525 4000

Bibliographic information:
Sunna Viðarsdóttir, 2019, *Hydrodynamic numerical model of waves and currents at Landeyjahöfn Harbour*, Master's thesis, Faculty of Civil and Environmental Engineering, University of Iceland, pp. 76.

Printing: Háskólaprent
Reykjavik, Iceland, June 2019

Abstract

Landeyjahöfn harbour is situated on the sandy southern coast of Iceland in a high-energy environment exposed to large waves and sediment transport. Since its opening in 2010, the harbour is often closed during winter time because a safe navigation depth cannot be maintained due to extensive sedimentation. Despite extensive bathymetric surveys and continuous wave, current and wind measurements, a better understanding of the sediment transport is required in order to conduct preventive dredging operations based on weather forecasts. The thesis goal was to develop a 2D hydrodynamic numerical model of waves and currents that could be used as a foundation for sediment transport modelling at Landeyjahöfn harbour. The open source suite of solvers TELEMAC-MASCARET and the freeware QGIS and BlueKenue for pre- and post-processing data were used. The model was calibrated for a storm with wave height over 3 m from the prevalent southwest wave direction. The simulated waves and spatial variations of currents compared well to measured values from a wave buoy and a radar. The current direction pattern at different times in the tidal cycle was almost identical to the currents detected by the radar and the average simulated significant wave height at the buoy was within 2% of the measured significant wave height. The calibrated model could reproduce spatial current fields during a large storm from the less prevalent southeast direction, but the simulated wave height was underestimated. The reason for the deviation was a lack of realistic offshore wave data to use as boundary conditions.

Útdráttur

Landeyjahöfn er staðsett á suðurströnd Íslands, sandströnd sem er útsett fyrir háum, orkumiklum öldum og með miklum sandflutningum. Frá opnun hafnarinnar árið 2010 hefur hún oft verið lokuð á veturna þar sem ekki hefur tekist að viðhalda öruggu siglingadýpi. Þrátt fyrir tíðar dýptarmælingar og öldu-, straum- og vindmælingar er þörf á betri skilningi á sandflutningum á svæðinu, t.d. svo hægt sé að skipuleggja fyrirbyggjandi dýpkunaraðgerðir út frá veðurspám. Markmið verkefnisins var að gera tvívítt reiknilíkan af öldum og straumum sem hægt væri að nota sem grunn fyrir hermun á sandflutningum við Landeyjahöfn. Opni hugbúnaðarpakkinn TELEMAC-MASCARET var notaður ásamt frjálsa hugbúnaðinum QGIS og BlueKenue fyrir for- og eftirvinnslu. Líkanið var kvarðað fyrir veður með ölduhæð yfir 3 metrum úr suðvestri, sem er ríkjandi ölduátt og jafnframt sú orkumesta. Hermaðir straumar og öldur pössuðu vel við mæld gildi frá öldudufli og radar. Straumstefnumynstrið á mismunandi tímum á sjávarfallabylgjunni var nánast alveg eins og straumarnir sem radarinn mældi og meðalhæð hermaðrar kenniöldu við ölduduflið var innan við 2% frá mældri kenniöldu. Kvarðaða líkanið var notað til að herma storm úr suðaustri og staðbundnar straumstefnur voru í stórum dráttum í samræmi við radarmælingar en hermaða ölduhæðin var vanmetin. Ástæða fráviks í öldu var skortur á raunhæfum gögnum um úthafsöldu til að nota sem jaðarskilyrði í líkaninu.

Preface

After working at the harbour department of the Icelandic Road and Coastal Administration since June of 2017, I have gotten to know the difficulties of keeping the Landeyjahöfn harbour open. Through my work I also have access to a great amount of data and information relevant to this study at the office. They come in the form of informal memos and files on the hard drive as well as easy access to conversations with the experts who were involved in the design of the Landeyjahöfn harbour and have been responsible for investigations since its opening as well as its operation.

In 2018 a student at the Division of Water Resources Engineering at Lund University, Clemens Klante, wrote a thesis about sediment transport and bathymetric change at the Hornafjörður tidal inlet. He set up a numerical model using TELEMAC-MASCARET, the open source software that is used in this study. In the fall of 2018, he visited the IRCA and set up his model on the agency's servers. I was assigned the task of getting familiar with the software to be able to do further work with the Hornafjörður model. It was through this collaboration that the idea for the current thesis was born and both Clemens and his thesis have been of great help to me.

Table of contents

List of figures

List of Tables

Acknowledgements

I would like to thank my advisor, Sigurður Sigurðarson, for his guidance through this work. He was always available for discussions and his knowledge and genuine interest in the topic made it a pleasure to seek his advice. I would also like to thank my supervising professor, Hrund Ólöf Andradóttir, for her thorough review and comments.

I wrote this thesis while working at the Icelandic Road and Coastal Administration's harbour department. I am grateful to the IRCA for letting me do this research and especially to Sigurður Áss Grétarsson for making it happen.

Clemens Klante introduced me to the modelling software used and I would like to thank him for all his help. I would also like to thank Ingunn and Orri for their input and assistance and all my colleagues at the harbour department for their patience.

1 Introduction

1.1 Extreme wave climate on Iceland’s southern coast

Figure 1-1 The unlimited fetch of the southerly waves at the southern coast of Iceland.

Iceland is an island located in the Northern Atlantic. Historically, the country’s economy is based on fishing and most of its towns are by the sea. Towns on the country’s south coast are few and far between which can largely be blamed on the extreme wave climate.

Wave height depends on wind speed, storm duration, water depth and fetch (e.g. Kamphuis, 2000). Fetch is the distance the wind blows over the water to generate the waves. As seen in Figure 1-1 the fetch of the waves reaching the south coast of Iceland in southerly wind directions is unlimited, although changes in wind direction and the size of the extratropical lows reaching Iceland from southwest make it unlikely that effective fetch would be greater than 500 km. This causes the waves coming up to the south coast to reach extreme heights. The highest single wave measured on the Surtsey wave buoy, south of the Westman Islands, was over 25 m and the significant wave height on the buoy has reached 16.7 meters (Viggósson, 2006).

These extreme wave conditions along with the fact that Iceland’s south coast is mostly straight and sandy, without any fjords to provide shelter, makes it a difficult place to construct a harbour. In fact, apart from Landeyjahöfn, there is no operating harbour between Þorlákshöfn and Höfn í Hornafirði although the coastline stretching between them is close to 370 kilometres.

1.2 The need for Landeyjahöfn harbour

The Westman Islands are an archipelago located 12 km off the southern coast of Iceland as seen in Figure 1-2. The town of Vestmannaeyjar is located on the biggest island with a population of around 4000. The main industry in the town is fishing. Until 2010 the ferry to the Westman Islands sailed to Þorlákshöfn, a port approximately 70 km from the islands, marked with a green dot in Figure 1-2.

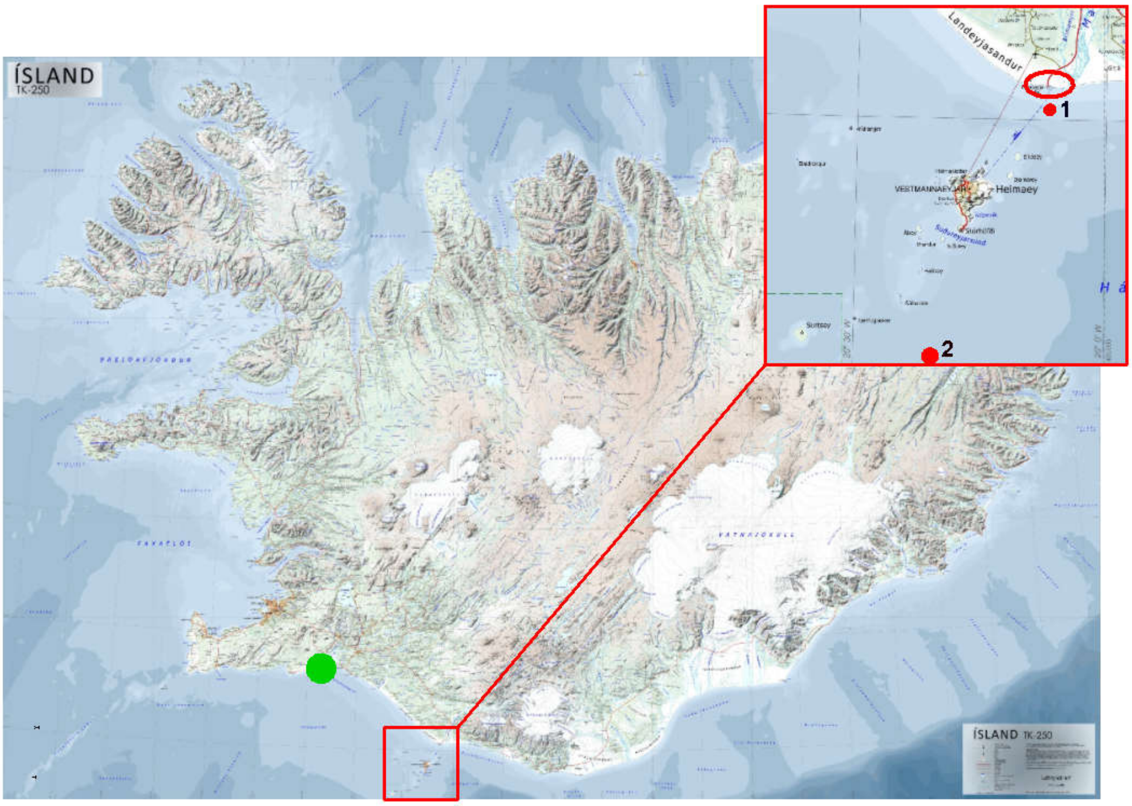

Figure 1-2 Location of the Westman Islands and Landeyjahöfn harbour (marked with a red ellipse). The Landeyjahöfn (1) and Surtsey (2) wave buoys are marked with red dots. Þorlákshöfn, the other ferry port serving the islands, is marked with a green dot.

In 2002 the islanders' demands to get better transportation routes were heard by the parliament and the minister of transport appointed a group to assess the issue. While the ferry from Þorlákshöfn was safe and reliable and met the demand for cargo transport, the 3 hour journey in sometimes very rough seas was considered to take too long (Vigfússon, 2003). Flights from Reykjavík and Bakki were available but they were expensive and did not offer the possibility of bringing a vehicle.

By 2003, three options to improve transportation to the island were being considered. The first one, an underwater tunnel was deemed too expensive and risky as the Westman Islands are one of the most volcanically active parts of Iceland. A faster ferry sailing to Þorlákshöfn was another option, but the operating cost for this was very high. The third option, building a new harbour in Landeyjar and acquiring a new ferry with shallower draft, was found to be the most economic option and giving the highest level of service.

As seen in Table 1-1 the total travel time from Reykjavík to the Westman Islands is shortened by 1.5 hours by sailing from Landeyjarhöfn compared to Þorlákshöfn. On top of that, the time on board the ferry, often in rough conditions which cause seasickness, is shortened from2.5 hours to 35 minutes. The third gain is the number of daily departures which increases the flexibility. Landeyjahöfn harbour puts the Westman Islands within reach for daytrips from Reykjavík, which in fact are hardly possible when the ferry sails from Þorlákshöfn as the last departure from the islands is only about 1 hour after the first arrival from the mainland. Flying is an option, but comes at approximately 6 to 14 times the price and does not offer the option to bring a car.

Table 1-1 Modes of transport to the Westman Islands

	Travelling time		Price of a single one way fare (ISK)	Daily departures
	Total from Reykjavík	From the mainland		
Ferry from Landeyjahöfn	2.5 hours	35 minutes	1,600	7
Ferry from Þorlákshöfn	4 hours	3 hours	1,600	2
Flight from Reykjavík	25 minutes	25 minutes	13,600- 19,100	1 - 2
Flight from Bakki	2 hours 5 min	10 minutes	8,500	4

Notes: Based on schedules as retrieved on 10.05.2019 from (1) www.herjolfur.is; (2) www.ernir.is (price variation depending on available discount seats); (3) www.flightseeing.is

The new harbour opened in August 2010 and the number of ferry passengers more than doubled, from 130,000 in 2008 to 290,000 in 2012 (Grétarsson & Sigurðarson, 2013). The ocean journey was shortened to 35 minutes and the Westman Islands saw an increase in tourism. According to Guðmundsson (2016) the total number of foreign visitors to the islands went from 12,000 in 2004 to 80,000 in 2012 and to 110,000 in 2016. The increase in tourism occurred in the months of May, September and October. Winter tourism, however, has been unchanged mainly because the Landeyjahöfn harbour is closed during the winter months due to a combination of sedimentation in the harbour and weather conditions.

The sedimentation has caused problems ever since the opening of the harbour. The necessity for some dredging was expected as is normal in harbours on sandy coasts. The dredged volume, however, has been 20-40 times what was estimated and during the winter months dredging is made difficult by the waves. This has resulted in the harbour being closed for 2-5 months every year depending on weather conditions.

1.3 **Principles of coastal sediment transport**

Sediments are transported along and perpendicular to the coast under the influence of winds, waves and currents (e.g. Van Rijn, 2012). The strong wave climate along the southern shore of Iceland, can as such, also generate unusually high sediment loads. Sediments can move as bed-load, suspended load or sheet-flow as graphically explained in Figure 1-3.

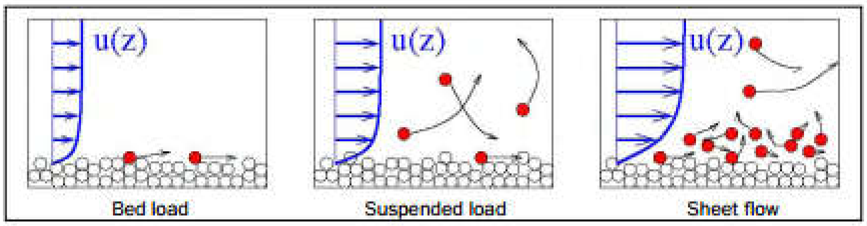

Figure 1-3 Modes of sediment transport (Camenen & Larson, 2007)

The definition for bed-load is not universally agreed upon but usually it is considered to be the transport of particles by rolling, sliding and saltating (Camenen & Larson 2007). Particles will start to move when the instantaneous fluid force on a particle is just larger than the resisting force related to the submerged particle weight and the friction coefficient. This movement occurs in continuous contact with the bed. This is strongly related to the local near-bed velocities as well as particle size, shape and position and all these parameters have some randomness to them.

When the bed-shear stress exceeds the fall velocity of the particle, it can be lifted to a level where upward turbulent forces are higher than the submerged weight of the particle and the particle may go into suspension. The horizontal velocity of suspended particles is almost equal to the fluid velocity and the sediment concentration decreases with distance up from the bed. This is called suspended load. Sheet flow occurs when sand grains under imposed stresses move in large quantities as a sheet layer.

The net transport at each point can be divided into current-related and wave-related parts. Outside the surf zone the transport is concentrated in a layer close to the bed in which bed-load and suspended load can be equally important. When the ratio of depth-averaged velocity and peak orbital velocity is small, bed load type transport dominates. As the strength of the tide- and wind-driven mean current increases, the suspended load becomes increasingly important due to turbulence-related mixing.

In the surf zone of sandy beaches the sediment transport is generally dominated by waves. Breaking waves as well as the near-bed wave-induced oscillatory water motion can bring large quantities of sand into suspension. The suspended load is then transported by the current. The wave-induced longshore current depends on the angle between the wave crest and the shoreline. Waves perpendicular to the shoreline do not induce a longshore current. Figure 1-4 shows the hydrodynamic forces determining conditions for longshore sediment transport.

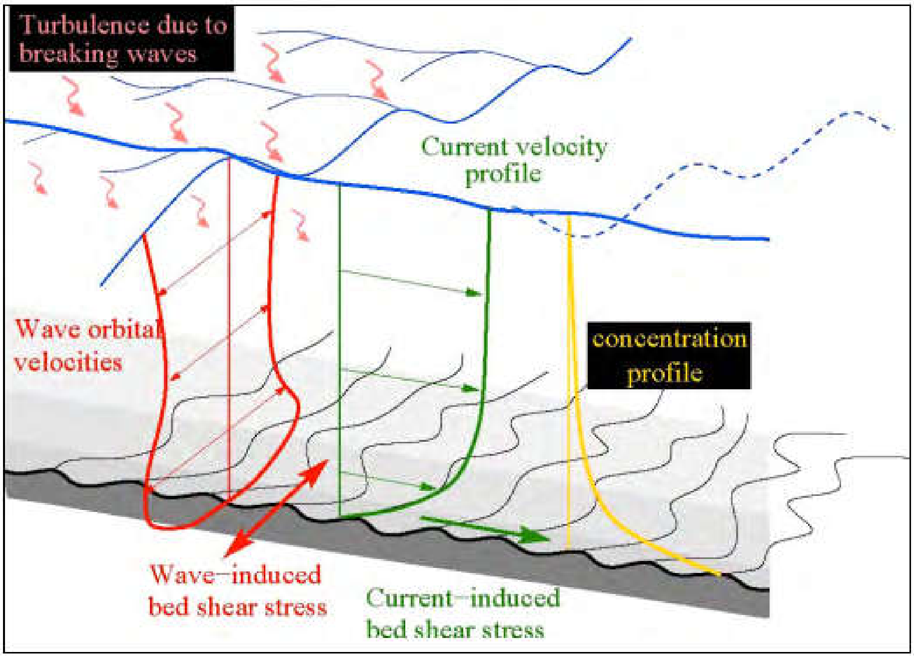

Figure 1-4 Hydrodynamic forcing determining conditions for longshore sediment transport (Camenen & Larson, 2007)

1.3.1 Formation of breaker bars

In deep water, waves travel with a constant wavelength and a nearly sinusoidal profile. When they enter shallow water – generally considered to start where the depth equals half a wavelength - they start touching the bottom and undergoing a transformation. They become asymmetric with peaked crests and wide troughs. This is called shoaling. When a wave has reached sufficient steepness it starts to break. The surf zone is the part of the coastal zone that is dominated by breaking waves and wave-induced currents. This process is shown graphically in Figure 1-5.

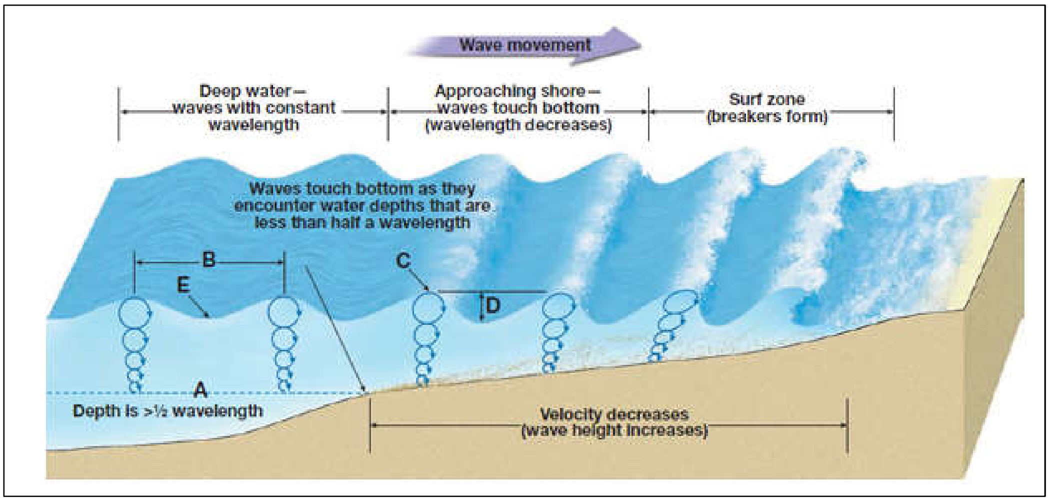

Figure 1-5 Waves approaching shore (https://surfwithamigas.com/how-to-read-a-surf-forecast-how-period-affects-wave-size/).

When the waves break, a large amount of water is pushed shoreward on the surface, stirring up great amounts of sediments. To accommodate all this water in the surface, a similar amount of water flows sea-ward close to the bottom causing an undertow. Because of the undertow and the sediment stirring the net cross-shore sediment transport under breaking wave conditions is sea-ward. As the depth increases, the velocity of the sea-ward moving water decreases, causing it to lose its sediment transport capacity. The sediments fall to the bottom, forming embankments parallel to the shore. These embankments are called breaker bars and serve as a natural protection for the inner part of the surf zone because the highest waves break on them and therefore hit the beach with reduced energy. There can be one or many breaker bars and they are highly dynamic.

As shown in Figure 1-6 there is usually a seasonal change in beach profiles. In calm conditions with non-breaking waves the net cross-shore sediment transport is shoreward directed. The smaller and not so steep waves move beach material back onshore, reducing the height of the bar and making the visible beach above water wider.

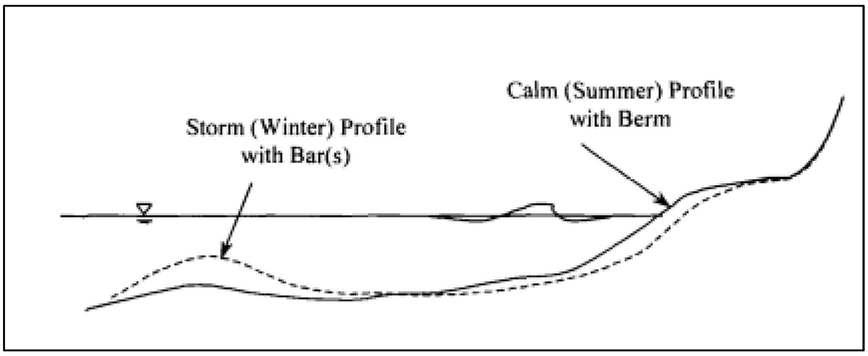

Figure 1-6 Typical winter and summer profiles of a sandy beach. (Kamphuis, 2000)

1.4 Pre-construction research of Landeyjahöfn harbour

A range of studies were conducted by eight different institutions from the time when the Icelandic Parliament agreed to allocate funding for investigation of the possibility of making a ferry harbour in Landeyjar to the time the harbour was constructed (see Table 1-2). Until 2009 the area was generally referred to as Bakkafjara in reports and elsewhere. In this study it will be referred to as Landeyjar. The part of the Icelandic Maritime Administration (IMA) overseeing the research is now the harbour department of the Icelandic Road and Coastal Administration (IRCA).

Table 1-2 Studies conducted before construction of the harbour

Topic	Conducted by	
Bathymetric surveys	IMA, Iceland	IRCA's database
Physical model study	IMA, Iceland	IRCA-memo, 2007
Quarry research	Stapi, Iceland	Stapi jarðræðistofa, 2007
Soil study - rating curves	IMA, Iceland	IRCA's database
Social impact study	Bifröst University, Iceland	Eyþórsson, Karlsson & Jóhannsdóttir, 2006
Risk assessment of shipping route	DNV, Norway	Johnsen & Tobiassen, 2007
Risk assessment of project	COWI, Denmark	COWI A/S, 2007
Environmental report	VSÓ, Iceland	VSÓ Ráðgjöf, 2008
Sediment transport study	DHI, Denmark	Jensen, Viggósson, Elfrink, Brøker & Grunnet, 2007

1.4.1 IMA's interim summary report

In 2006 the IMA published an interim report summarizing the results of research that had been conducted until that point and design suggestions based on those results.

As the wave rose in Figure 1-7 shows, the dominating wave direction offshore of the Westman Islands is south-westerly. In this prevalent wave direction, the shelter provided by the islands is greatest at Landeyjahöfn, causing the area to have the smallest waves of any place along the south coast.

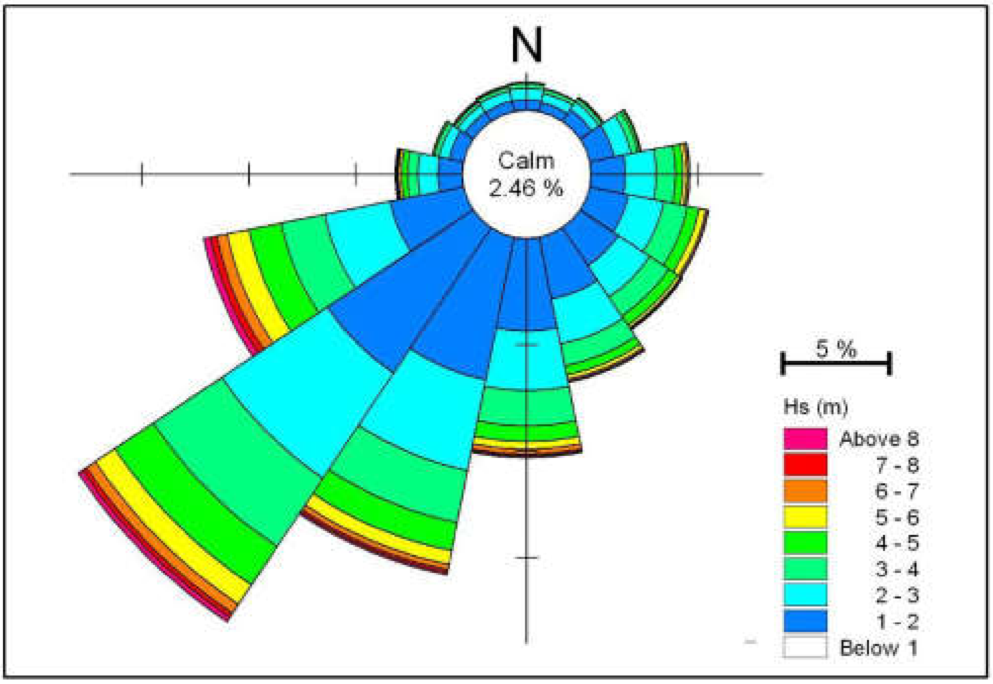

Figure 1-7 Offshore wave statistics (Viggósson, 2006)

The coast is made up of sand and both the coastline and nearshore bathymetry are continuously changing due to the breaking waves and the sediment transport they cause. As a result, the coastline never reaches the equilibrium it seeks and sediment transport occurs both longshore and cross-shore. Due to the substantial differences in weather between seasons the beach profile varies on a seasonal basis, as explained in Chapter 1.3.1. The breaker bar which is found approximately 800 meters offshore is typically more pronounced in winter and flatter in summer as is characteristic of seasonal profiles.

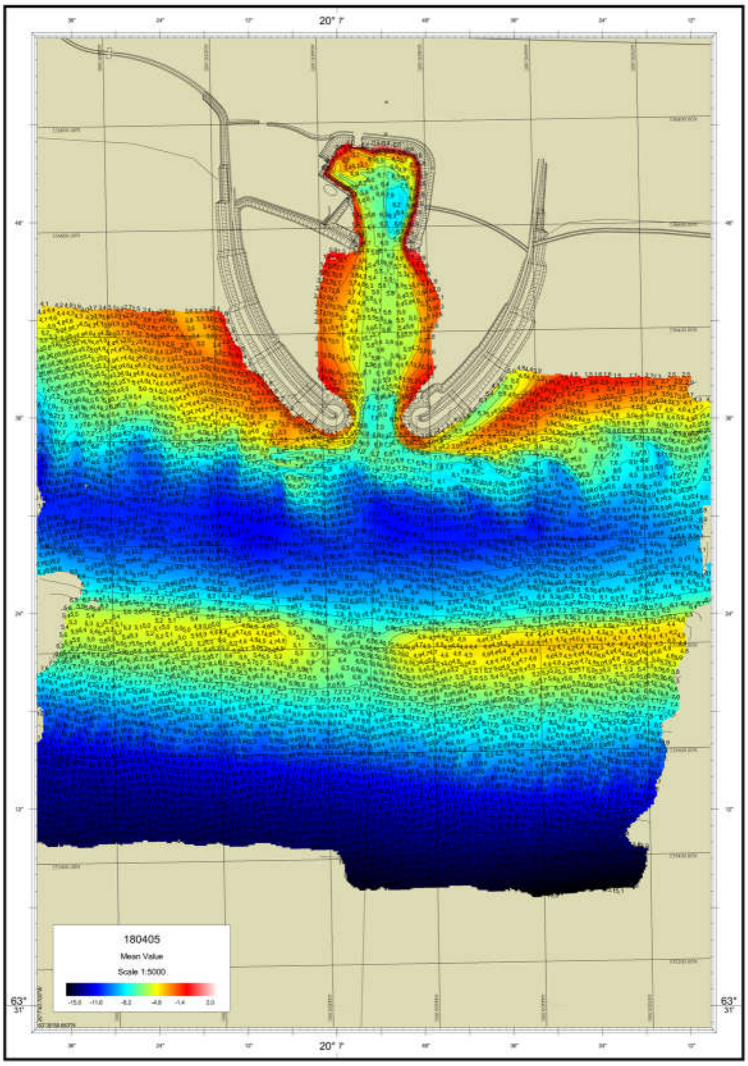

Figure 1-8 Bathymetric survey from 05.04.2018, showing clearly the opening in the breaker bar.

The depth at the breaker bar is typically 5.5 to 7 meters, but there is a naturally occurring opening or gate in the bar where the depth is approximately 1 meter more (Viggósson, 2006). Historical bathymetric surveys of the area were studied to evaluate whether the gate is stable and it was found that in the period 1979 to 2005 the gate had moved at most 400 meters to the west and 140 meters to east. This gate is important to the navigability of the harbour and its location was chosen so that the gate is in front of the harbour entrance as seen in Figure 1-8. The opening in the bar and the shelter provided by the Westman Islands from the dominant south-westerly waves were the main considerations in choosing the exact location for the harbour.

The research undertaken before making the final decision, including numerical modelling of sediment transport in the area, concluded that the location was viable. One of the assumptions made in those studies was that with the new harbour would come a new ferry with a shallower draft. It is only now, 9 years later, that the new ferry is expected to arrive. The new ferry will require 1.5 meter less depth to navigate than the current ferry.

Echo soundings to map the bathymetry, in particular the breaker bar, were done every season for three consecutive years from 2002 to 2005. This was redeemed necessary because of the changing nature of the sandy beach and the fact that the short-term changes are seasonal and the long-term changes are dependent on waves and currents. A wave buoy was set up at 30 meters water depth south of Landeyjar in 2003.

A physical model of the harbour was built, including the bathymetry off the coast, and used to study the effect of the ocean movements on the breakwaters. Experiments were also done with a remotely controlled model ferry. Many other aspects involved in choosing the location of the harbour and its preliminary design, as well as characteristics of the new ferry are discussed in the report.

Viggósson's (2006) overall conclusion, based on the abovementioned studies, was that the best possible location for the harbour with regard to shelter from waves and the breaker bar off the coast had been found and that a suitable harbour entrance with sufficient safety for navigation had been developed. Moreover, studies suggested that operating costs due to sedimentation would not be excessive and that the number of days of non-navigability would be within reason.

1.4.2 DHI modelling investigation

As part of these investigations, the Danish Hydrological Institute (DHI) was contracted to do a study of the waves, currents, sediment transport and morphology in the area. Elfrink, Brøker and Viggósson (2006) carried out analysis of near-shore wave conditions. The overall sediment budget was evaluated as well as the stability of the bar and shoreline fluctuations. Sedimentation inside the harbour and currents in front of the harbour are also evaluated based on a numerical model of a harbour in Thorsminde in Denmark where conditions were considered similar to those in Landeyjar. This first phase was completed in January 2006 and the conclusions drawn in the IMA report were largely built on this.

In phase II of the DHI study, Jensen et al. (2007) used coupled numerical 2D models for current, waves and sediment transport to investigate the overall stability of the outer bar, sedimentation rates into the harbour and equilibrium depth in front of and in the entrance. The bathymetry used for the model was obtained in a bathymetric survey in May 2006 and the software used was MIKE 21 FM, developed by DHI. The simulation periods, chosen to include both south-easterly and south-westerly historical storms, were selected from a 27 year time series of waves and longshore transport. They cover approximately 70 days in total.

MIKE 21 SW was used to simulate the propagation of waves. A regional wave model was used to transform the waves from an offshore location to the boundary of the model. Since the wave parameters vary significantly along the shore, 6 different sets of parameters are used as boundary conditions in the nearshore wave model. The regional wave model was validated against measured waves from the Landeyjahöfn wave buoy.

The flow was simulated using MIKE 21 HD. Tidal elevations and velocities were extracted from a tidal model run at the IMA and the flow model calibrated against those current speeds and surface elevations. The annual discharge at the mouth of the river Markarfljót has been evaluated and found to be on average 96 m^3/s but with significant seasonal variations. The calculated hydrograph for the simulation period was used as the river boundary conditions.

The sediment transport in the area was modelled with MIKE 21 ST based on information about waves and flow, from MIKE 21 SW and MIKE 21 HD respectively, in every time step. An extensive number of sediment samples were collected to evaluate the mean grain size, standard deviation and relative density of the sand, which are also required as input for the sediment model.

The two simulated periods, November 1985 and February 1989, both include waves from south-westerly and south-easterly directions. However, the main storm in November 1985 is south-easterly dominated and the overall trend in the sediment transport field is to the west. The coastline on the western side of the breakwater advances 60 meters and erosion occurs on the eastern side. The overall trend in the simulation of February 1989 is sediment movement to the east and the coastline near the breakwaters advances on both sides. Morphological activity seen in both simulation periods include accretion of sediment near the river, changes along the outer side of the bar and a formation of a bar in front of the harbour entrance. No significant changes in the deep trough between the harbour mouth and the bar are seen and only small changes in navigation depth in the harbour mouth.

Among other aspects investigated are waves, currents and bed levels along navigation line, coastal impact of the intended harbour facility, sedimentation inside the harbour and equilibrium water depth in front of the harbour entrance.

1.5 Post-construction research

Soon after the opening of the harbour, morphological changes led to unsafe navigation conditions at the harbour entrance. Additional studies were carried out in 2010 in an attempt to understand those changes. For the next two years, significant morphological changes occurred in the area and it was suggested that these changes were caused by the construction of the harbour. In 2013, DHI's Grunnet & Kristiensen published a report titled "Landeyjahöfn – Further Investigations," which had the overall objective to study the possibility to ensure a 5.5 meter equilibrium water depth in front of and in the entrance to the harbour.

They performed a morphometric study of the area, in which the historically observed changes to the morphology were quantified. By comparing beach profiles from surveys done from 2002 to 2012 it was confirmed that the bar dynamics had changed considerably. The main concern was the disappearance of the bar in 2010 which resulted in an increased exposure to waves on the upper shore face. The bar is barely present in the 2011 survey but recovers in 2012. The report concludes that the disappearance of the bar is not a consequence of the construction of the harbour but rather an extraordinary absence of waves from the west, causing landward migration of the bar.

The wave hindcast model which was set up for the previous study was revised. Numerous sensitivity runs on key model parameters were done. Most parts of the model were found to be valid but two boundary condition problems were identified and the boundary conditions changed. The sediment budget was also revised, the fixed bed model and morphological model were calibrated and solutions to the sedimentation problems screened.

The study estimates that on average the net sediment transport is 400,000 m^3/year towards east due to prevailing south-westerly wave climate. Normally the coastline on the updrift side of a harbour will advance further than the downdrift side and problems with sedimentation and reduced navigation depth will be associated with transport in the main direction. The opposite was experienced at Landeyjahöfn.

Another important element is that due to the eruption of Eyjafjallajökull volcano in April 2001, the Markarfljót river deposited around 1.6 million m^3 of sand and gravel east of the harbour compared to approximately 200,000 m^3 in an average year. The study concludes that the sand accumulation east of the harbour is responsible for the problems of sedimentation and reduced navigation depth during and after south-easterly winds.

1.6 **Objective**

To date, the Landeyjahöfn harbour sedimentation modelling has been conducted by the external expert consultancy DHI, using their proprietary numerical modelling software MIKE. This service has been conducted on ad-hoc basis at a considerable cost. There is a dire local need for an open source hydrodynamic model.

The objective of this study was to develop a 2D numerical hydrodynamic model of waves and currents around Landeyjahöfn harbour using open source software that can be coupled with a sediment transport model and used to improve harbour operations in the future.

A model of the astronomical tides, including temporal and spatial variation of the sea level, were calibrated against tide tables. This is an important base to be coupled with the wave model for two reasons. The waves' behaviour changes with water depth and thus the sea level. The tides also generate their own current which must be represented in the model to see how it interacts with the wave induced longshore current.

A storm from the prevalent south-westerly directions was simulated and the model calibrated against wave measurements from a wave buoy and visually compared to radar images of the surface currents in front of the harbour.

Finally the model's performance for a storm with waves from the southeast will be checked and compared to the measured values.

2 Methods

All software used to construct the numerical hydrodynamic model and generate the input data files in this study is either freeware or open source software. TELEMAC-MASCARET was chosen as the hydrodynamic model solver, primarily because of the promising results it had given in a sedimentation study for a different harbour in Iceland (Klante, 2018). Wave and weather time series and large point data sets are handled using R Studios, an open source data analysis software. QGIS, a free and open source geographic information system, is used for visualisation of bathymetric surveys and pre-processing of data. BlueKenue is a free data preparation, analysis and visualization tool for hydraulic modellers, developed by National Research Council of Canada and is used to create the triangular bathymetry mesh.

2.1 Hydrodynamic model

The TELEMAC-MASCARET system is an open source integrated suite of solvers for numerical modelling of free-surface flow (http://www.opentelemac.org). The system was developed by Laboratoire National d'Hydraulique, a department of Electricité de France. The system consists of seven simulation modules which all use high-capacity algorithms based on the finite-element method. The modules are

- MASCARET for one-dimensional free-surface flow modelling.
- TELEMAC-2D for two-dimensional free-surface flow modelling.
- TELEMAC-3D for three-dimensional free-surface flow modelling.
- TOMAWAC for modelling wave propagation in coastal areas.
- ARTEMIS for numerical simulation of wave propagation towards the shore and agitation into harbours.
- SISYPHE for modelling sediment transport and bed evolution.
- NESTOR for modelling dredging operations in the river bed.

All the simulation modules share a single library of numerical algorithms which makes for consistency throughout the system. For the purpose of this thesis the modules used are TELEMAC-2D and TOMAWAC.

2.1.1 TELEMAC 2D

TELEMAC 2D uses the finite-element method to solve the depth-averaged Saint-Venant equations in a triangular mesh. The main results at each node are water depth and the depth-averaged velocity components (Ata, 2018). The program is capable of taking into account various phenomena which can occur in free-surface flow, including but not limited to the following which are all relevant to the current study:

- propagation of long waves,
- friction on the bed,
- effects of meteorological phenomena such as wind,
- turbulence,
- supercritical and subcritical flows,
- dry areas in the computational field,
- wave induced currents through coupling with TOMAWAC
- coupling with sediment transport.

To run a simulation in TELEMAC-2D a set of input files is needed. The three mandatory files needed for every case are the steering file, the geometry file and the boundary conditions file. Depending on the nature of the project a variety of other input files can be included.

The steering file contains the configuration of the computation. It is where the input and output files are specified and all kinds of parameters such as which equation to solve, what kind of discretization to use and number and length of time-steps.

In the case of this study a binary data base containing tidal information is also included.

The TELEMAC-2D code solves the following hydrodynamic equations in each node point simultaneously:

$$\frac{\delta h}{\delta t} + \boldsymbol{u} \cdot \boldsymbol{\nabla}(h) + hdiv(\boldsymbol{u}) = S_h \qquad \text{continuity}$$

$$\frac{\delta u}{\delta t} + \boldsymbol{u} \cdot \boldsymbol{\nabla}(u) = -g\frac{\delta Z}{\delta x} + S_x + \frac{1}{h}div(hv_t\boldsymbol{\nabla u}) \qquad \text{momentum along x}$$

$$\frac{\delta v}{\delta t} + \boldsymbol{u} \cdot \boldsymbol{\nabla}(v) = -g\frac{\delta Z}{\delta y} + S_y + \frac{1}{h}div(hv_t\boldsymbol{\nabla v}) \qquad \text{momentum along y}$$

$$\frac{\delta T}{\delta t} + \boldsymbol{u} \cdot \boldsymbol{\nabla}(T) = S_T + \frac{1}{h}div(hv_T\boldsymbol{\nabla T}) \qquad \text{tracer conservation}$$

in which

- h (m) is water depth
- u,v (m/s) are velocity components in x- and y-directions respectively
- T (g/l) is non-buoyant tracer
- g (m/s^2) is gravity acceleration
- v_t,v_T (m/s^2) are momentum and tracer diffusion coefficients
- Z (m) is free surface elevation
- t (s) is time
- x,y (m) are horizontal space coordinates
- S_h (m/s) is source or sink of fluid
- S_T (g/l/s) is source or sink of tracer
- S_x,S_y (m/s^2) are source terms representing wind, Coriolis force, bottom friction and a source or sink of momentum within the domain.
- h, u, v and T are the unknowns.

An explanation of how TELEMAC-2D solves the equations is available in the TELEMAC-2D user manual.

2.1.2 TOMAWAC

TOMAWAC is the module of the TELEMAC system that can be used to model wave propagation. It is a scientific software which models the changes, both in time and space, of the power spectrum of wind-driven waves and wave agitations (Awk, 2018).

TOMAWAC's application domain may be divided into three sections based on the relative depth which is defined as d/L where d denotes the water depth and L the wave length. Each section has its own characteristics which must be taken into account in the steering file.

In the ocean domain, where the relative depth is over 0.5, the dominant physical processes are wind driven waves, whitecapping dissipation and non-linear quadruplet interactions. In the continental seas and the medium depths, with relative depths between 0.05 and 0.5, bottom friction, shoaling and refraction due to bathymetry and currents must also be taken into account. Finally, areas with relative depth lower than 0.05 are referred to as the coastal domain. There bathymetric breaking, non-linear triad interactions between waves and unsteady sea level and currents should be included.

How waves evolve and behave depends on an array of physical factors such as bathymetry and bottom geometry, atmospheric circulation, tide pattern, three dimensional oceanic circulation currents and sea level variations caused by exceptional weather events. The interactions between those physical factors and the waves are generally rather complex to model. The TOMAWAC module models wave-bathymetry interaction, wave-atmosphere interaction and wave-current interaction.

Some of the processes involved in wave physics are well known and understood but the numerical modelling of the various processes is a subject still being investigated and improved. The processes taken into account and modelled by TOMAWAC can be divided into three categories depending on the kind of effect they have on the waves.

- **Processes supplying or dissipating energy** are wind driven interactions with atmosphere, whitecapping dissipation, bottom friction induced dissipation, dissipation through bathymetric breaking and dissipation through wave blocking.
- **Non-linear energy transfer conservative processes** are of two different kinds – resonant quadruplet interactions at great depths and triad interactions at small depths.
- **The wave propagation-related processes** are wave propagation due to wave group velocity, depth-induced refraction, shoaling, current-induced refraction, interactions with unsteady currents and diffraction.

The current version of the diffraction model in TOMAWAC is able to represent some diffraction effects but has some limitations. Reflection from a structure or pronounced depth irregularity is not addressed. Where diffraction and reflection are of high importance the use of a phase-resolving model is recommended. This presents the limitation to the application domain that it does not include harbour areas.

A presentation of how these processes are modelled is available in the TOMAWAC user manual.

2.2 Simulations

The simulations run for this study are outlined in Table 2-1. The astronomical tides alone can only be calibrated against the tide table issued by the bathymetric department of the Icelandic Coast Guard. The tables are based on another model but have been in use for decades and proven themselves reliable. The simulation of the tides alone cannot be compared to measurements as there are always other factors present in nature, such as storm surge and barometric surge.

Table 2-1 Simulations run

No.	Simulation	Duration	Module used	Compare to
1	**Astronomical tides**	14 day	TELEMAC2D	Tidal table
2	**SW waves only**	2 hours	TOMAWAC	MIKE SW
3	**SE waves only**	2 hours	TOMAWAC	MIKE SW
4	**SW waves with tides**	24 hours	TELEMAC2D + TOMAWAC	Measurements
5	**SW + tides + inner bar**	12 hours	TELEMAC2D + TOMAWAC	Simulation 4
6	**SE waves with tides**	24 hours	TELEMAC2D + TOMAWAC	Measurements

The reason for running the waves alone without the tides was to evaluate the spatial development of the waves. Wave measurements are only conducted at two points within the modelled area and therefore the results of that simulation was compared with another model. The simulated waves were compared visually to the results from the MIKE SW model to see if the patterns were similar. This was only a rough comparisons to check for major errors in the model.

The simulated storms were chosen based on data from the Landeyjahöfn wave buoy. The criteria was a significant wave height of at least 3.0 meters and a relatively steady wave height and direction for a period of 24 hours.

Then the tidal simulations were coupled with the wave simulations and the outcomes compared to measurements of currents and waves. A simulation was run with and without the estimated inner bar (see Chapter 2.3.1). It had no visible effect on the results in the area in front of the harbour so it was excluded from further simulations.

2.3 Data input

2.3.1 The geometry file

The coastline and outline of the model are drawn on an aerial photo in QGIS and imported into BlueKenue. The mesh area is quite large in the longshore direction and reaches further to the west than to the east. This is crucial for describing the longshore variation in wave height caused by the Westman Islands. The BlueKenue is used to make a triangular mesh, which is quite coarse at the outer boundaries with 500 meter maximum edge length. The edge length is gradually decreased towards the area of interest by drawing polygons as seen in as seen in Figure 2-1 and setting the edge length for each polygon. A higher node density results in higher accuracy in the calculations but also takes up more computational power which is why a lower density is used for the largest part of the study area but a higher density for areas of particular interest

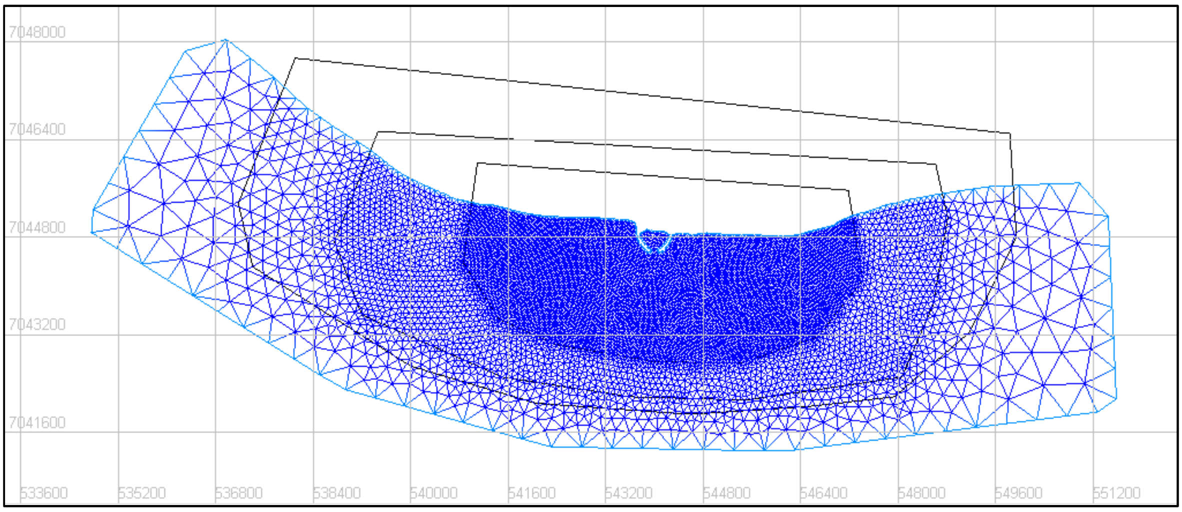

Figure 2-1 Triangular mesh with 500m, 250m, 100m and 50m edge lengths

The bathymetric data is then imported to BlueKenue. The offshore bathymetric data has been collected from years of measurements by the Hydrographic Department of the Icelandic Coast Guard. The near-shore bathymetric data comes from the IRCA's survey. The IRCA measures the bottom around Landeyjahöfn frequently (46 surveys in 2018) to monitor the sea bed, both with regard to navigability and progress of dredging operations. The bathymetry changes constantly due to the waves and currents and in turn the waves and currents are influenced by the bathymetry so some thought had to be put into which survey to use. A survey conducted on November 26th 2018 was chosen as it covered a large area in front of the harbour and 2 days later a storm fulfilling the selection criteria occurred.

The IRCA's bathymetric surveys are performed from a boat with a multi-beam echo sounder. The boat must sail over the seabed it is measuring which limits the surveys to about 3 meters depth. Any sea bed features shallower than that are not included. However, from Figure 2-2 it is known that an inner breaker bar exists west of the harbour. What is not known is how often the bar is there, its exact location and depth. In one version of the model the bar was manually added with estimated dimensions.

Figure 2-2 Photo taken on 31.03.2013 showing the inner breaker bar.

Near-shore and off-shore bathymetric data is imported to BlueKenue as XYZ coordinates. The program interpolates the point data and maps the triangular mesh to the bathymetry as seen in Figure 2-3.

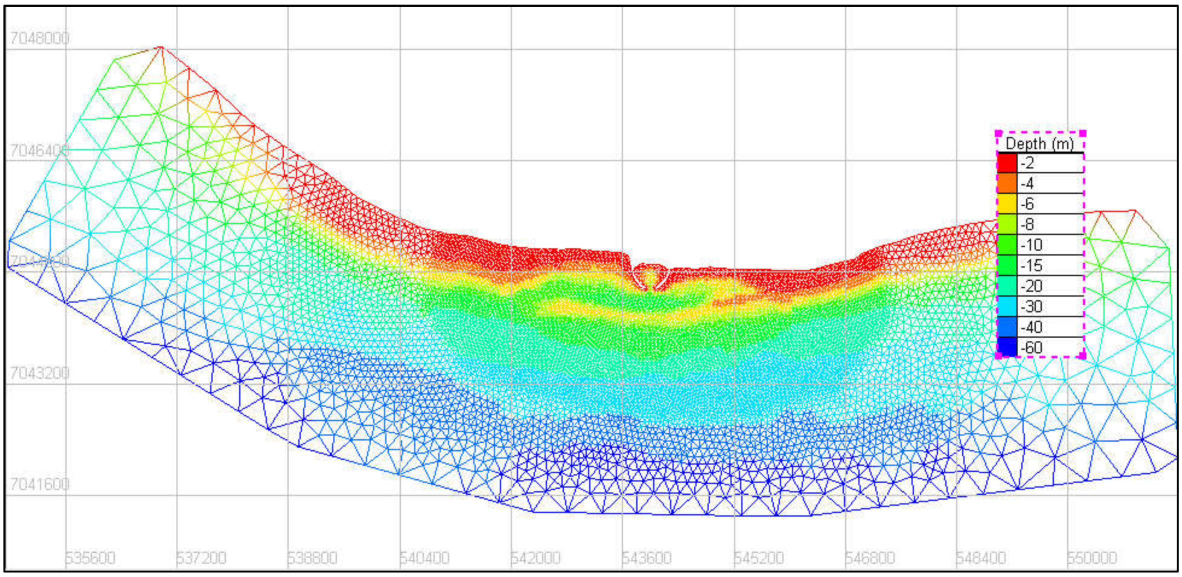

Figure 2-3 Interpolated mesh with colours representing water depth.

Finally, boundary conditions are set using BlueKenue. The open sea boundary has prescribed elevation and velocity described by the tidal binary database as well as wave conditions. The Markarfljót outlet has a prescribed flow which is set to the average flow of 100 m^3/s. This information is stored in a separate boundary conditions file.

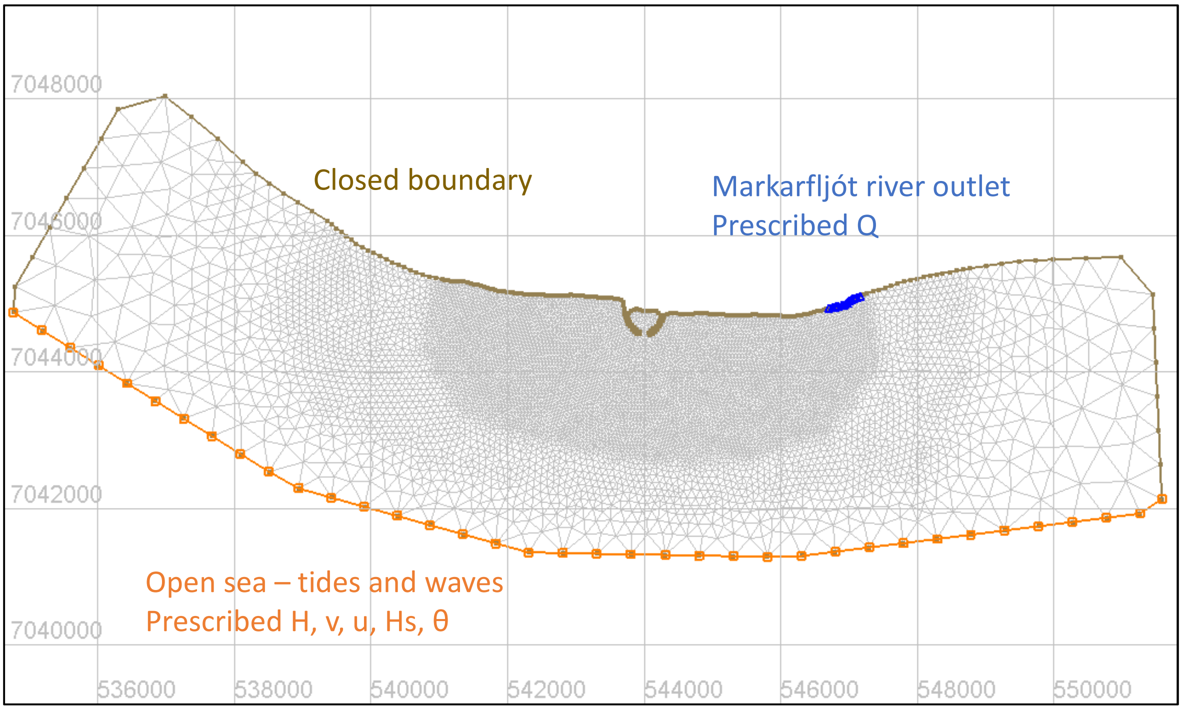

Figure 2-4 Boundary conditions in BlueKenue. The brown lines represent a closed boundary. The blue line represens the Markarfljót river outlet with a prescribed flow. The orange line represents the open sea with prescribed water level and flow velocities variable in space and time and wave characteristics variable in space.

2.3.2 Tidal data

The tidal input data comes from TPXO, a series of fully-global models of astronomical ocean tides. The models are based on the Laplace Tidal Equations and altimetry data and the tides are provided as complex amplitudes of earth-relative sea-surface elevation for 13 harmonic constituents. Egbert and Erofeeva (2002) describe the methods used to compute the model in detail. Some local tidal solutions have also been obtained which generally fit the data significantly better in shallow water and for complex topographic areas. Such a solution for Iceland is available with a resolution of 1/60°. The model provides both elevation and velocity. The data can be downloaded from http://volkov.oce.orst.edu/tides/ and TELEMAC2D can be made read this data by setting the option TIDAL DATA BASE in the steering file. The coordinate system used by the TPXO model is WGS84 so the mesh for the hydrodynamic model must also be in that coordinate system.

2.3.3 Wave input

As mentioned in Chapter 2.2 the storms to simulate were chosen based on measurements from the Landeyjahöfn wave buoy. The IRCA runs the wave buoy and 72 hour time series are available at www.vegagerdin.is. Longer time series were obtained from the IRCA's internal servers. The criteria for the selection of the storms was a significant wave height of around 3 meters and a relatively steady wave direction and height for 24 hours. One event with waves from south-westerly directions was simulated and one with waves from south-easterly directions. Figure 2-5 shows the significant wave height and direction at the Landeyjahöfn wave buoy in November and December of 2018. One storm with direction above (SW) the red line and one with direction below (SE) it were chosen. The yellow circles highlight the events simulated.

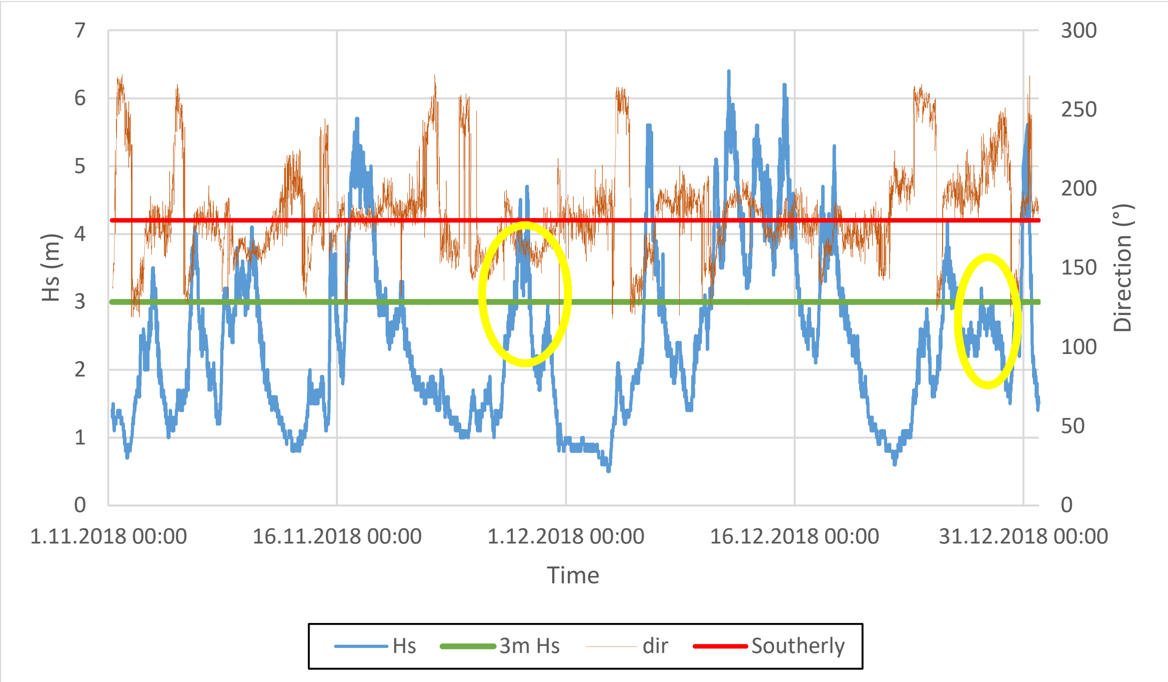

Figure 2-5 Significant wave height and direction at Landeyjahöfn wave buoy in November and December 2018. Simulated events are marked with a yellow circle.

To get the conditions at the model boundary, the IRCA's regional MIKE SW wave model was used and the results for the corner points of the TELEMAC model extracted. The input boundary conditions for the MIKE SW model are time series of significant wave height, wave direction and peak wave period from the European Centre for Medium-Range Weather Forecasts. The bathymetry is based on the same collection of measurements from the Hydrographic Department of the Icelandic Coast Guard as the offshore bathymetry in the TELEMAC model. The water level is a time series of measured water levels and the wind forcing comes from EMCWF. It is not deemed necessary to include wind forcing in the TELEMAC model as the effects of wind on the waves are already present in the imposed boundary conditions which are extracted from MIKE SW. Any additional effects of wind in the 4 km wide TELEMAC model are assumed to be negligible.

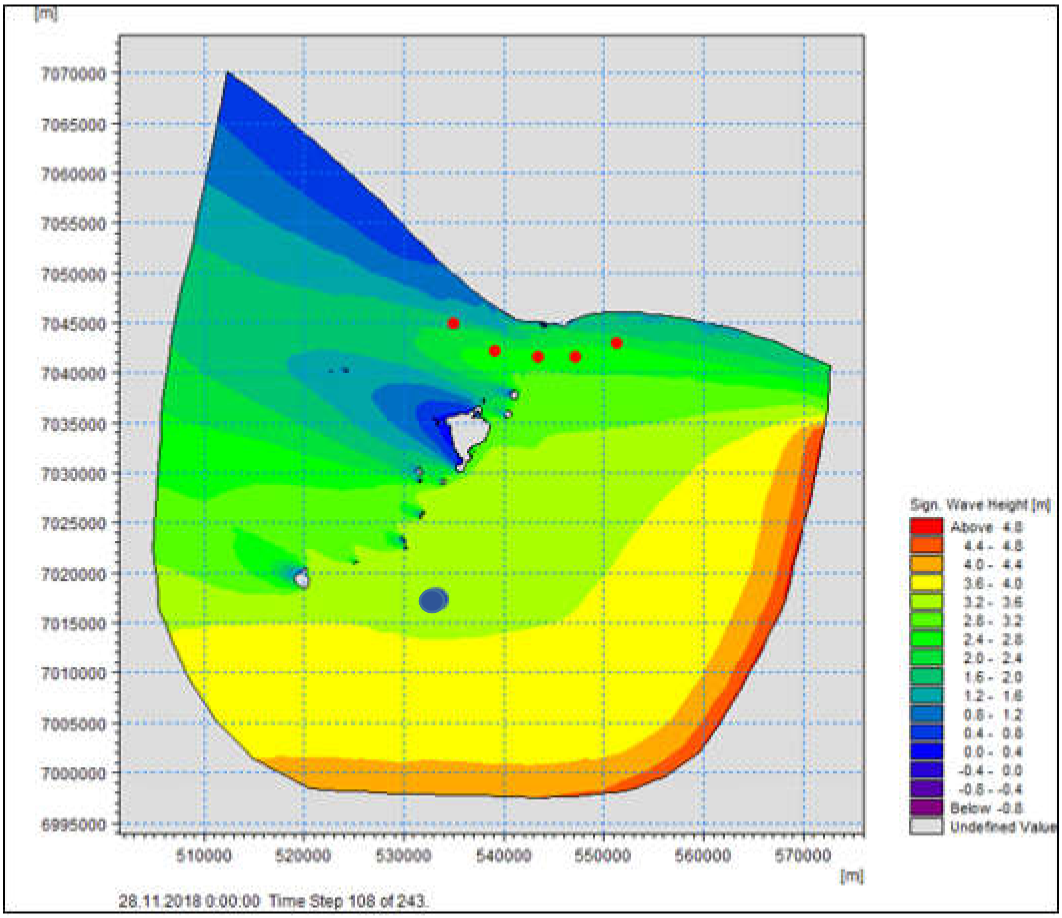

Figure 2-6 Results of the regional MIKE SW wave model at midnight of 28.11.2018 from which the wave boundary conditions for the south-easterly storm were taken. The red dots represent the corner points, P1 to P5, of the TELEMAC model. The blue dot represents the Surtsey wave buoy.

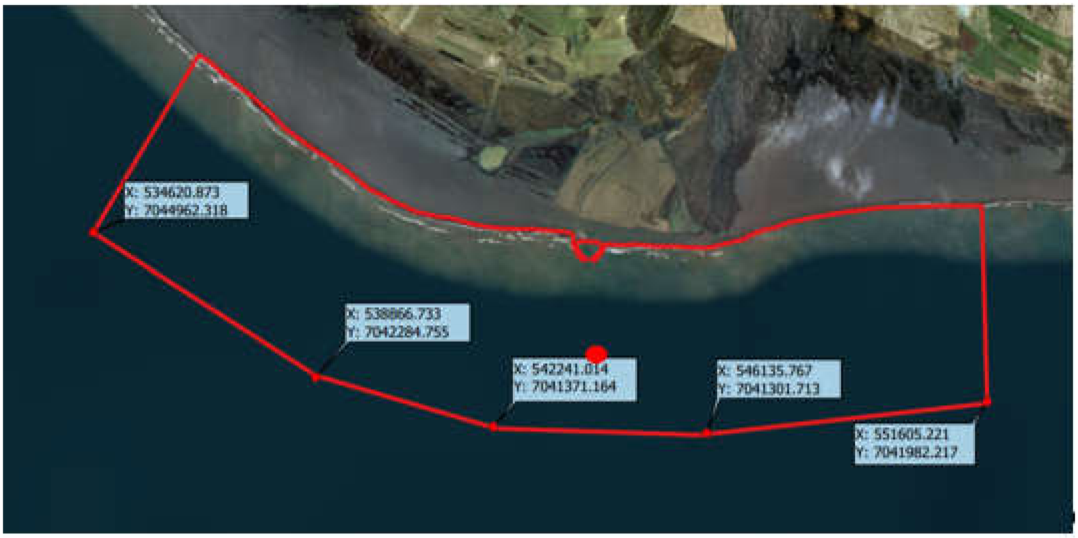

Figure 2-7 The points for which results from the regional MIKE SW wave model were extracted. The red line represents the outline of the TELEMAC model. The red dot represents the Landeyjahöfn wave buoy.

Because of the sheltering effects of the Westman Islands it is important to have spatially varying boundary conditions on the TELEMAC model. The results at the points in Figure 2-7 were interpolated and imposed on every node of the open sea boundary. The boundary conditions are however constant in time which increases the importance of choosing a storm with relatively constant wave heights and directions for the duration of the simulation. The results from the regional MIKE SW model for the beginning of the two events, south-easterly event in November and south-westerly event in December, at the boundary points, as well as the measured values from the Landeyjahöfn wave buoy are shown in

Table 2-2. It is worth noting that the spatial variation in wave height is much greater in the south-westerly event from December and how big the sheltering effect of the Westman Islands is in the middle point.

Table 2-2 Results from regional MIKE SW wave model at boundary points of TELEMAC model at the beginning of the simulated periods. P1 is the western most point and P5 the one furthest to the east. The measurements from the Landeyjahöfn wave buoy is included for comparison.

00:00 28.11. SE event	Significant wave height (m)	Peak wave period (s)	Mean wave direction (°)
P1	1.8	8.8	124
P2	2.4	8.9	120
P3	2.6	8.9	117
P4	2.7	8.9	117
P5	2.5	8.8	119
Wave buoy	4.0	9.9*	175

06:00 28.12. SW event	Significant wave height (m)	Peak wave period (s)	Mean wave direction (°)
P1	4.39	10.79	230
P2	3.70	10.79	240
P3	2.62	10.74	242
P4	3.31	10.74	222
P5	3.58	10.76	217
Wave buoy	3.1	8.3*	233

Note: The peak wave period for the buoy is calculated with T_p=1.3 x T_z (see Chapter 3.2.3)

The wave heights at the boundaries in the south-easterly event are significantly lower than the ones measured by the Landeyjahöfn wave buoy. In fact, looking at Figure 2-6, it is clear that only on the eastern boarder of the model that the wave height is are similar to the measured 4.0 meters and from there they only get smaller. SW simulation results for other south-easterly storms in November and December were examined and they all had lower wave heights than measured by both the Landeyjahöfn and the Surtsey wave buoys. Data from the EMCWF forecast points, which are used as input into the MIKE SW model, were then examined for the biggest south-easterly storms of 2018 and the wave heights were consistently lower than expected. However, these results are the only available source of the wave conditions at the boundary points of the TELEMAC model and will thus be used as input. This discrepancy must be kept in mind when analysing the results.

It is possible that the forecast underestimates waves coming from the southeast since the low pressure systems are always coming from the southwest. That means that the south-easterly winds are more unstable and the time series from ECMWF only have a value every 6 hours. Further speculation about what might cause errors in the ECMWF's forecast will not be undertaken here but it is an issue well worth investigating.

2.3.4 Steering files

The two modules of the TELEMAC suite used in this study, TELEMAC2D and TOMAWAC each have their own steering file and can be run separately. They specify input and output files as well as various parameters, physical and computational options.

It is possible to consider tides and stationary currents through keywords in the TOMAWAC steering file but that way only the effects of the current on the waves is taken into account. When the TOMAWAC and TELEMAC2D simulations are coupled the wave-current interactions are represented both ways. TELEMAC transfers updated values of current velocities and water depths to TOMAWAC at each time step and TOMAWAC in turn transfers updated values of wave driving forces acting on the current.

This added precision and the fact that the tidal current is not stationary are the reasons for choosing to couple the simulations.

2.3.5 Calibration Data

The IRCA operates 11 wave buoys around the country, one of which is located 1.05 nautical miles south of Landeyjahöfn harbour at 30 meters water depth. The buoy sends out information about significant wave height, average zero-crossing period, wave length and wave direction 4 times every hour. This data is available at the IRCA's website (http://www.vegagerdin.is/vs/StationsDetails.aspx?ID=110).

There is also a WaMos II Radar located on land in the harbour which measures the waves and current in the area outside the harbour. A screenshot of the radar can be seen in Figure 2-8. The radar is located in the centre of the circle and the small dot south of the eastern breakwater is the observation point. Wave characteristics such as significant wave height, wave length, wave direction and peak period at the observation point are stored every 2 minutes in an ASCII file. In addition, the High Resolution Current Analysis (HRC) software installed on the radar allows the collection of temporal and spatial varying surface current fields and sea state from sequences of nautical X-band radar image.

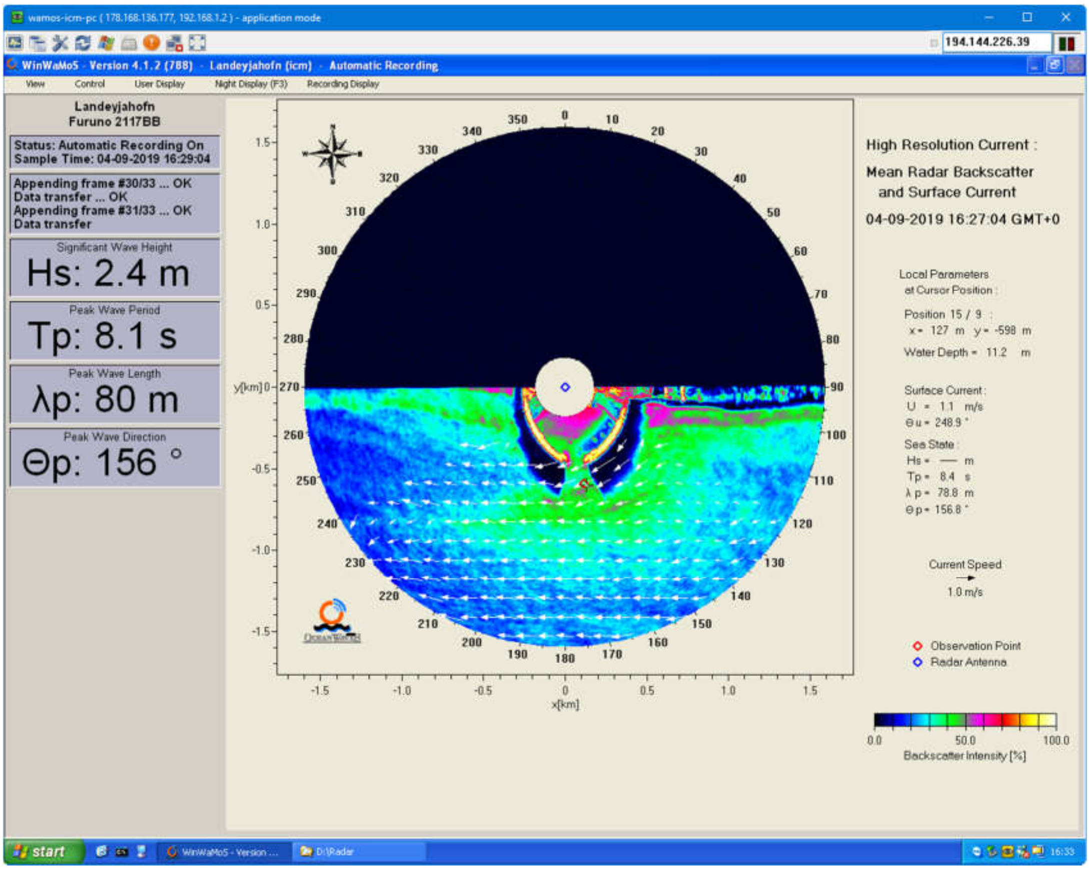

Figure 2-8 Screenshot of the WAMos II Radar in Landeyjahöfn

3 Results

3.1 Calibration of tides

A simulation was run with tides only for a period of 2 weeks. The results were compared to the tide table data for Landeyjahöfn from the hydrographic department of the Icelandic coast guard and the three calibration coefficients in TELEMAC2D adjusted until the result in Figure 3-1 was obtained. The maximum error is 18 cm and the average absolute difference is 5 cm. The largest errors occur during ebb and apart from those peaks, the maximum error is 6 cm. The simulated amplitude is sometimes larger and sometimes smaller than the tide table amplitude and the difference between the average values is 1.6 cm. The model used by the hydrographic department and the TPXO model used by TELEMAC are completely independent of each other.

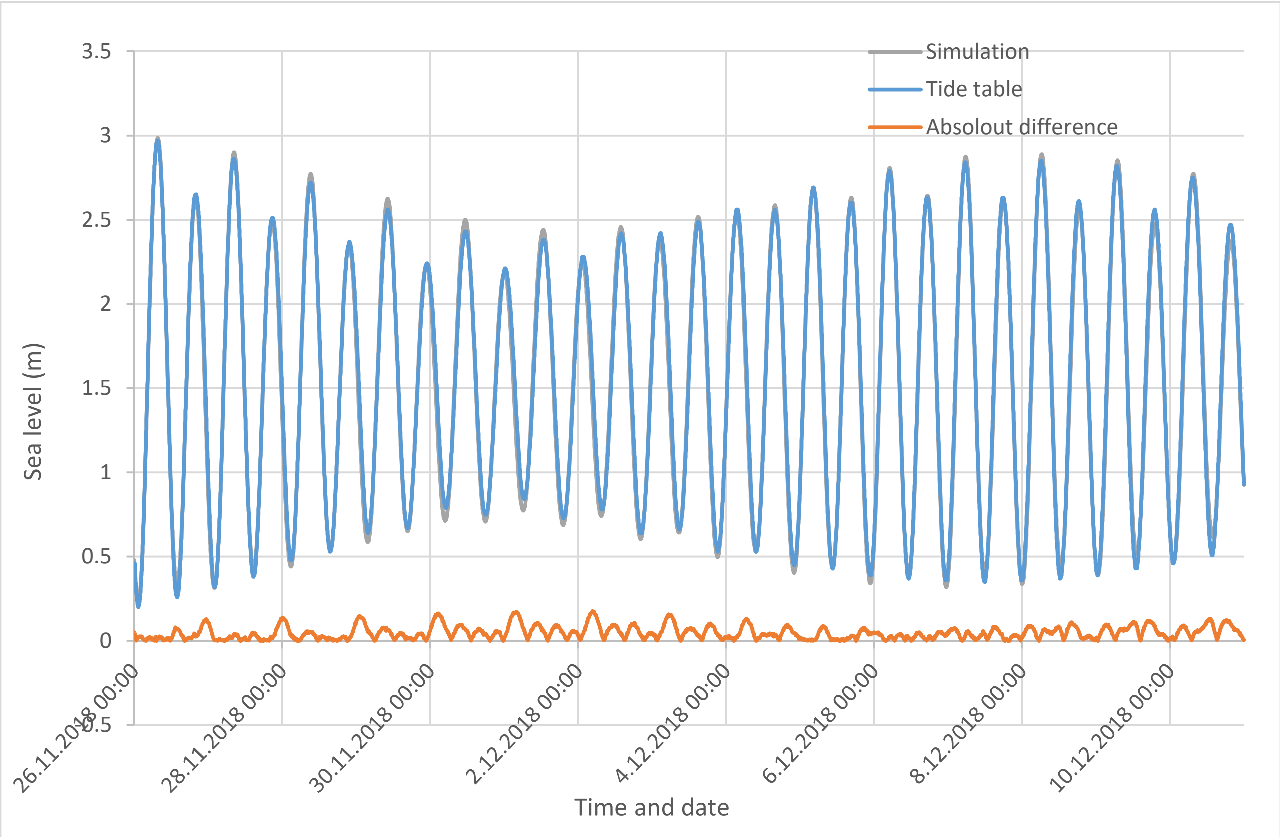

Figure 3-1 Simulated tides and local tide table

3.2 **Southwestern storm**

3.2.1 Tides

The southwestern event simulated is a 24 hour period starting at 06:00 on December 28th 2018. Simulated sea level was compared to measured sea level and tide table sea level. As seen in Figure 3-2 the simulated sea level follows the tide table quite closely but the measured sea level is on average 34 cm lower. The tide table is based on calculations of the astronomical tide and does not include storm surge or barometric surge. In Iceland, measured sea level is usually higher than tide table sea level as storm surge and barometric surge are almost always positive. One possible explanation for measured sea level being lower than tide table sea level is a deep low pressure system somewhere off the coast pulling the water away from the coast. A difference of -34 cm is unusually large so a more likely explanation is that the zero in these measurements is not properly adjusted. This theory is supported by looking at the data over a longer period of time, as the measured sea level is almost always lower than the tide table sea level.

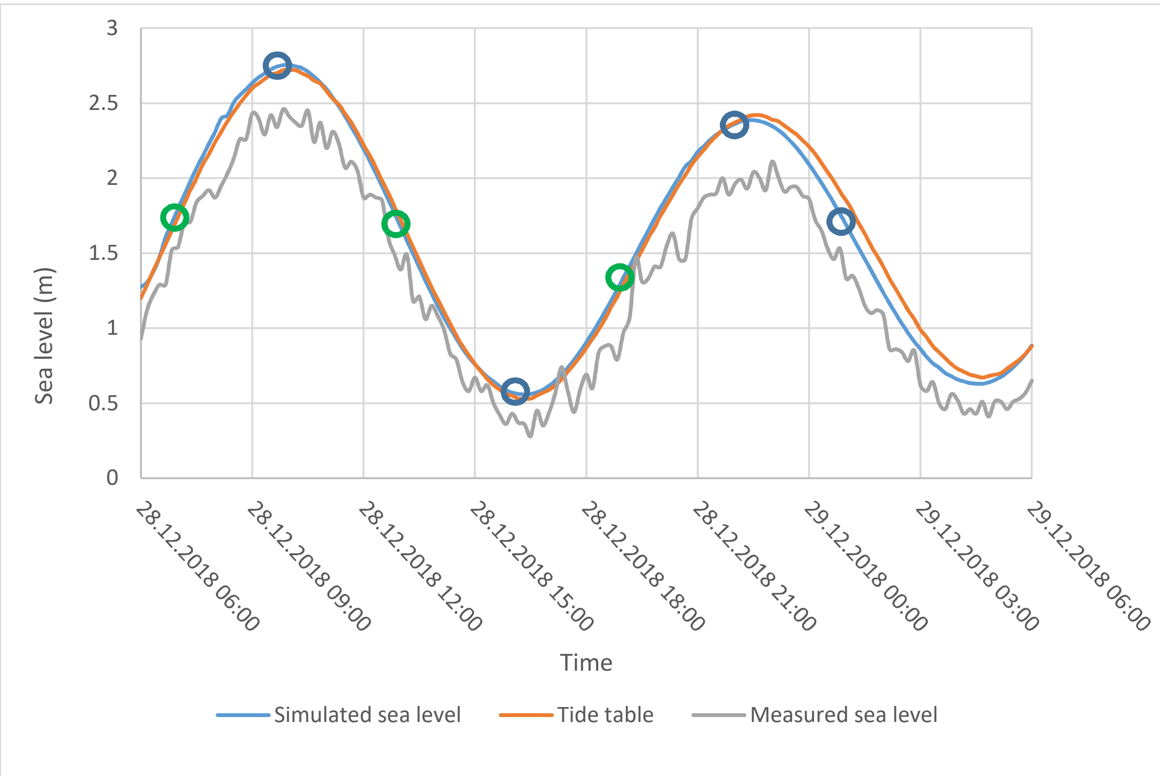

Figure 3-2 Measured, simulated (TELEMAC2D) and forecast (Hydrographic department of the Icelandic Coast Guard) sea level on December 28th. The circles represent times when screenshots were taken of the simulation results to include in this thesis. All the screenshots can be found in Appendix A. The screenshots marked with a green circle are also to be found in the following chapter.

3.2.2 Current Velocities

During flood the tide-induced current flows to the west. When the waves come in from the southwest they cause a longshore current to the east. This can be seen clearly in Figure 3-3 which shows a larger area of the simulation than the radar measures.

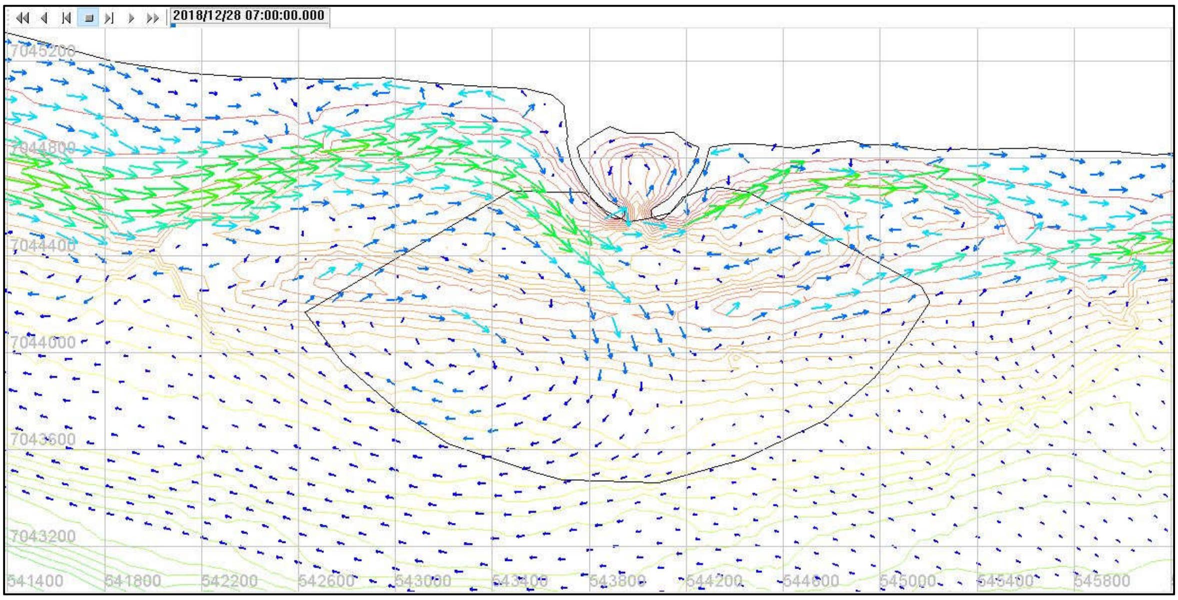

Figure 3-3 Simulated current velocities during flood tide and southwesterly waves at 07:00 on December 28th 2018. The outline of the area captured by the radar is also shown.

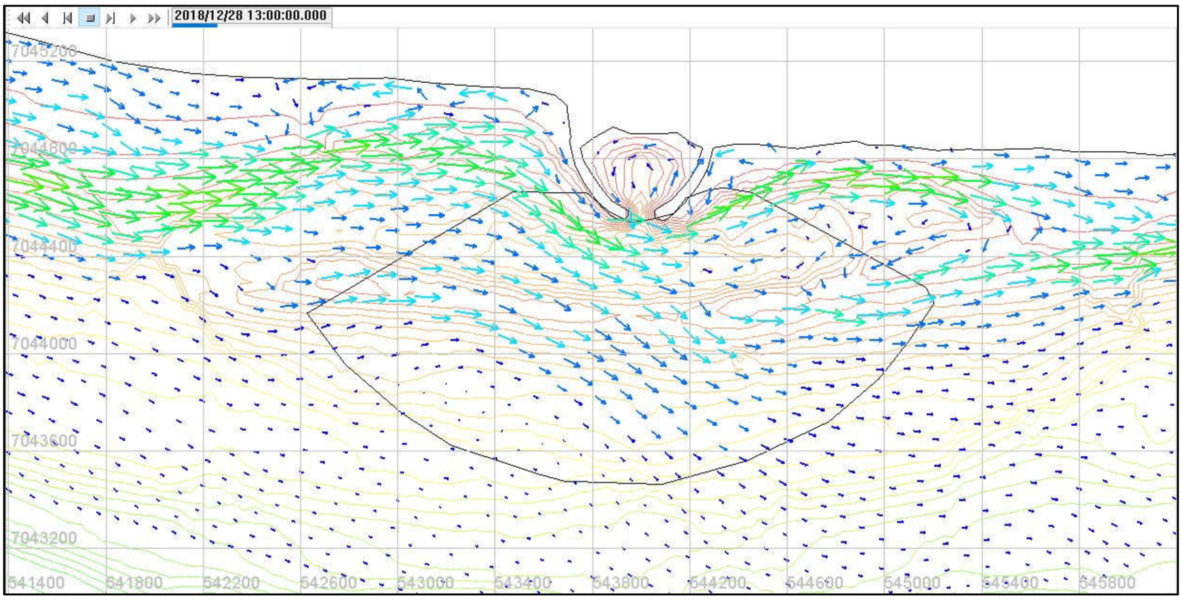

Figure 3-4 Simulated current velocities during ebb and south-westerly waves at 10:00 on December 28th 2018.

Outside the breaker bar the westward tidal current is dominant. As the waves start breaking on the bar, they produce a stronger current to the east. The current travels along and inside the breaker bar until it reaches the opening in the bar where a big part of the current swerves to the south through the opening. This is the rip current that keeps the opening there as it carries the sediments with it. Figure 3-4 shows the same area during ebb. The current outside the bar is to the east.

Figure 3-5 shows the simulated depth averaged current velocities within the area captured by the radar during flood tide at 19:00 on December 28th 2018. Figure 3-6 shows the surface current velocities measured by the radar at the same time. In appendix A, the development of the current at different phases of the tidal cycle can be seen as similar images are provided for flood, high tide, low tide and ebb conditions. The model results have been cropped to show the same area as the radar data and the spacing between the arrows has been adjusted to facilitate comparison between the two. Figures similar to Figure 3-3 and Figure 3-4 showing a larger area and the contour lines is also supplied for each phase of the tidal cycle.

Examining these images reveals a very good agreement in directional patterns between the radar measurements and the simulation results. The magnitude of the vectors cannot be directly compared as the model shows depth averaged velocities and the radar surface velocities. There is, however, a strong resemblance between the images with regard to where the velocity is high and where it is low.

The most notable difference is at the far east end of the depicted area. Both images show a part of the longshore current continuing to the east but the large arrows on the radar are further to the north than on the simulation. This could be explained by the bathymetries not being exactly the same. The bathymetry in the model is from a survey taken a month earlier. As can be seen in Figure 2-5 the period between the survey and the event simulated in December was dominated by powerful storms which very likely changed the bathymetry to some extent.

The simulation shows a clear westward flow north of the abovementioned eastward wave-induced current but this is not clearly present in the radar image. It is present in the radar image from the 07:00 flood but also in that case it is more prominent in the simulation. From Figure 3-3 and Figure 3-4 it is clear that this is an eddy current as it is also present during ebb when the tidal flow is to the east. Another eddy current is visible next to the eastern breakwater.

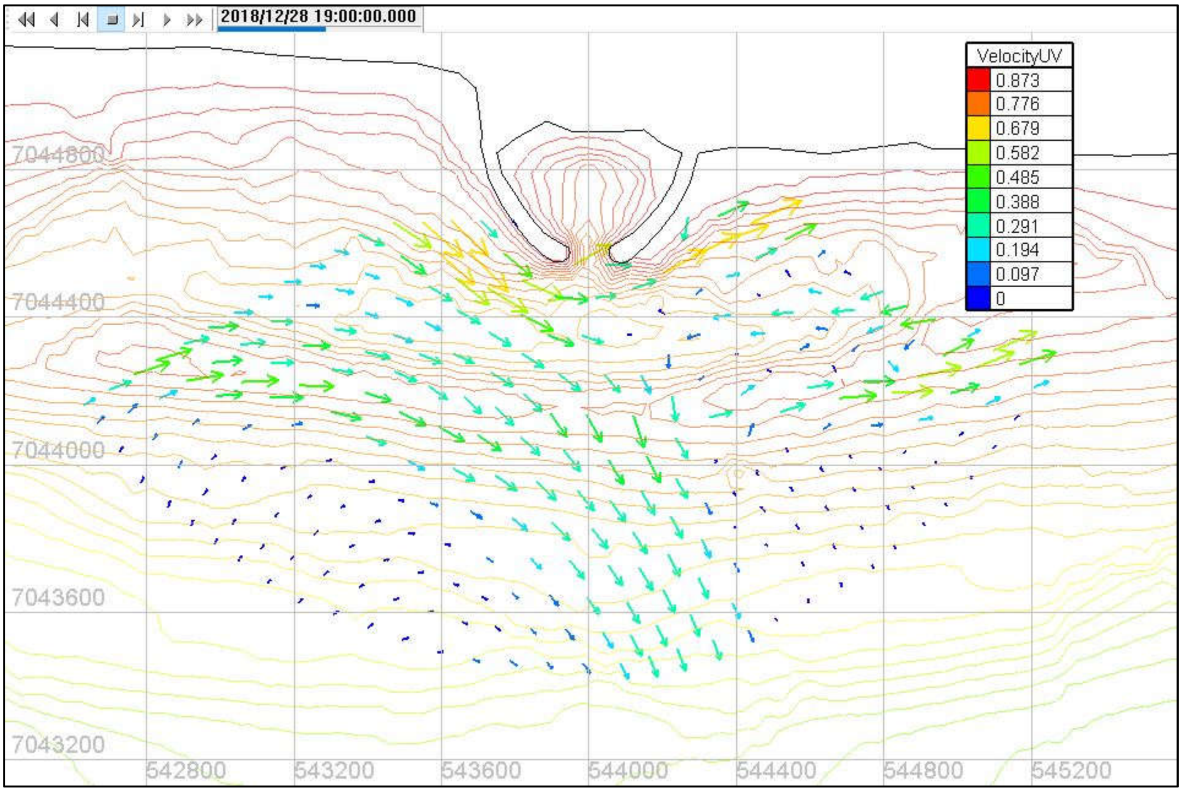

Figure 3-5 Simulated current velocities during flood tide at 19:00 on December 28th 2018

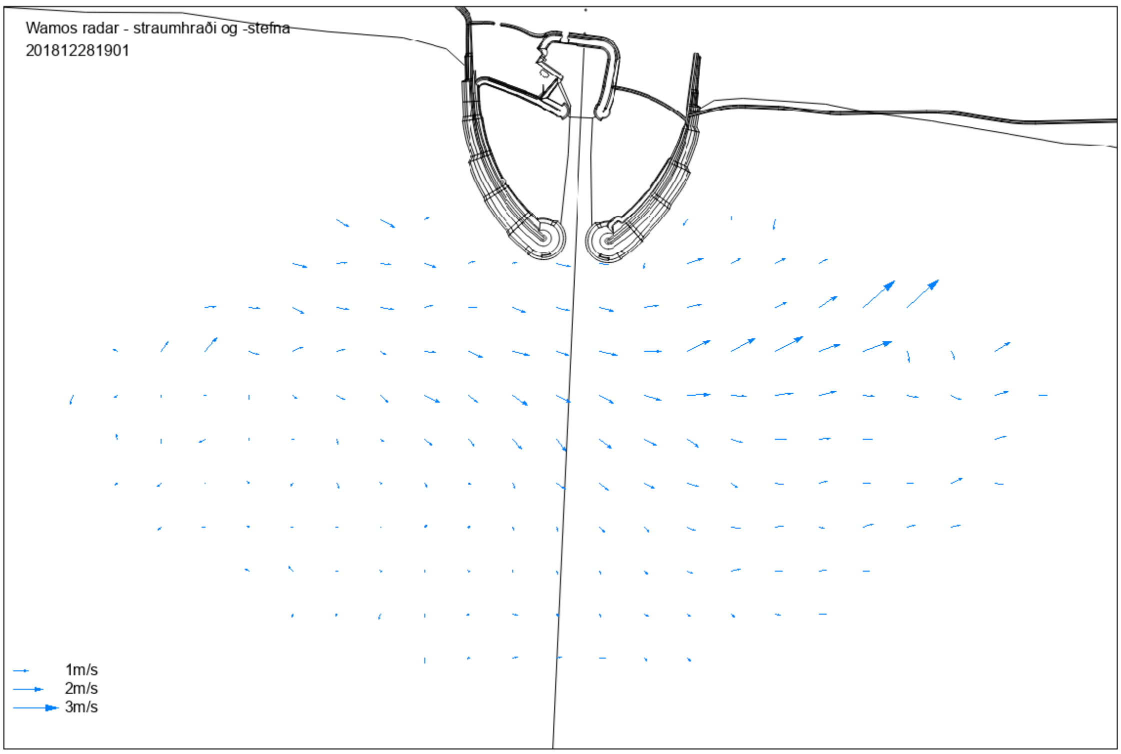

Figure 3-6 Current velocities from the radar during flood tide at 19:01 on December 28th 2018

3.2.3 Wave characteristics

Figure 3-7 shows simulated significant wave heights at 19:00 on December 28th 2018. The boundary conditions are constant in time meaning that any differences inside the model from one time to another are due to effect of the tides. The wave heights imposed on the boundary which are taken from the MIKE SW regional wave model clearly include the shelter effect from the Westman Islands.

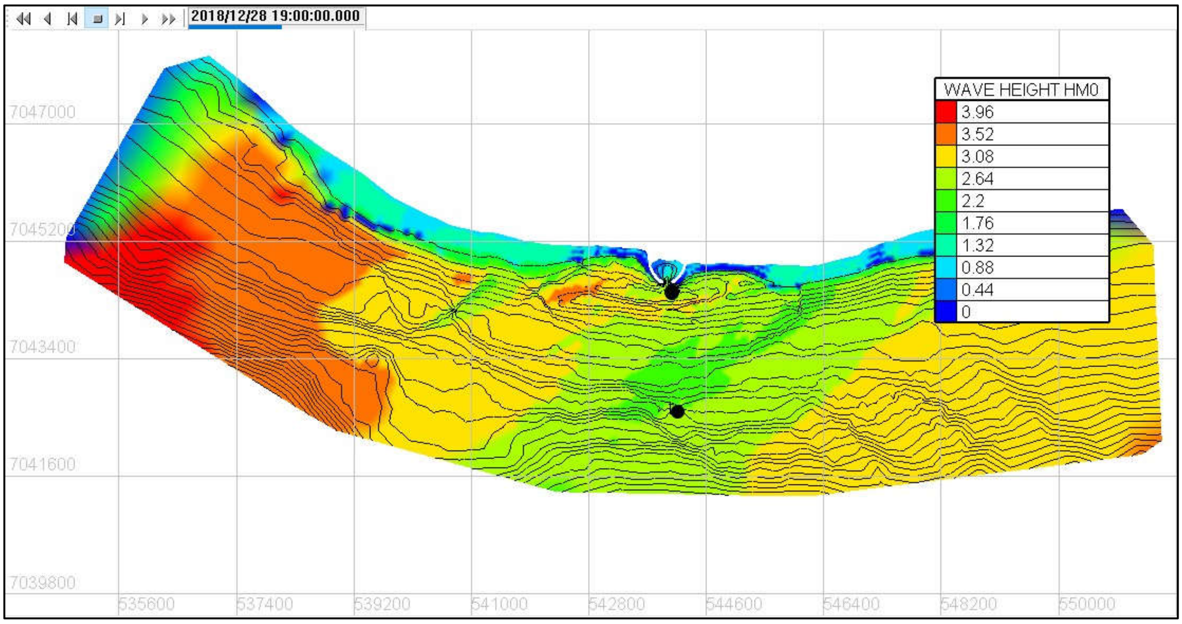

Figure 3-7 Simulated significant wave height in meters at 19:00 on December 28th 2018 with 2 meter contour lines and location of Landeyjahöfn wave buoy and radar observation point (next to the harbour).

Unlike the current velocities, the wave characteristics can be compared quantitatively to measurements. The black dots in Figure 3-7 represent the two points where measurements of wave height, direction and period are taken. The one closer to land is the radar observation point and the one further out is the Landeyjahöfn wave buoy. Table 3-1 shows the average values of measured and simulated H_0, T_p and θ at the two measuring points over the simulated period. Figure 3-8 through Figure 3-10 show the time series of the same variables.

Table 3-1 Average values for measured and simulated H_0, T_p and θ on December 28th

	Buoy		Radar	
	Measured	Simulated	Measured	Simulated
H_0 (m)	2.7	2.7	3.4	2.7
T_p (s)	7.9	9.8	10.8	10.0
Θ (°)	218	231	207	223

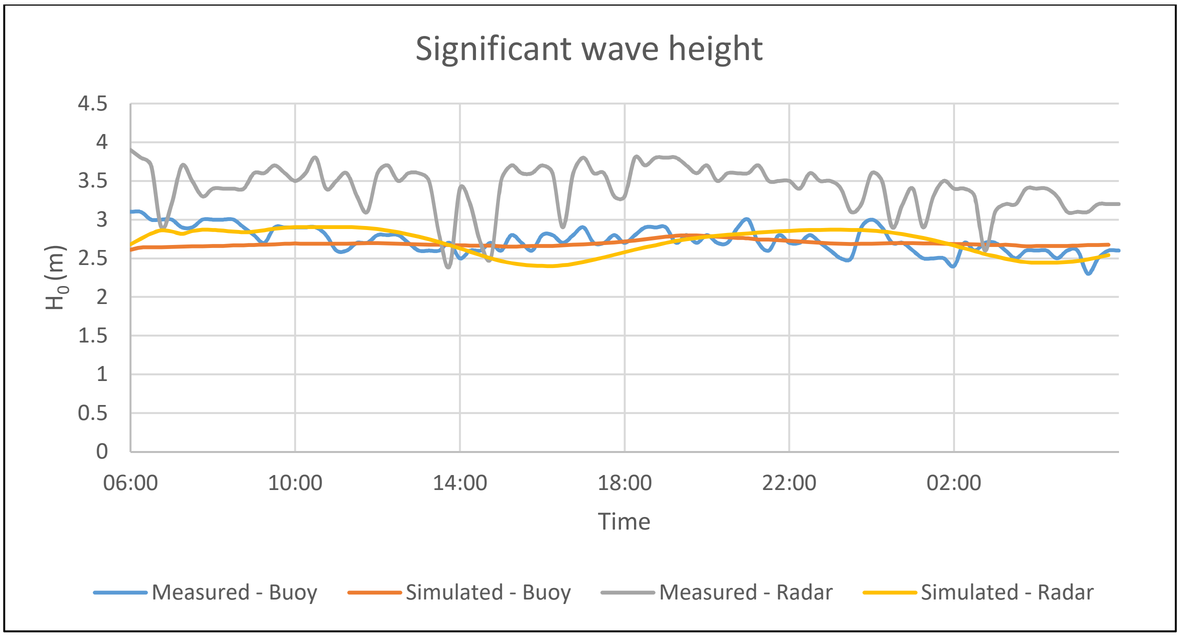

Figure 3-8 Measured and simulated significant wave height at wave buoy and radar observation point

The measured wave heights have bigger fluctuations than the simulated ones. This is to be expected as the wave conditions imposed on the boundary are constant in time whereas natural waves are highly irregular. The fluctuations in the simulated wave heights are solely due to the tidal current and the tidal change in sea level. This effect of the tides on the waves is stronger at the radar observation point which is in agreement with expectations as it is closer to land than the wave buoy. The maximum wave height occurs about an hour after high tide and the minimum wave height is right around the time of low tide.

The simulated wave height at the wave buoy falls within the measured range indicating that the input boundary conditions were reasonable. The average simulated wave height at the wave buoy and the radar observation point are almost the same. The average measured wave height at the radar is 0.73 meters higher. Whether this is due to underrepresented shoaling in the model or overestimation by the radar is not entirely clear. A comparison between MIKE SW simulations and the radar measurements which was done for two periods in 2016 and 2017 shows that radar measurements were on average 0.3 meters higher than simulated wave heights. The radar is does not measure weave height directly and must be calibrated somehow but whether a measuring device should be calibrated to a computational model is debatable. This demonstrates one of the many difficulties in collecting data in the coastal environment.

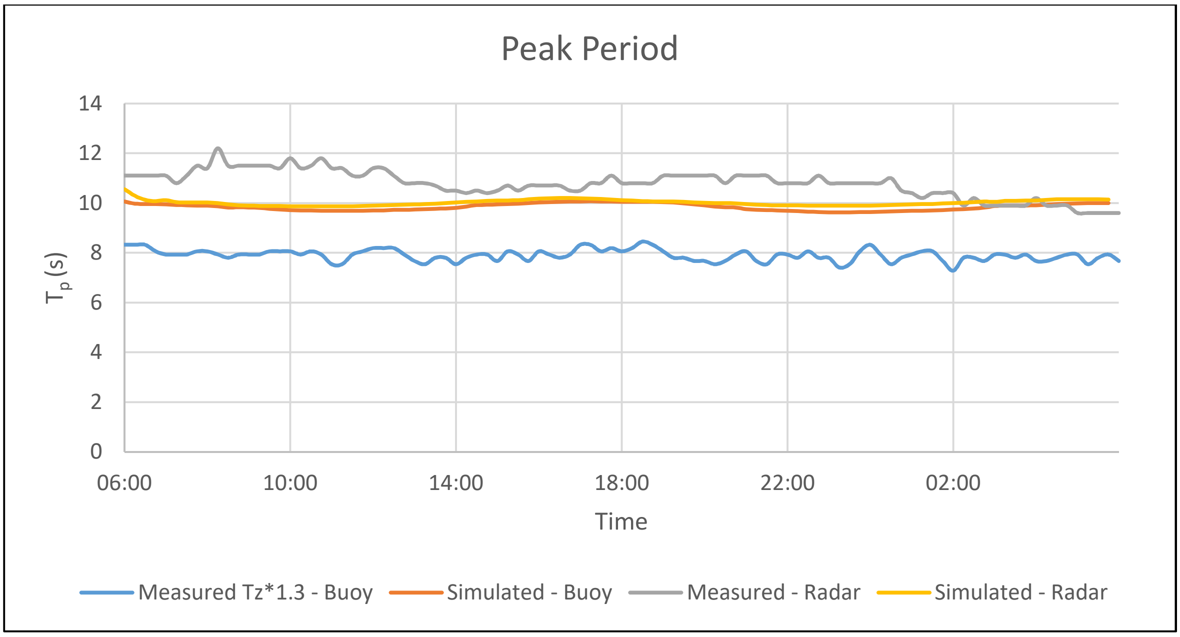

Figure 3-9 Measured and simulated peak period at wave buoy and radar observation point

The simulated peak period hardly changes at all from the buoy to the radar and is close to the measured value from the radar. The wave buoy does not measure peak period (T_p) but zero crossing period (T_z). There is not a fixed relationship between the two but a rule of thumb usually applied by IRCA is $T_p \approx 1.3 \times T_z$

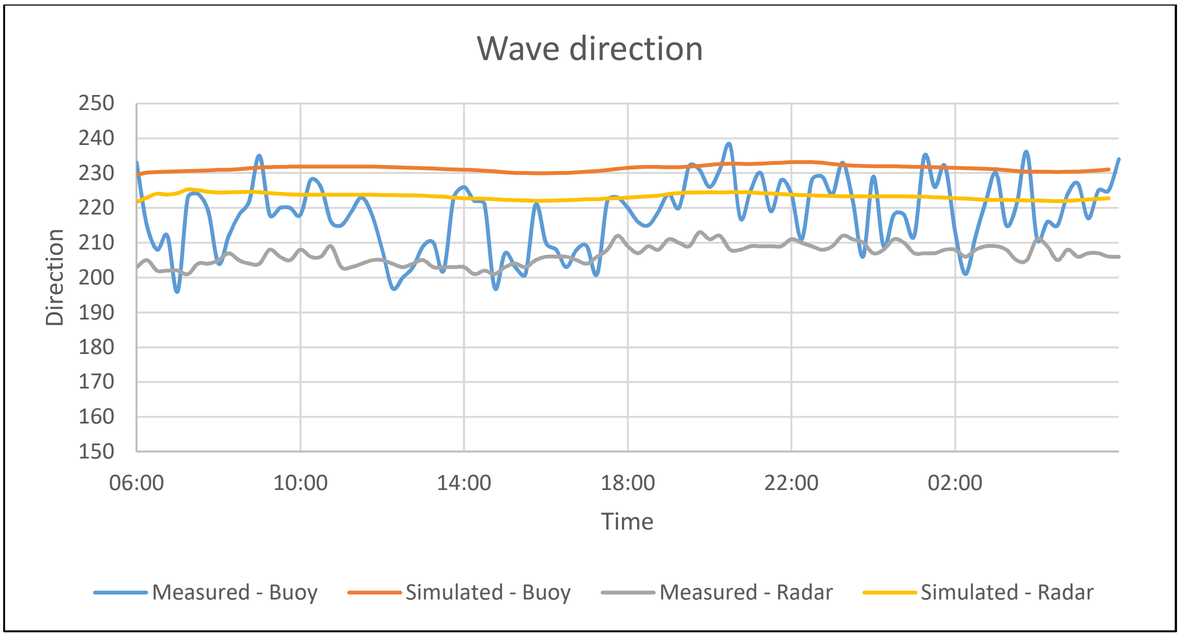

Figure 3-10 Measured and simulated wave direction at wave buoy and radar observation point

The simulated wave direction is more westerly than measured direction at both points. The effect of refraction turning the waves to be more perpendicular to the coast is represented and is of similar magnitude as the difference between the two measurements.

3.3 **South-eastern storm**

3.3.1 Tides

The simulated period with waves from the southeast is the storm of 28.11.2018. The simulation starts at midnight and the duration is 24 hours. Figure 3-11 shows the measured, simulated and forecast sea level during that period.

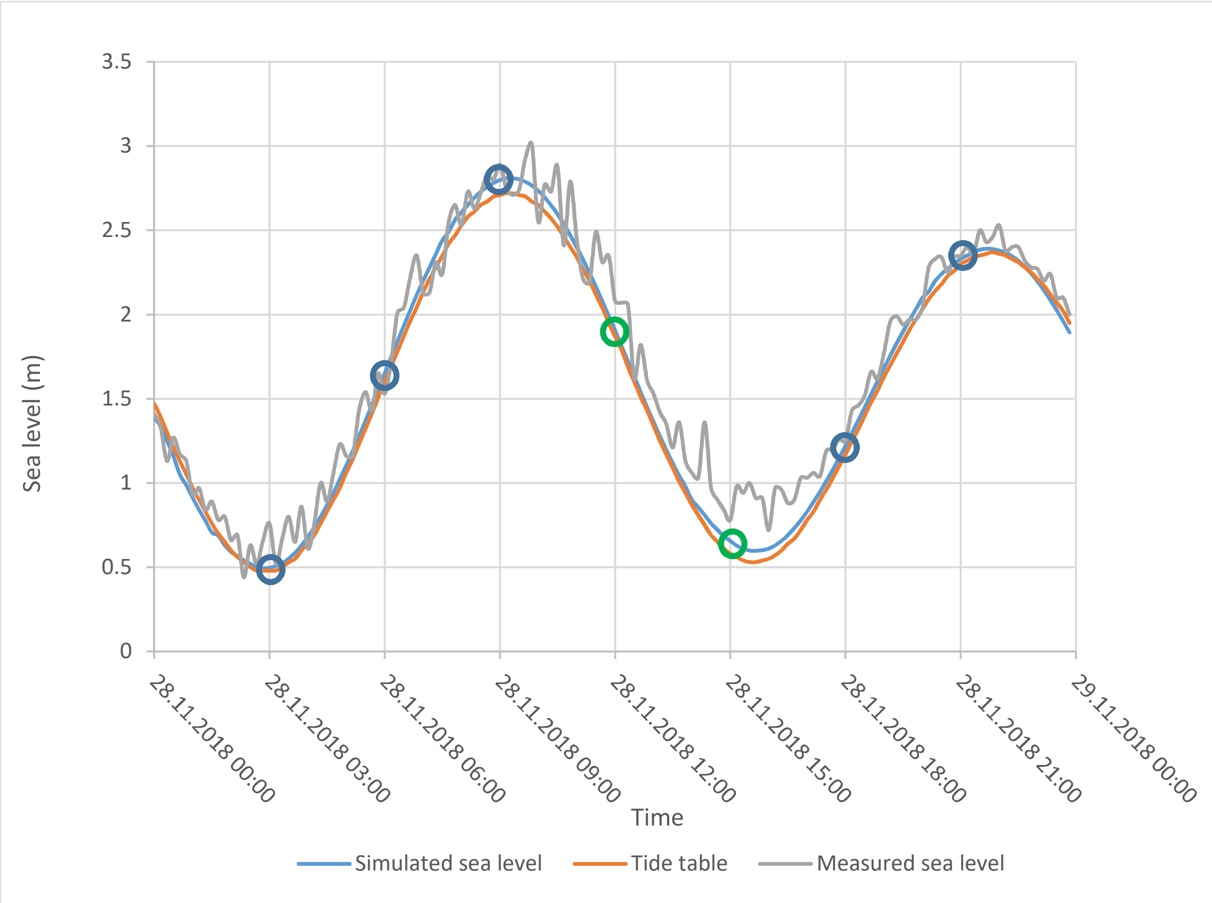

Figure 3-11 Measured, simulated (TELEMAC2d) and forecast (Hydrographic Department of the Icelandic Coast Guard) sea level on November 28th 2018. The circles represent times when screenshots were taken of the simulation results to include in this thesis. All the screenshots can be found in Appendix B. The screenshots marked with a green circle are also to be found in the following chapter.

Here, the measured sea level and the simulated sea level are slightly higher than the tide table as is expected because of surge. If the conclusion drawn in Chapter 3.2.1 that the zero for the measured sea level is too high is correct, the difference in reality is larger.

3.3.2 Currents

The simulated currents behave as expected. The wave induced longshore current is to the west and the current outside the breaker bar is to the west during flood and to the east during ebb. No big rip current is visible although a part of the longshore current seems to escape south through the opening in the bar to join with the eastward tidal current as depicted in Figure 3-12.

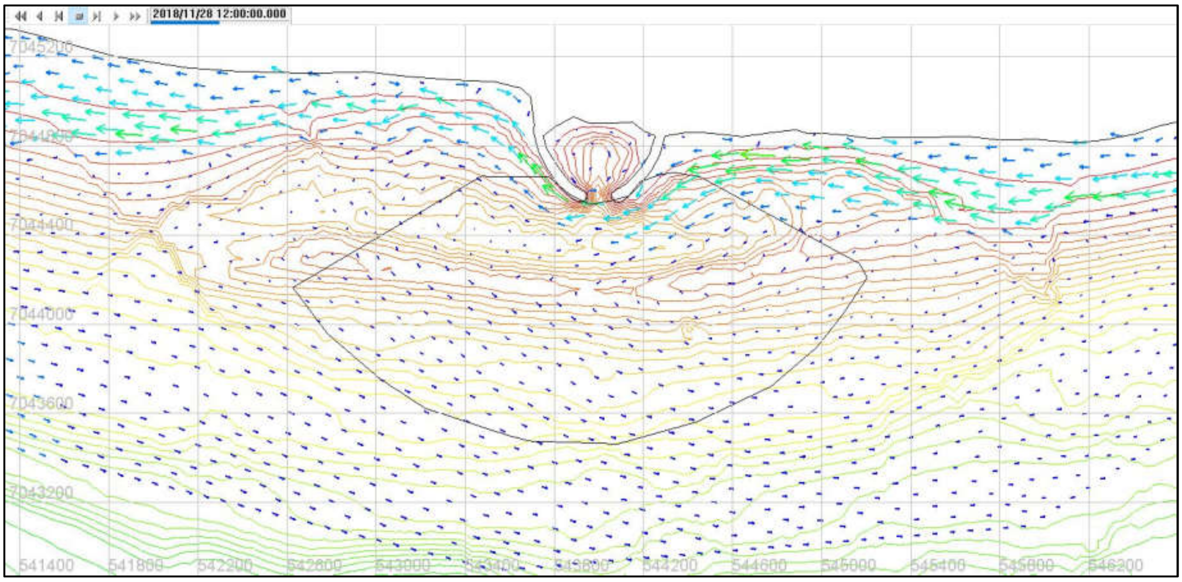

Figure 3-12 Simulated Currents at 12:00 on 28th of November 2018. Ebb tide.

The radar data from this period has a lot of irregularities as can be seen in Figure 3-14 and in Appendix B. The radar does not measure the current directly, but tries to identify phenomena in the surface and calculate the current velocities from their location. One of the factors that can confuse the radar is if the waves are very small, which is not the case here. Precipitation can also cause a disturbance in its view and strong winds can cause irregularities in the phenomena the radar is trying to follow. According to the Icelandic Met Office, there was no precipitation this day. There was however a northerly wind direction (www.vedur.mogt.is) which, although not very strong, might cause irregularities in the surface pattern of south-easterly waves. It is generally assumed that a large vector next to small ones is a measurement error. By looking only at the smaller vectors there seems to be some resemblance to the simulated currents although not as good as in the simulation of the south-western storm.

Looking at Figure 3-13 and Figure 3-14, which show the simulated and measured currents at low tide at 15:00 on November 28th, the current is generally to the west in all areas. In both figures, three swirls or spirals can be seen along the top of the bar.

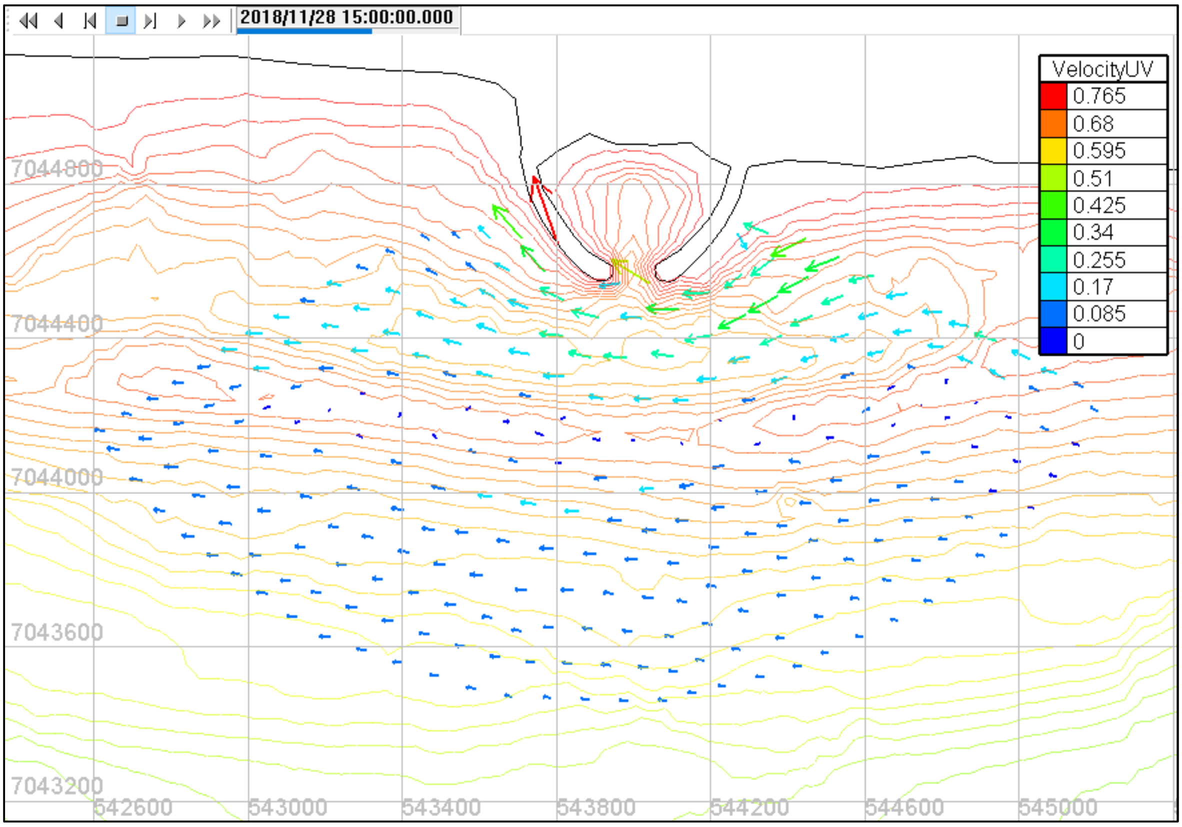

Figure 3-13 Simulated current velocities at 15:00 November 28 2018. Low tide.

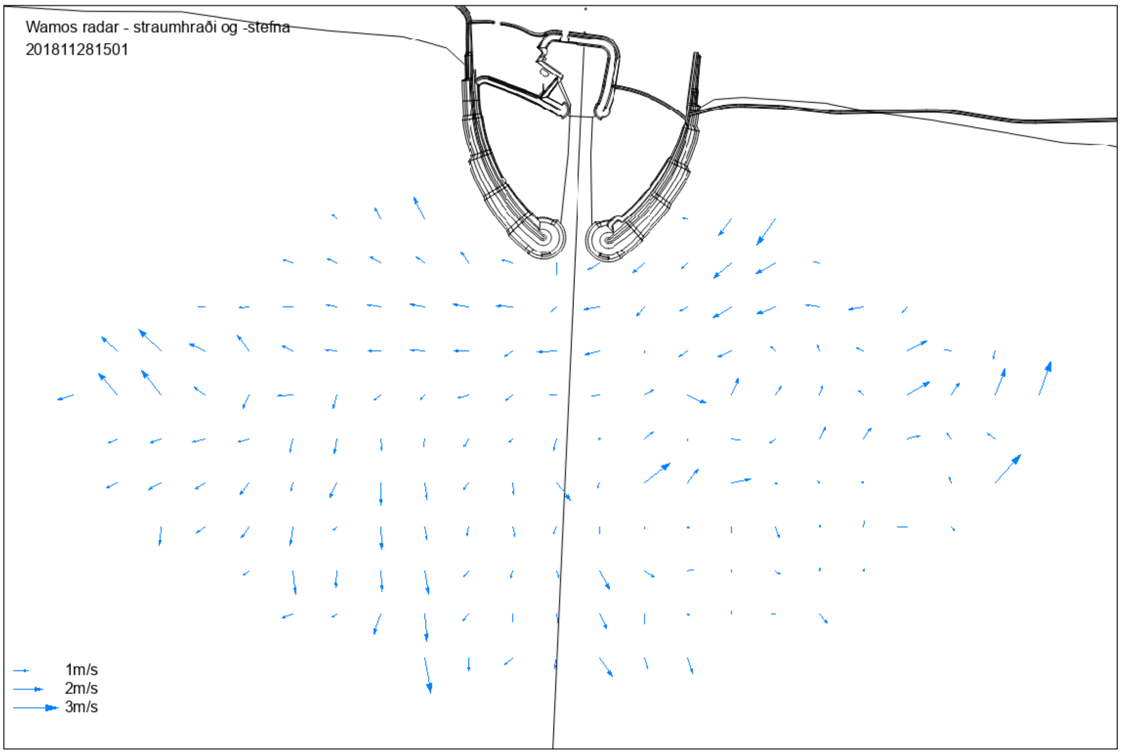

Figure 3-14 Measured surface velocities at 15:00 November 28 2018. Low tide.

The simulation shows a large current along the western breakwater where the radar shows not much at all. That could be explained by this being a blind spot for the radar as the breakwater blocks its view. One of the sand transportation processes around the harbour that has been noticed by the IRCA is the flushing from the western breakwater. In some bathymetric surveys there is an unexplained hole next to the breakwater which could be caused by the current depicted in the simulation but is missed by the radar as it is in its blind spot. Figures similar to Figure 3-12, Figure 3-13 and Figure 3-14 representing other times in the tidal cycle are provided in Appendix B.

3.3.3 Wave characteristics

As explained in Chapter 2.3.3 the wave data input for the south-eastern storm does not look realistic. The output of a model is never better than its inputs so it is no surprise that the results of the simulation do not fit the measured data. The simulated wave height is lower than the measured wave height as expected since the input wave heights on the model boundary were lower than the wave heights from the buoy and the radar. The average simulated and measured wave characteristics are shown in Table 3-2 and the significant wave height in meters is shown in Figure 3-15. The simulated waves turn toward the coast as they should because of refraction. The measured direction hardly changes at all, and the one degree it does turn is in the wrong direction which gives reason to doubt the radar measurement.

Table 3-2 Average values for measured and simulated H_0, T_p and θ on November 28th.

	Buoy		Radar	
	Measured	Simulated	Measured	Simulated
H_0 (m)	3.3	2.1	4.4	1.8
T_p (s)	9.9	8.1	11.6	8.2
Θ (°)	162	128	161	143

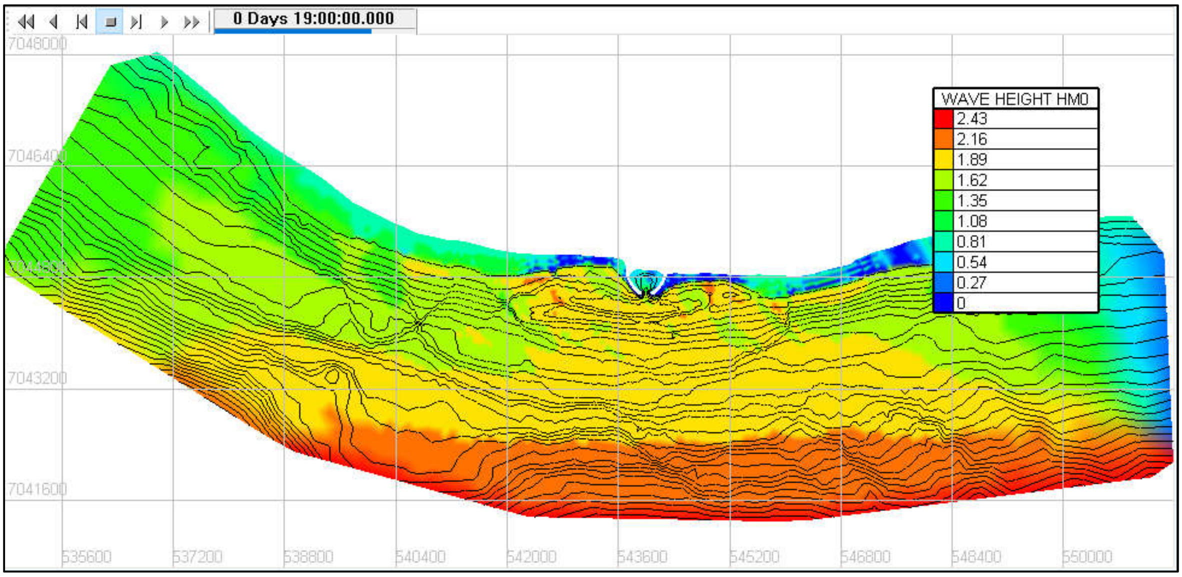

Figure 3-15 Simulated significant wave heights at 19:00 on November 28th 2018 with 2 meter contour lines.

Graphs of H_0, T_p and θ are shown in Figure 3-16. Compared to the December simulation the fluctuation in wave height with the tides is much smaller – in fact it is hardly detectable. The simulated waves have a short period, more like wind waves rather than swell. The radar observation point is at a water depth of approximately 8 meters and the bottom would not interfere with short 2 meter waves at that depth so it is logical that the tides do not have a visible effect on the wave height.

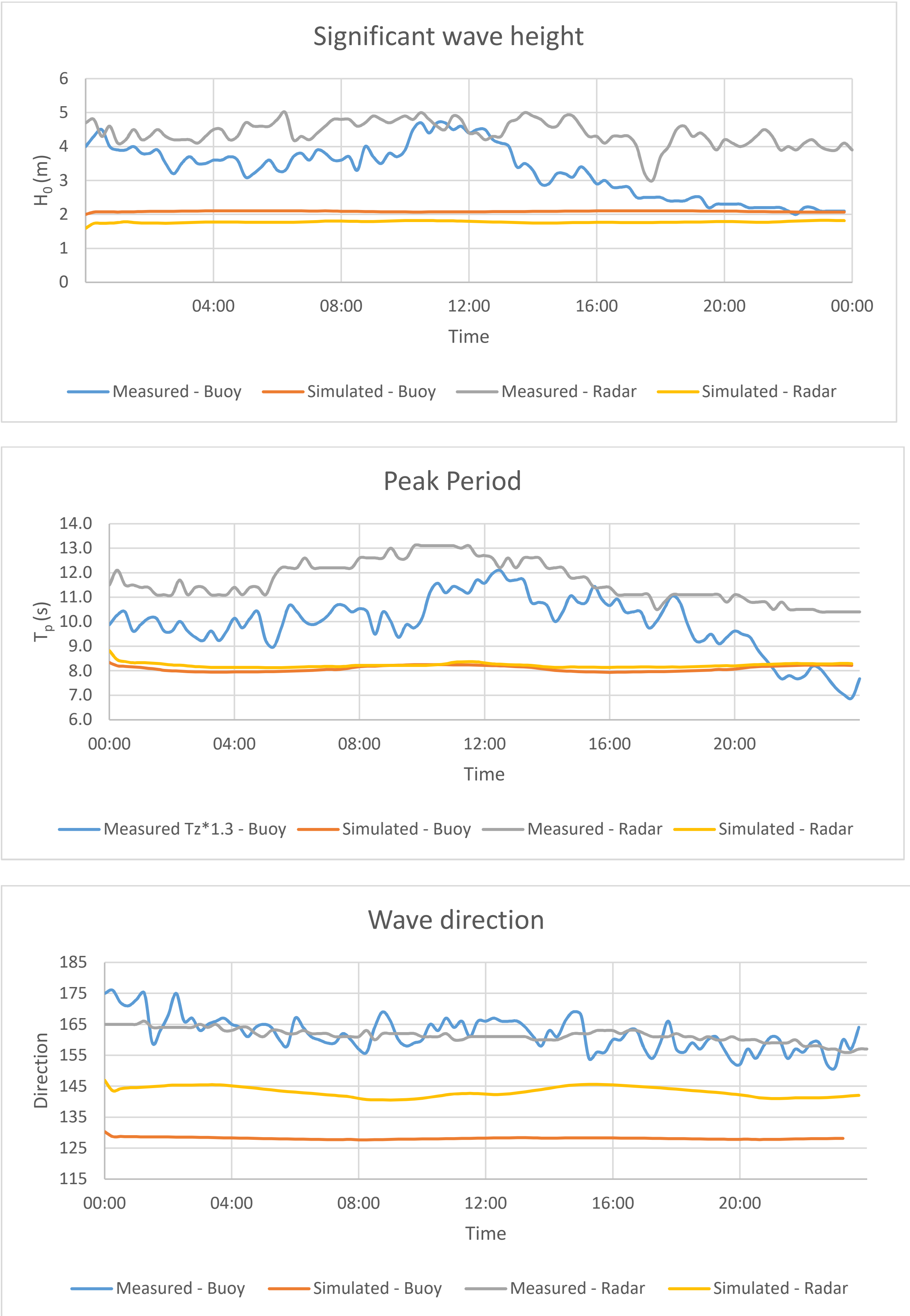

Figure 3-16 Measured and simulated wave characteristics for November 28th

3.4 **Model limitations**

A model's output is never better than its inputs so the lack of reliable input wave data for south-easterly wave directions is a concern. It is, however, a problem outside the scope of this study that should be investigated further.

The bathymetry is another factor that limits the accuracy of the model. The bathymetry in a high energy environment with a sandy bottom is changing continuously. An attempt was made to minimize the error due to this by first selecting an event to simulate and building the model based on a bathymetric survey taken 2 days before that event. It wasn't until later in the process that the lack of reliable input wave data for that storm was realized. The other storm simulated, which had realistic looking wave data, happened a month later. The results from that simulation were very good, suggesting that the changes to the bathymetry over that month were not significant. This particular location has the advantage that the bathymetric surveys are carried out frequently (46 surveys in 2018) in connection with dredging operations. Each survey covers a limited area but most frequently the opening of the harbour and the opening in the breaker bar are included. For future use it would be possible to update the model bathymetry according to the most recent survey.

The shoreline presents a similar problem as the bathymetry. The model shoreline is based on an aerial photo and set to an elevation which is estimated from the size of the visible part of the breakwaters. As the bathymetry changes, the shoreline moves and this movement is not included in the IRCA's frequent surveys as the area that can be covered is limited by the boat's draft. The bathymetry of the nearshore area in the model is created by interpolating between this arbitrarily set shoreline and the nearest points covered by the survey so there is some uncertainty in that area. The shoreline also changes with the tides and this is not represented by the model. The exact location of the shoreline is probably not important for the results extracted from the simulations in this study but could present a problem when it comes to the intended use of the model to map the sediment transport in the area.

Cross-shore sediment transport is known to be an important part of the sediment transport at Landeyjahöfn – but just how important is not known. One of the speculations as to why DHI´s investigation underestimated the sediment transport into the harbour so grossly is that cross-shore processes are a bigger part of the total sediment transport than was assumed. As explained in Chapter 1.3.1 the undertow is a sea-ward current under a land-ward surface current. A depth-averaged two-dimensional model cannot represent this phenomenon adequately. Moreover, SISYPHE, the sediment transport and bed evolution module of the TELEMAC-MASCARET suite of solvers does not consider cross-shore sediment transport. It is being worked on, but as of September 2018 the development was still in its early stages (TELEMAC-MASCARET Forum). It might be worth considering developing the model in 3D if simulations coupled with the sediment module don't give adequate results.

Lastly, every model's quality is affected by the modeller's level of skill. This is the author's first attempt at making a hydrodynamic model of a coastal region and there is surely much room for improvement. Both TELEMAC2D and TOMAWAC have many adjustable parameters that were left at their default value. Doing a sensitivity analysis of some of these parameters and comparing some different physical and numerical options would have been useful. The time frame did not allow for that as there were some time consuming technical obstacles to overcome as a first time user of the software.

4 Summary

The southern coast of Iceland is exposed to extreme wave conditions and as it is made up of sand and lacks fjords or other landforms that provide shelter, does not offer any natural harbours. Building a harbour to service the Westman Islands closer to the islands than the already existing harbour in Þorlákshöfn, was recognized as a challenging task from the beginning. Extensive research was conducted prior to building the harbour and many of the findings of that research, which led to choosing the harbour's exact location, have been confirmed. However, the amount of sediment transport into the harbour was vastly underestimated based on the data available pre-construction. Consequently, the difficulties related to maintaining a safe navigational depth in and in front of the entrance have led to the harbour being non-operational for 2 to 5 months every year, mostly in the winter time. This severely limits the transportation between the mainland and the Westman Islands, reduces frequency and adds time to the journey. As well as limiting the islanders' possibilities for reaching the mainland, this heavily impacts tourism, a growing industry in recent years, in winter.

The Icelandic Road and Coastal Administration (IRCA), the government body responsible for the operation of the harbour, has undertaken extensive data collection of varying wave, weather and bottom bathymetry conditions. Yet, the hydrodynamics driving sediment transport processes are complex and not fully understood. There is a dire local need for an open source hydrodynamic model that can be updated with regularly monitored data, and used to improve day-to-day dredging operations and for future structural improvements of the harbour. In this thesis, the first step was undertaken to develop a local 2D computational model. The open source TELEMAC-MASCARET modelling system was chosen as it had successfully simulated currents in another harbour on the Southern Shore of Iceland undergoing similar wave climate. The model´s offshore bathymetry was based on a large collection of bathymetric surveys from the hydrographic department of the Icelandic Coast Guard and the nearshore bathymetry on a survey done by the IRCA two days before the first simulated storm. The wave input on the open sea boundary was obtained from a MIKE SW regional wave model which uses data from the European Centre for Medium-Range Weather Forecasts (ECMRWF) as boundary conditions.

The simulated storms were chosen based on data from the Landeyjahöfn wave buoy. The model was calibrated for a storm with wave height over 3 m from the prevalent southwest direction. A good agreement was found between simulated and measured values of wave height and currents from a wave buoy and from a radar with high resolution current analysis software.

The calibrated model was then used to simulate a storm of similar strength but from the less prevalent southeast direction. The simulation captured the measured spatial variability of the currents near the harbour entrance. Moreover, the simulation identified a strong current right next to the western breakwater which is not captured by the radar. The IRCA's bathymetric surveys have shown occasional unexplained flushing from this location which could be explained by this current that there was no record of previously. This gives hope that the model may prove useful in better understanding the sedimentation processes in the area.

The wave height at the Landeyjahöfn wave buoy and at the radar was severely underestimated in the simulated south-easterly storm. The deviance between measurements and simulation was attributed to the input offshore wave data from ECMWF. Many other south-easterly storms were investigated and the offshore wave data was found to be consistently lower than measured data. The reasons for this discrepancy are unknown, and future efforts need to find ways of overcoming this shortcoming in the data input. This research thus highlights the importance of having access to reliable input data and the complications of obtaining it in coastal modelling.

The next step to further develop the model is to validate it against another south-westerly storm as reliable input data is readily available for that direction. Better wave input data needs to be found for south-easterly storms and the model validated for those. Effects of wind must also be investigated. The decision not to include wind in the current model was based on the assumption that the effects the wind might have on the waves over the breadth of the model would be negligible. This assumption is still valid but wind-induced currents might have an effect in very shallow water. After the abovementioned steps are completed the model must be coupled with the sediment module from the TELEMAC-MASCARET suite and the results compared to pre- and post-event bathymetric surveys.

References

Ata, R. (2018). *Telemac2d User Manual. Version v7p3.* TELEMAC-MASCARET Consortium.

Awk, T. (2018). *Tomawac User Manual. Version v7p3.* TELEMAC-MASCARET Consortium.

Camenen, B. & Larson, M. (2007). *A Unified Sediment Transport Formulation for Coastal Inlet Application.* Washington, DC. USA. US Army Corps of Engineers.

COWI A/S (2007). *Bakkafjara Ferry Port. Review of IMA provided reports.* Lyngby. Denmark.

Egbert, Gary D., & Erofeeva, Svetlana Y. *Efficient inverse modeling of barotropic ocean tides.* Journal of Atmospheric and Oceanic Technology 19.2 (2002): 183-204. (https://journals.ametsoc.org/doi/full/10.1175/1520-0426%282002%29019%3C0183%3AEIMOBO%3E2.0.CO%3B2)

Elfrink, B., Brøker, I., & Viggósson, G. (2006). *Bakkafjara – Sediment Transport and Morphology. Phase 1.* Hørsholm, Denmark. DHI.

Eyþórsson, G. Þ., Karlsson, V. &Jóhannesdóttir, K. (2006). *Áhrif ferju um Bakkafjöruhöfn á samfélag og byggð í Vestmannaeyjum og á öðrum svæðum Suðurlands.*

Fredsøe, J. (1984). *Sediment transport in current and waves.* Lyngby, Denmark. Technical University of Denmark.

Guðmundsson, R. (2016). *Ferðamenn og íbúar í Vestmannaeyjum 2016 – samanburður við 2012.* Hafnarfjörður. Rannsóknir og ráðgjöf ferðaþjónustunnar ehf.

Grétarsson, S., Viggósson, G., Sigurðarson, S. Ómarsson, B & Sveinbjörnsson, P. (2017). *Landeyjahöfn – Verkfræðilegt afrek eða mistök.* [PowerPoint slides]. Retrieved from https://www.vfi.is/media/frettir/Landeyjahofn-verkfraedilegt-afrek-eda-mistok_net.pdf

Grunnet, N. & Kristensen, S. (2013). *Landeyjahofn – Further investigations.* Hørsholm, Denmark. DHI.

IMA-memo (2007). *Líkantilraunir af ferjuhöfn við Landeyjahöfn í rannsóknastöð Siglingastofnunar 2005 og 2006.* Unpublished. Retrieved from the IRCA's internal database.

IRCA-memo (2019). *Dýpkun – samantekt aflaskýrslna 2011-2018.* Unpublished. Retrieved from the IRCA's internal database.

Jensen, J. H., Viggósson, G., Elfrink, B., Brøker, I. & Grunnet, N. (2007). *Bakkafjara – Sediment Transport and Morphology. Phase 1 and Phase 2 – Final Report.* Hørsholm, Denmark. DHI.

Johnsen, T. & Tobiassen, H. (2007). *Risk Assessment of Ferry Bakkafjara – Vestmannaeyjar*. Report No. 2161-2006. Det Norse Veritas (2007). Høvik. Norway. Net Norske Veritas.

Kamphuis, J. W. (2000). *Introduction to Coastal Engineering and Management.* Singapore. World Scientific Publishing Co. Pte. Ltd.

Klante, C. (2018). *Sediment transport and bathymetric change at Hornafjörður tidal inlet – Field data analysis and mathematical modelling.* Lund, Sweden. Lund University.

Mangor, K., Drønen, N.K., Kærgaard, K.H. & Kristensen, S.E. (2017). *Shoreline Management Guidelines.* Hørsholm, Denmark. DHI.

Rijn, L. C. van. (1993). *Principles of sediment transport in rivers, estuaries and coastal seas.* Ruinen, The Netherlands: Aqua Publications.

Rijn, L. C. van. (2012). *Principles of sedimentation and erosion in rivers, estuaries and coastal seas.* The Netherlands: Aqua Publications.

Rijn, L. C. van. (2013). *Basic Hydrodynamic Processes in the Coastal Zone.* Retrieved from https://www.leovanrijn-sediment.com/index.html

Stapi jarðfræðistofa (2007). *Bakkafjöruhöfn - Grjóntmámskönnun 2006.* Reykjavík. Iceland.

US Army Corps of Engineers (2002). *Coastal Engineering Manual – Part III.* Retrieved from https://www.publications.usace.army.mil/USACE-Publications/Engineer-Manuals/

Viggósson, G. (2006). *Ferjuhöfn við Bakkafjöru. Áfangaskýrsla um rannsóknir og tillögur.* Siglingastofnun.

Vigfússon, K. (2003). *Lokaskýrsla starfshóps um samgöngur til Vesmannaeyja.* Reykjavík. Samgönguráðuneytið. Retrieved from http://www.vegagerdin.is/vefur2.nsf/ 15.03.2019

VSÓ Ráðgjöf (2008). *Bakkafjöruhöfn, bakkafjöruvegur og grjótnám á seljalandsheiði. Matsskýrsla.* Reykjavík. Iceland.

Appendix A

Simulation results for southwestern storm

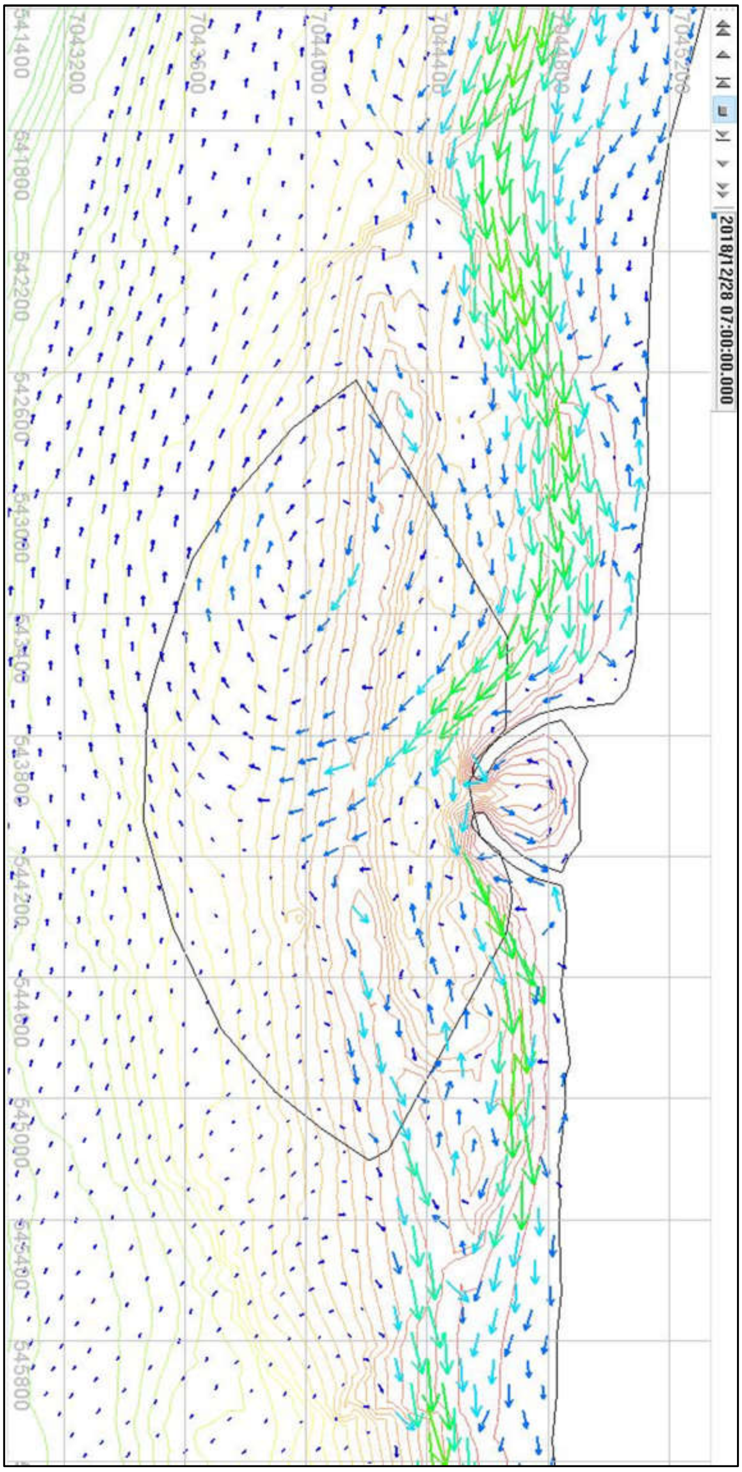

Figure A-1 Simulated current velocities at 07:00 on December 28th 2018. Flood.

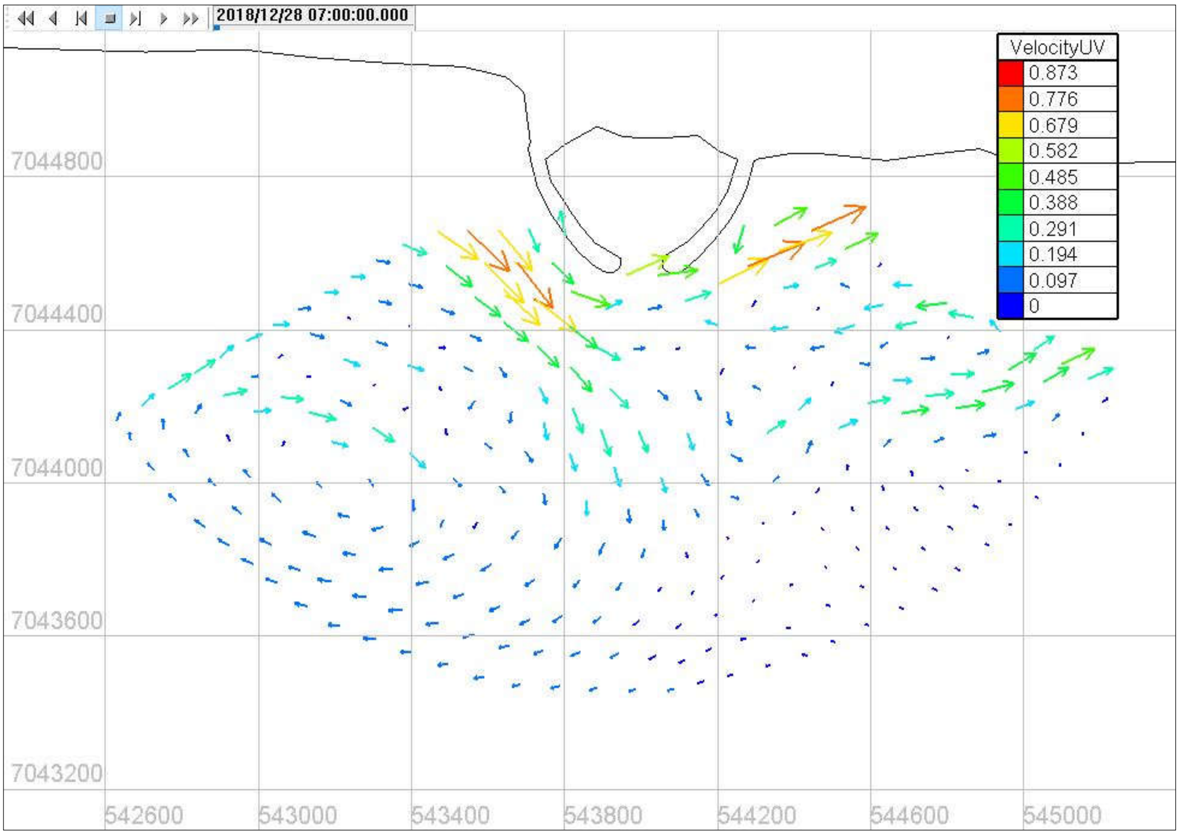

Figure A-2 Simulated current velocities at 07:00 on December 28th 2018. Flood.

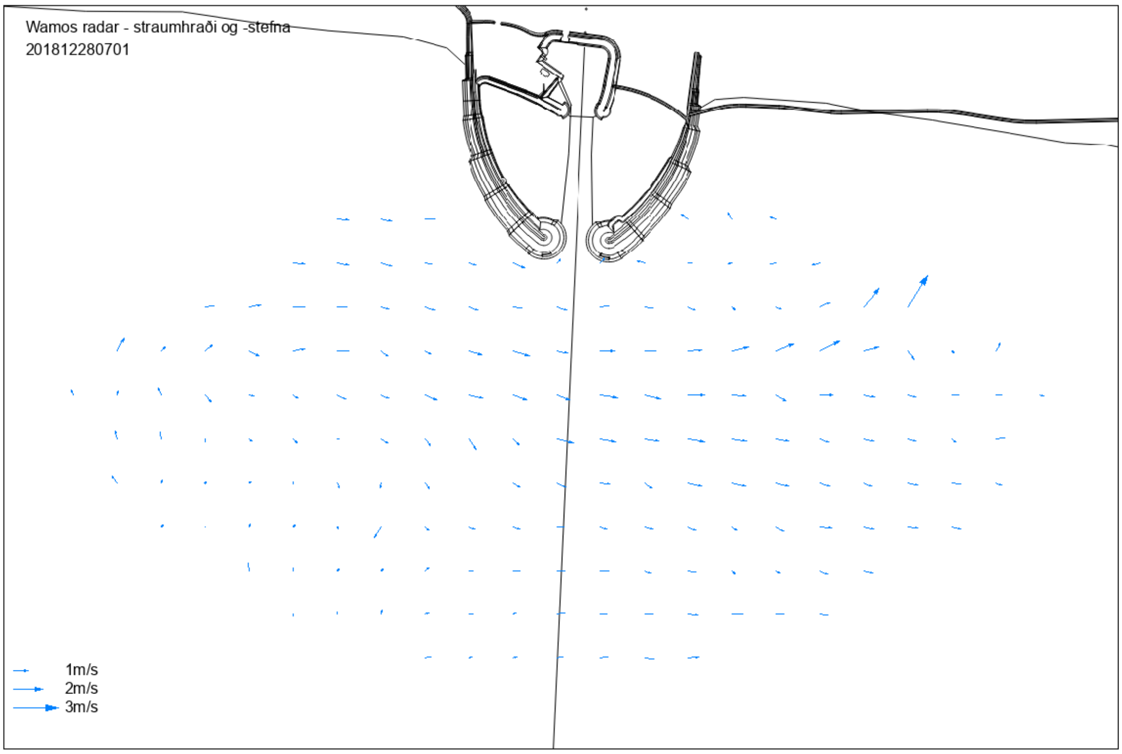

Figure A-3 Measured current velocities at 07:00 on Decemberr 28th 2018. Flood.

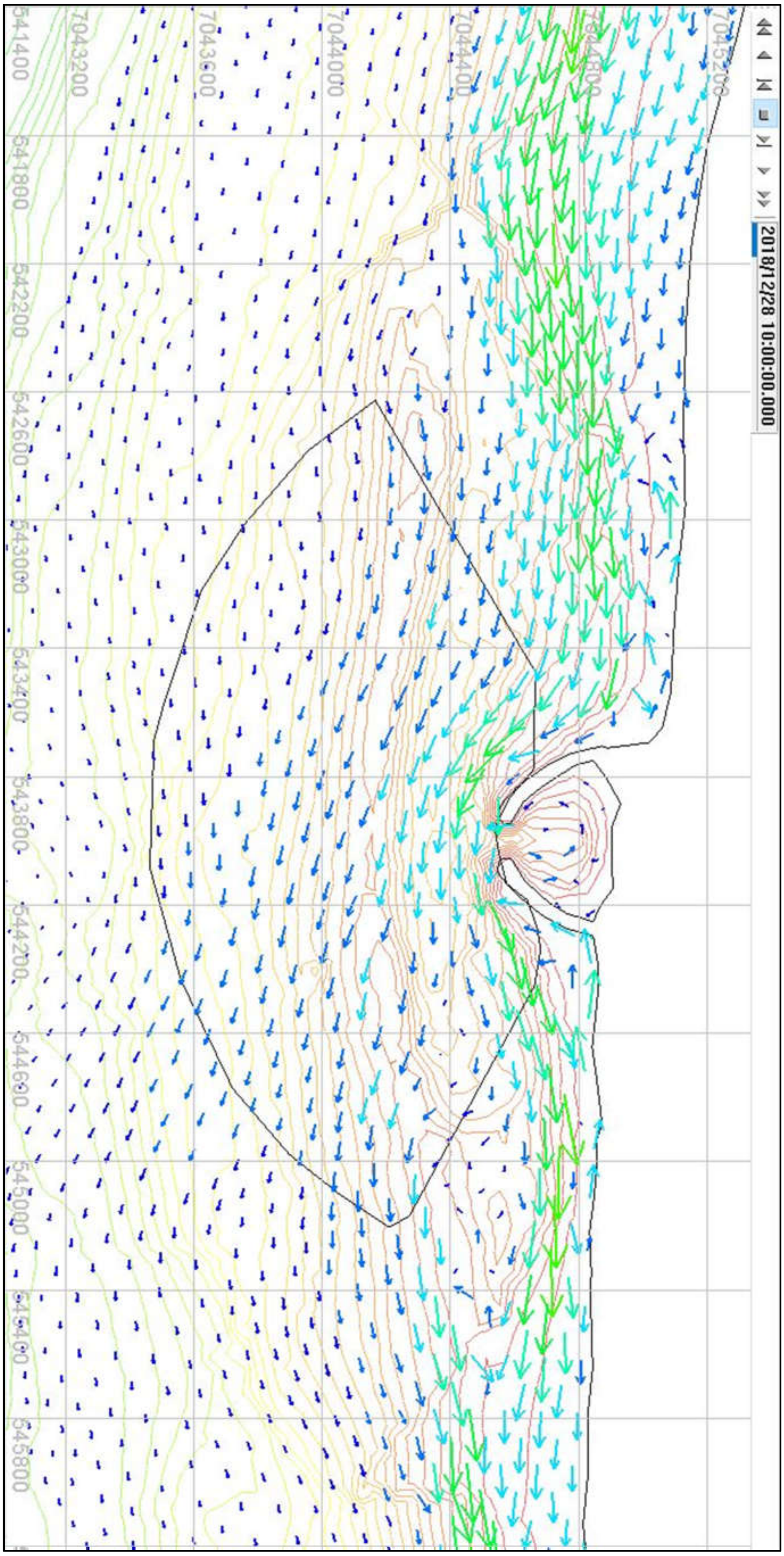

Figure A-4 Simulated current velocities at 10:00 on December 28th 2018. High tide.

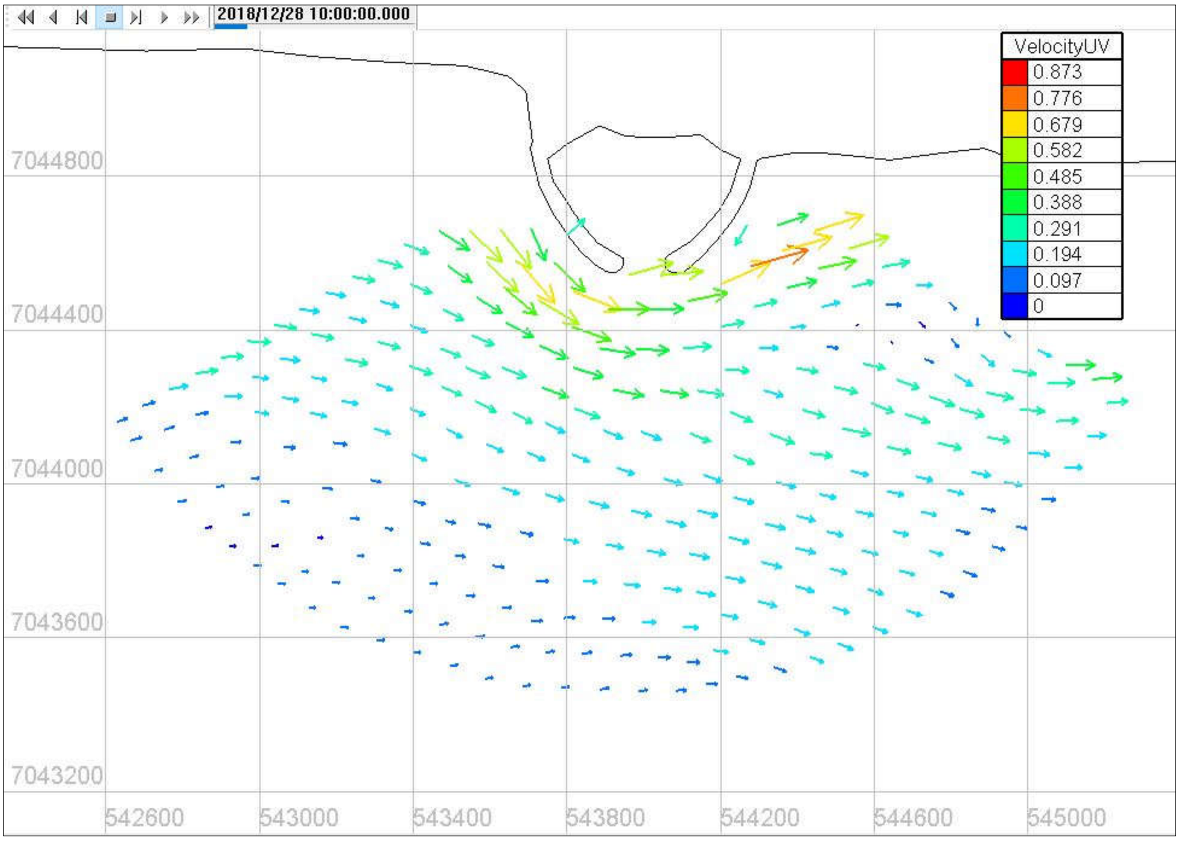

Figure A-5 Simulated current velocities at 10:00 on Decemberr 28th 2018. High tide

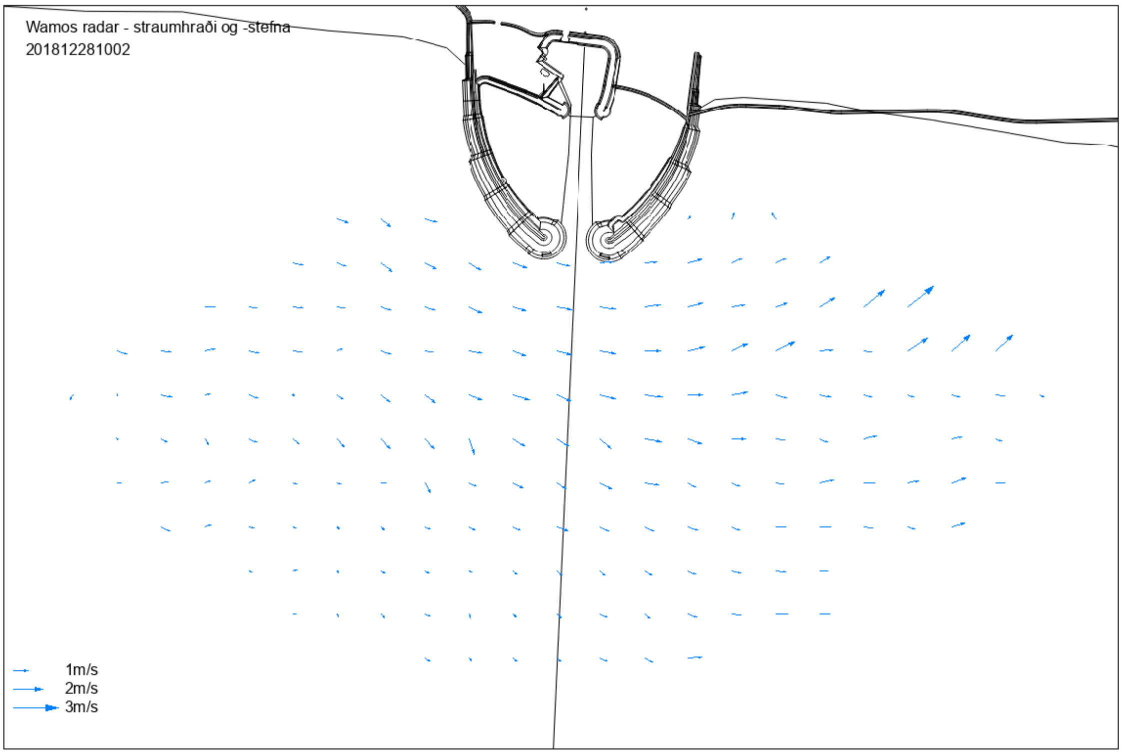

Figure A-6 Measured current velocities at 10:00 on December 28th 2018. High tide

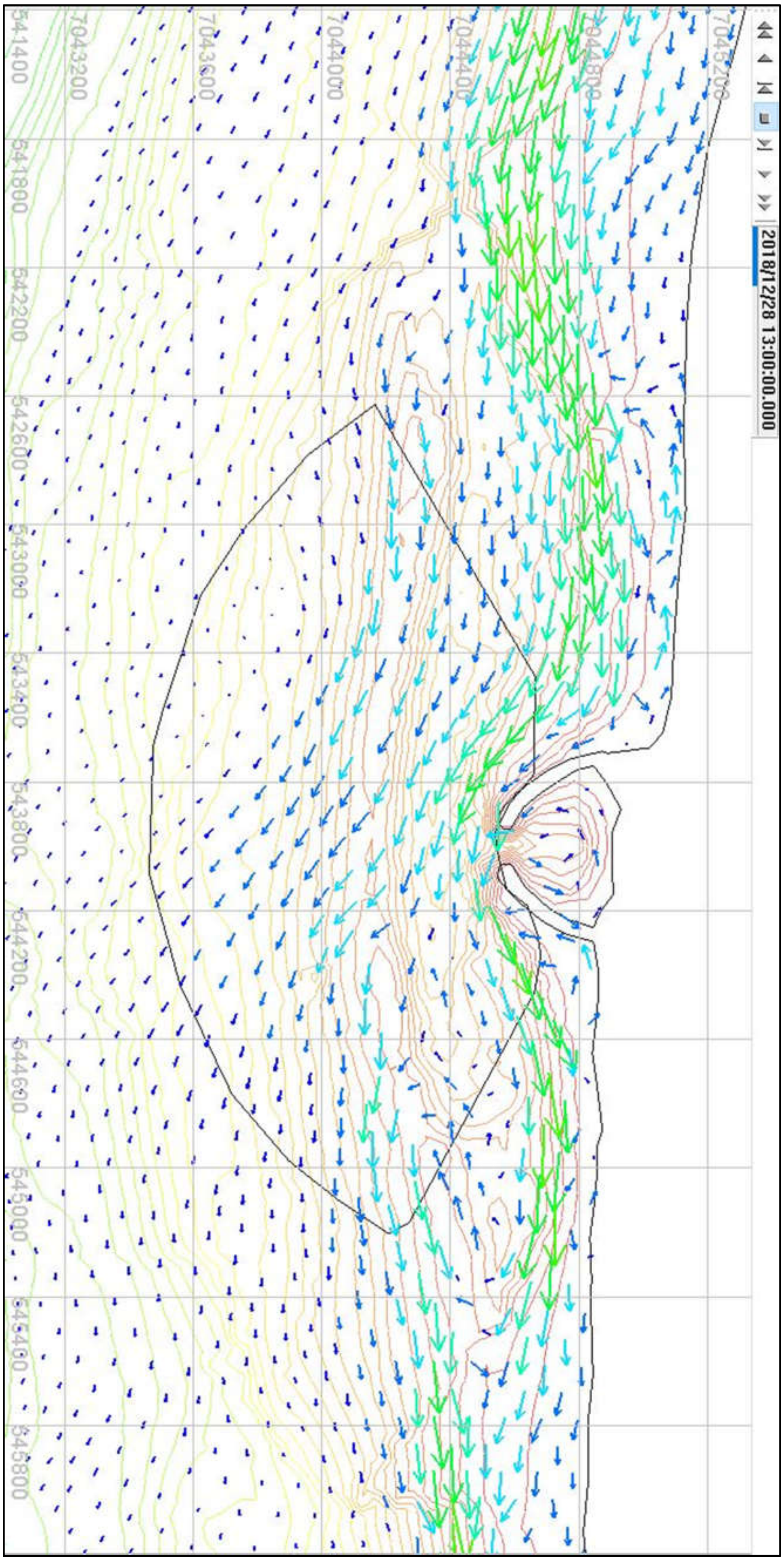

Figure A-7 Simulated current velocities at 13:00 on December 28th 2018. Ebb.

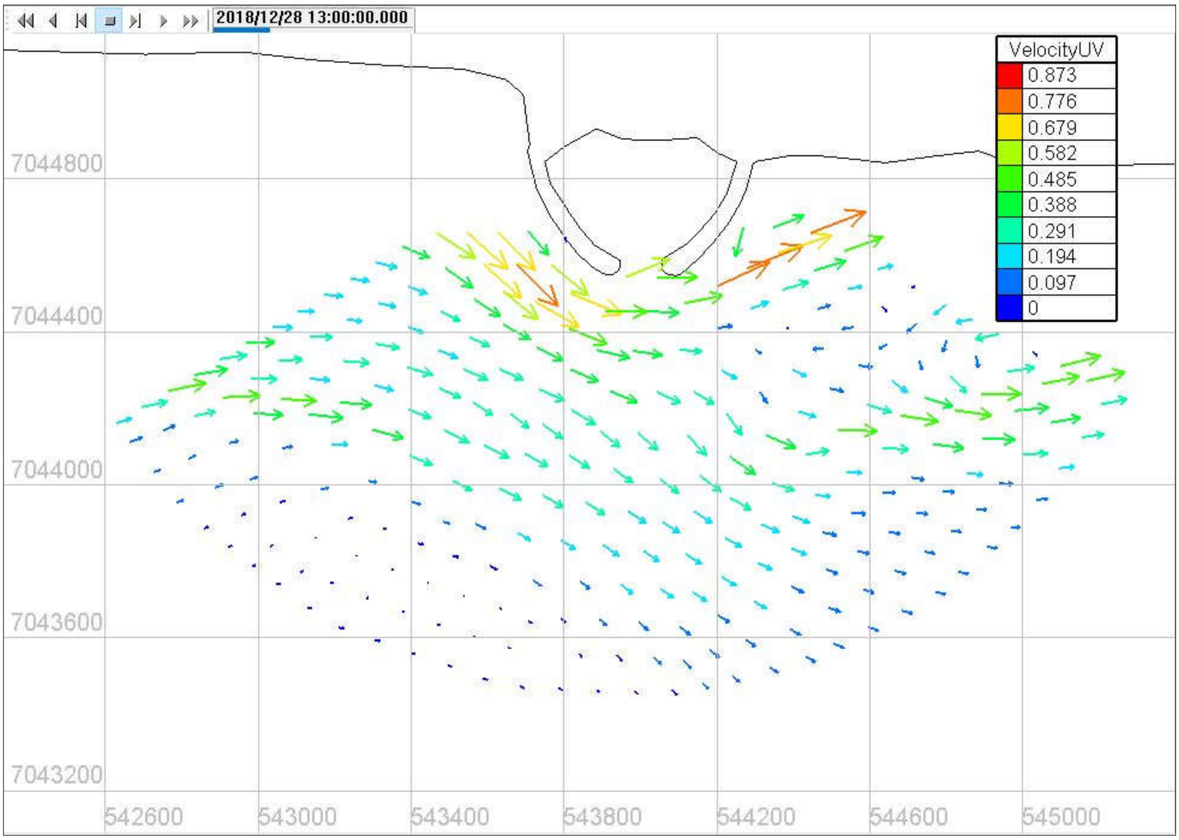

Figure A-8 Simulated current velocities at 13:00 on December 28th 2018. Ebb.

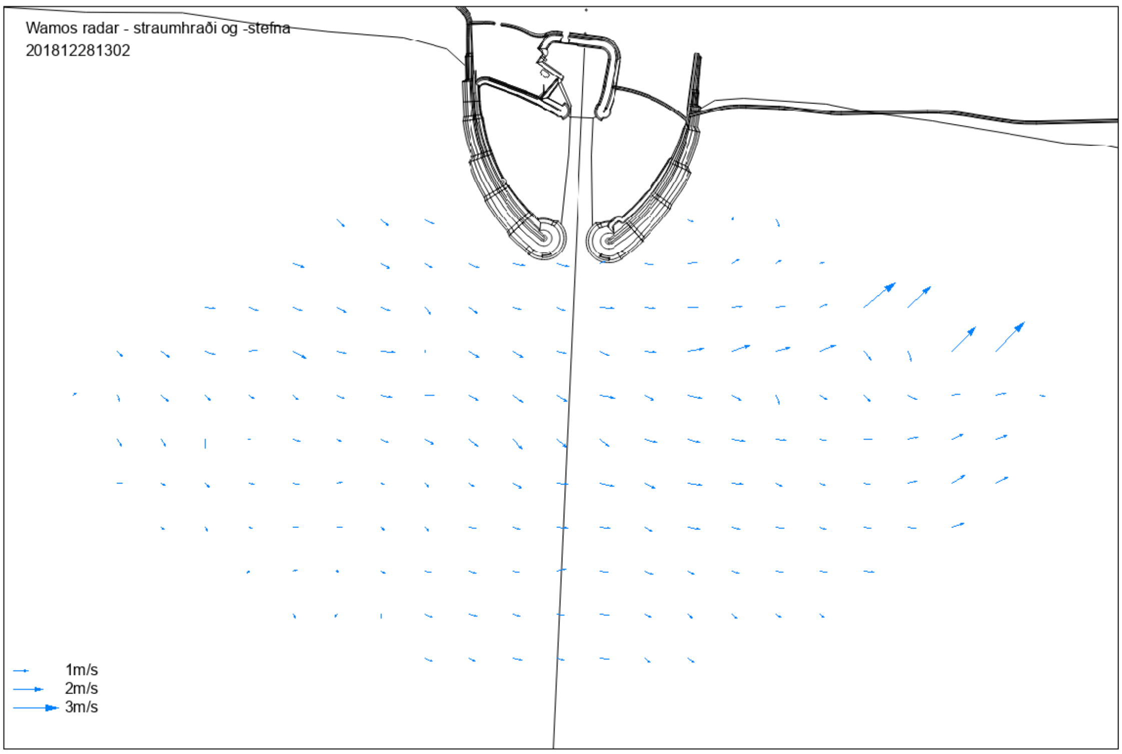

Figure A-9 Measured current velocities at 13:00 on December 28th 2018. Ebb.

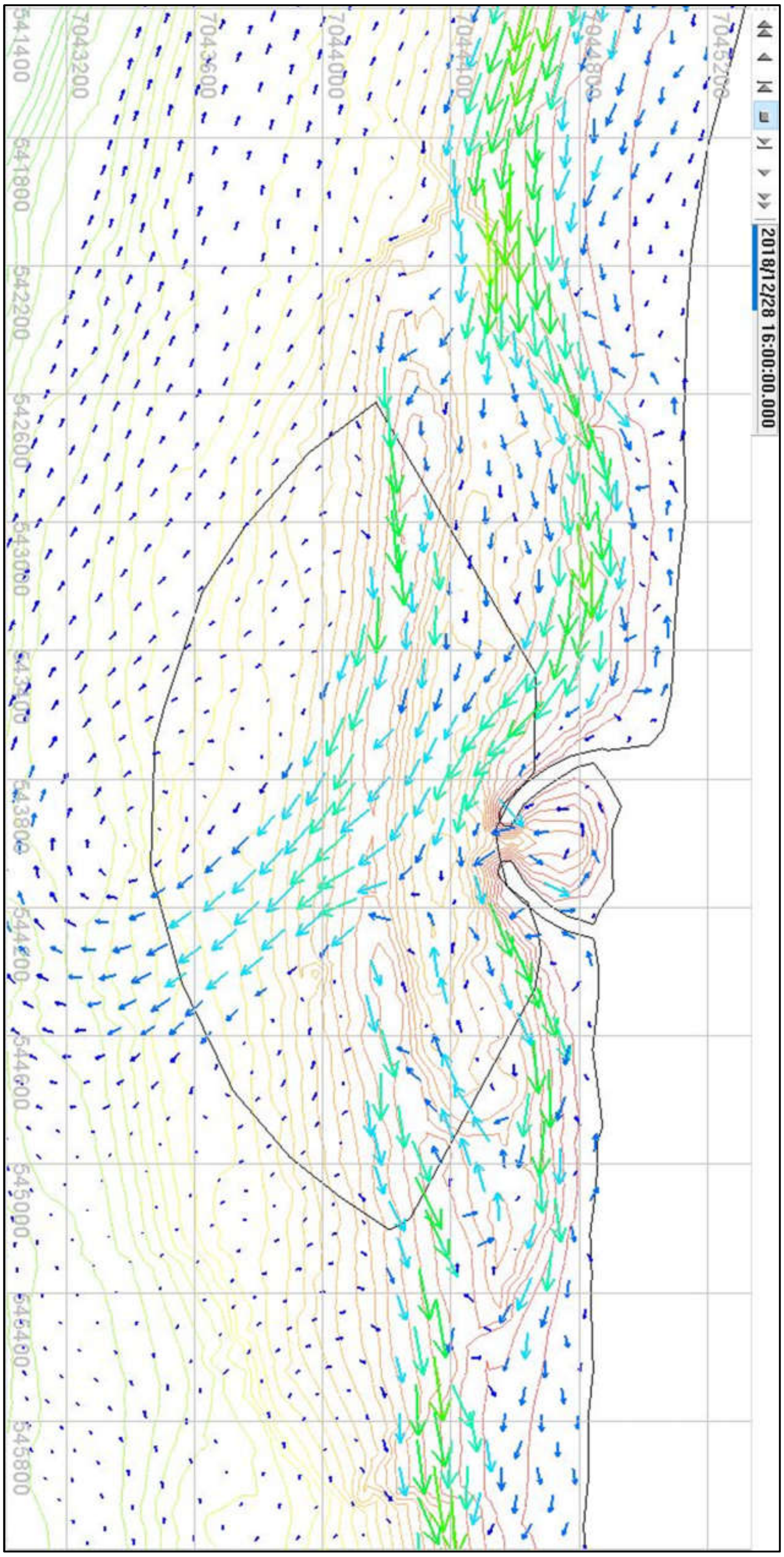

Figure A-10 Simulated current velocities at 16:00 on December 28th 2018. Low tide.

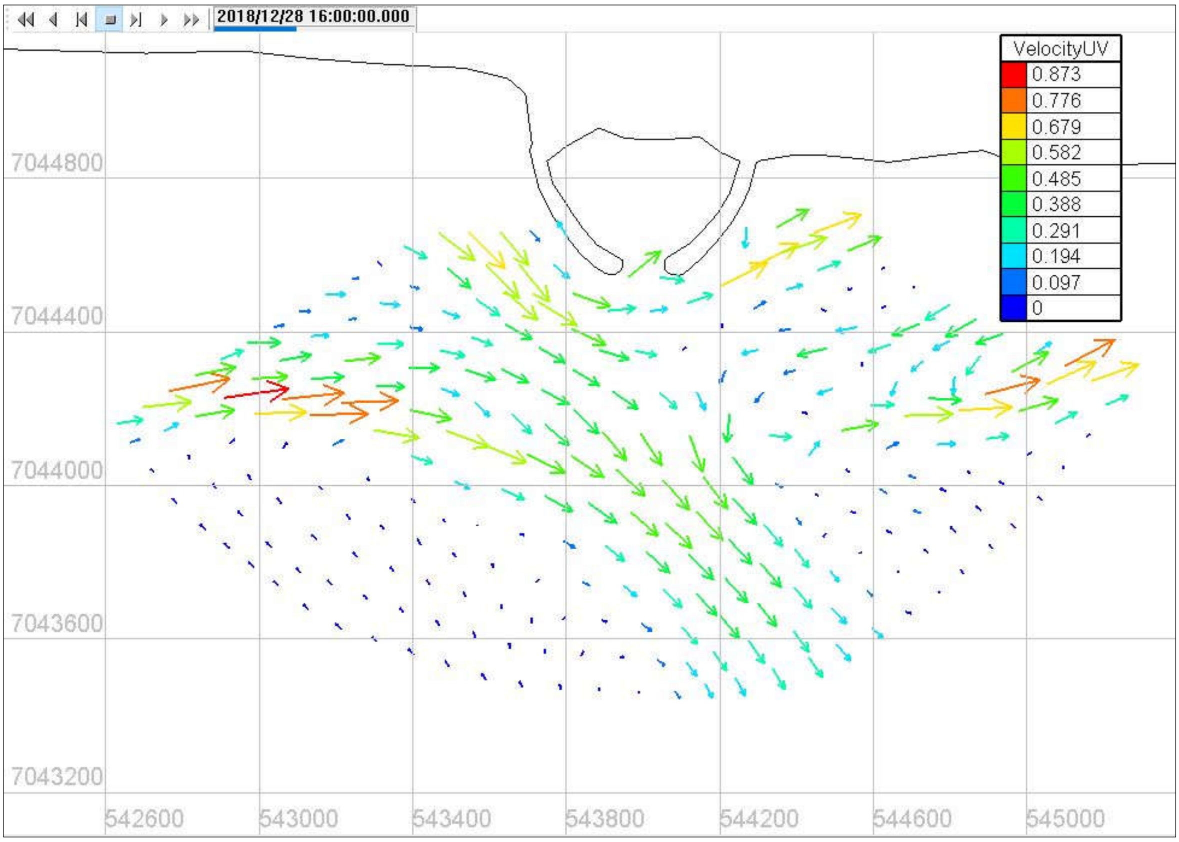

Figure A-11 Simulated current velocities at 16:00 on December 28th 2018. Low tide.

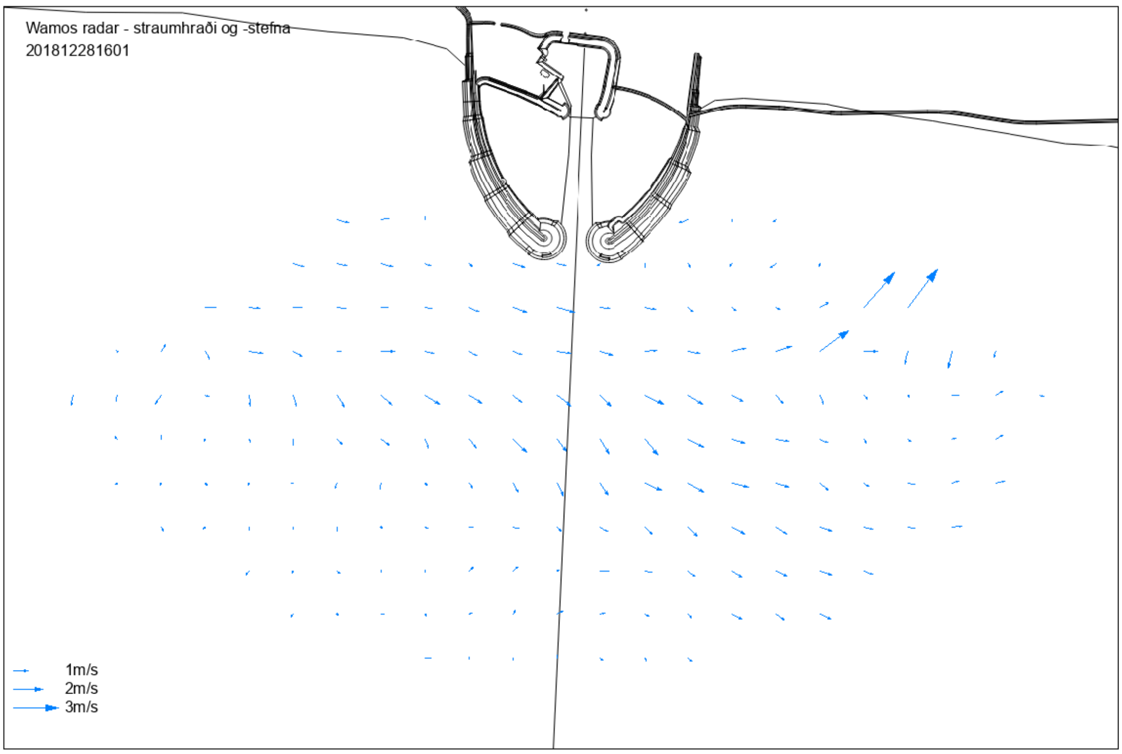

Figure A-12 Measured current velocities at 16:00 on December 28th 2018. Low tide.

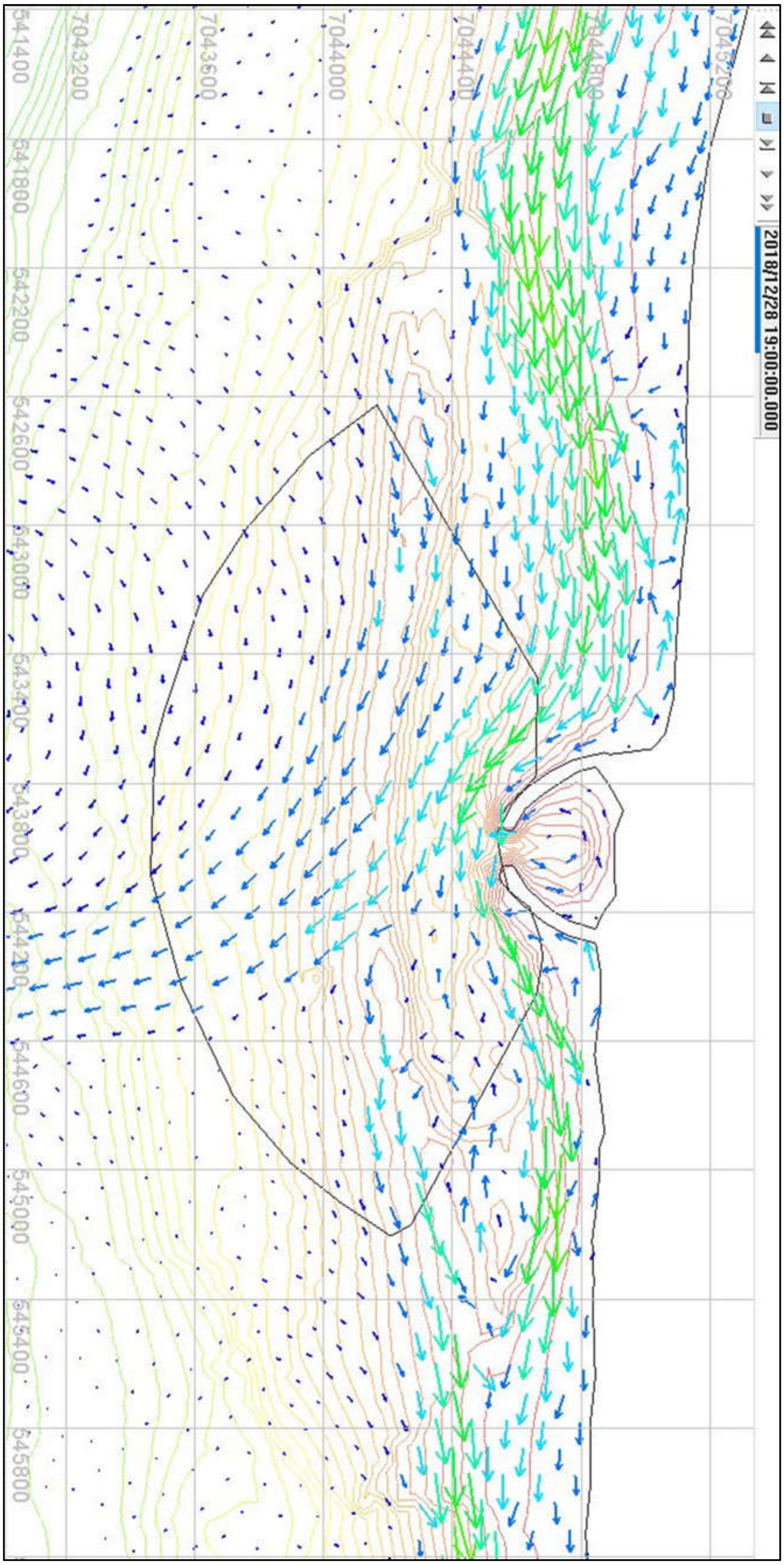

Figure A-13 Simulated current velocities at 19:00 on December 28th 2018. Flood.

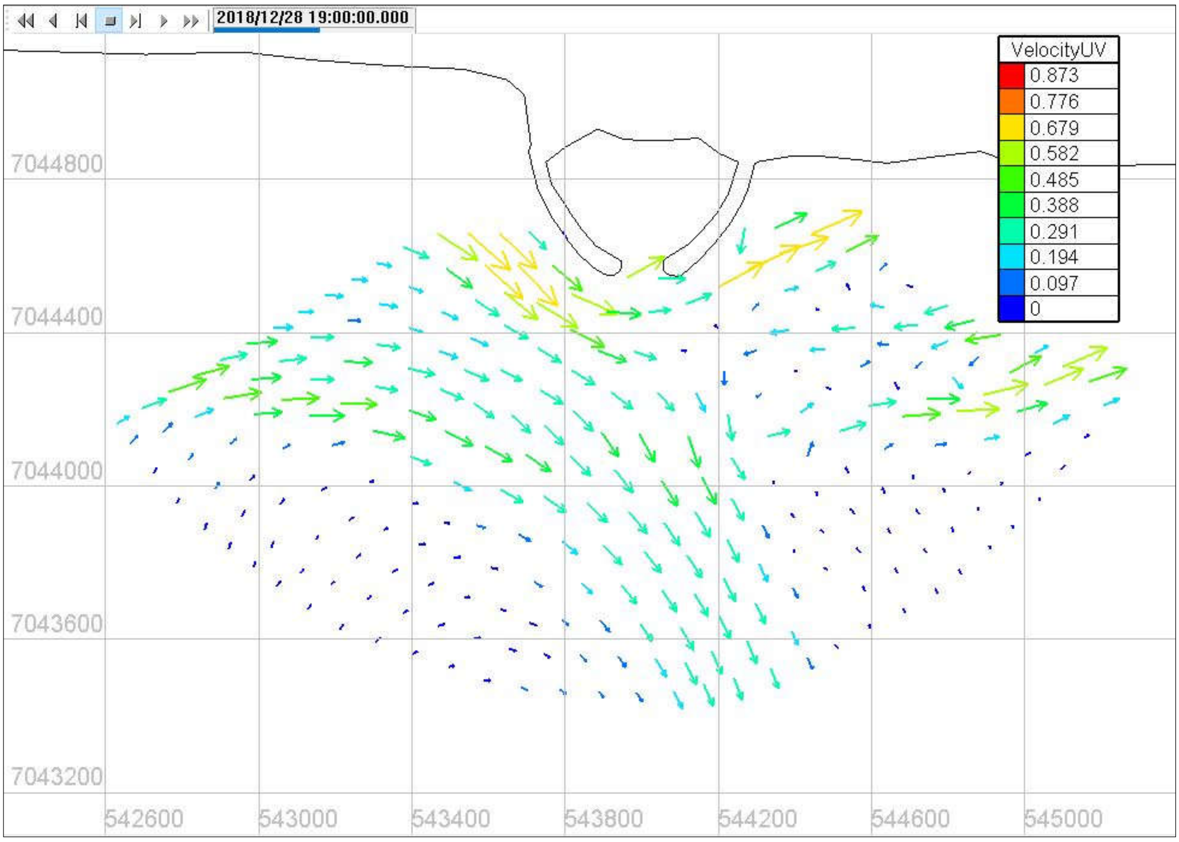

Figure A-14 Simulated current velocities at 19:00 on December 28th 2018. Flood.

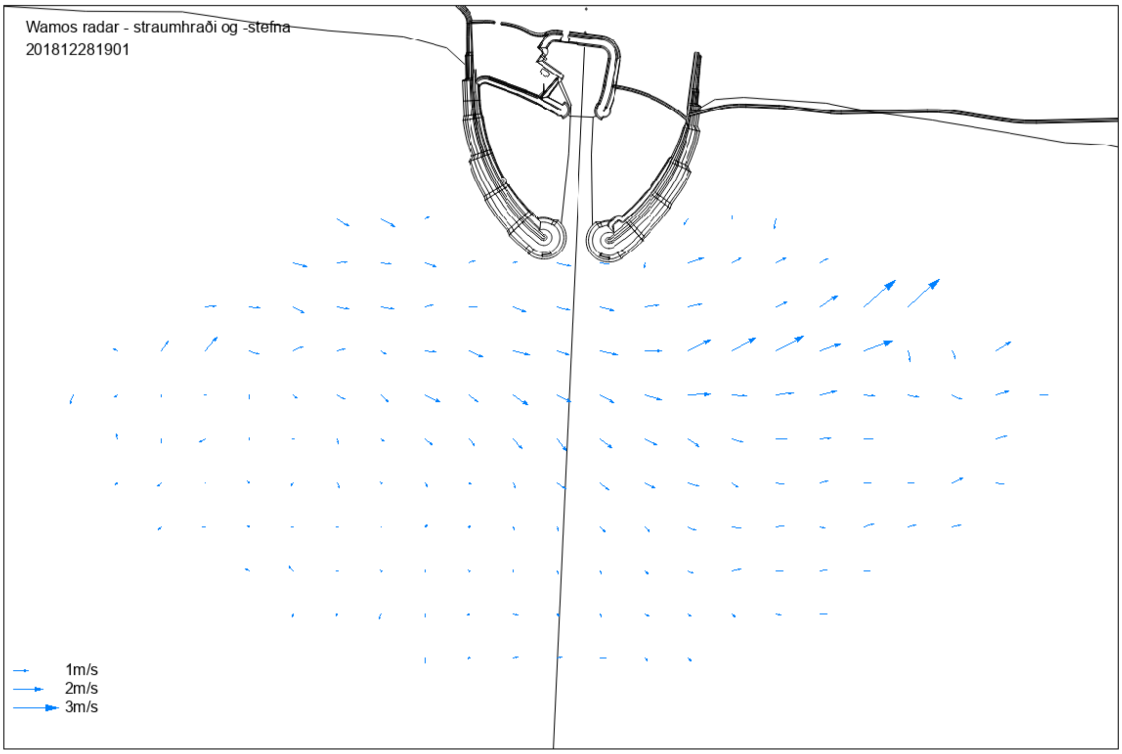

Figure A-15 Measured current velocities at 19:00 on December 28th 2018. Flood.

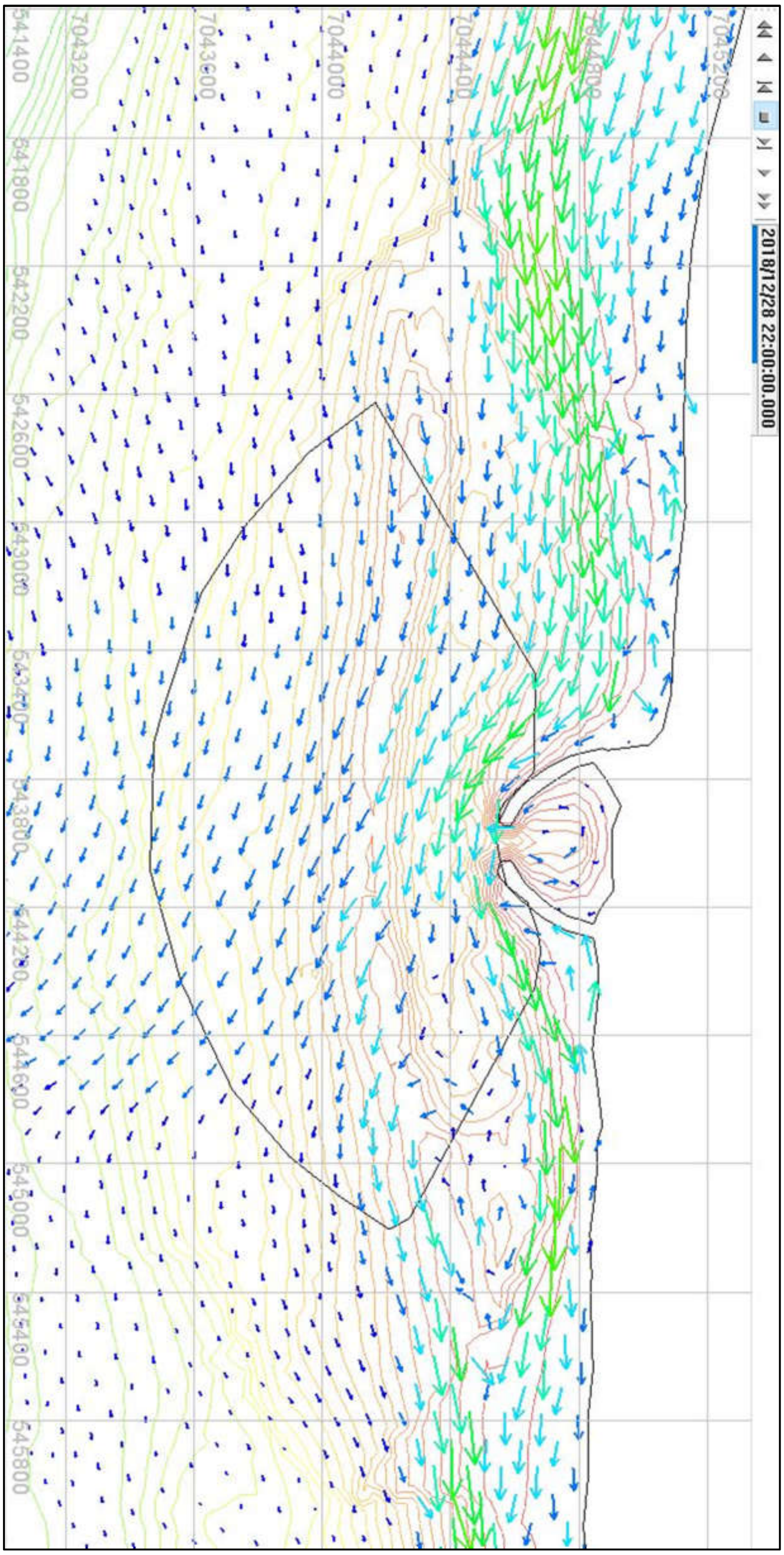

Figure A-16 Simulated current velocities at 22:00 on December 28th 2018. High tide.

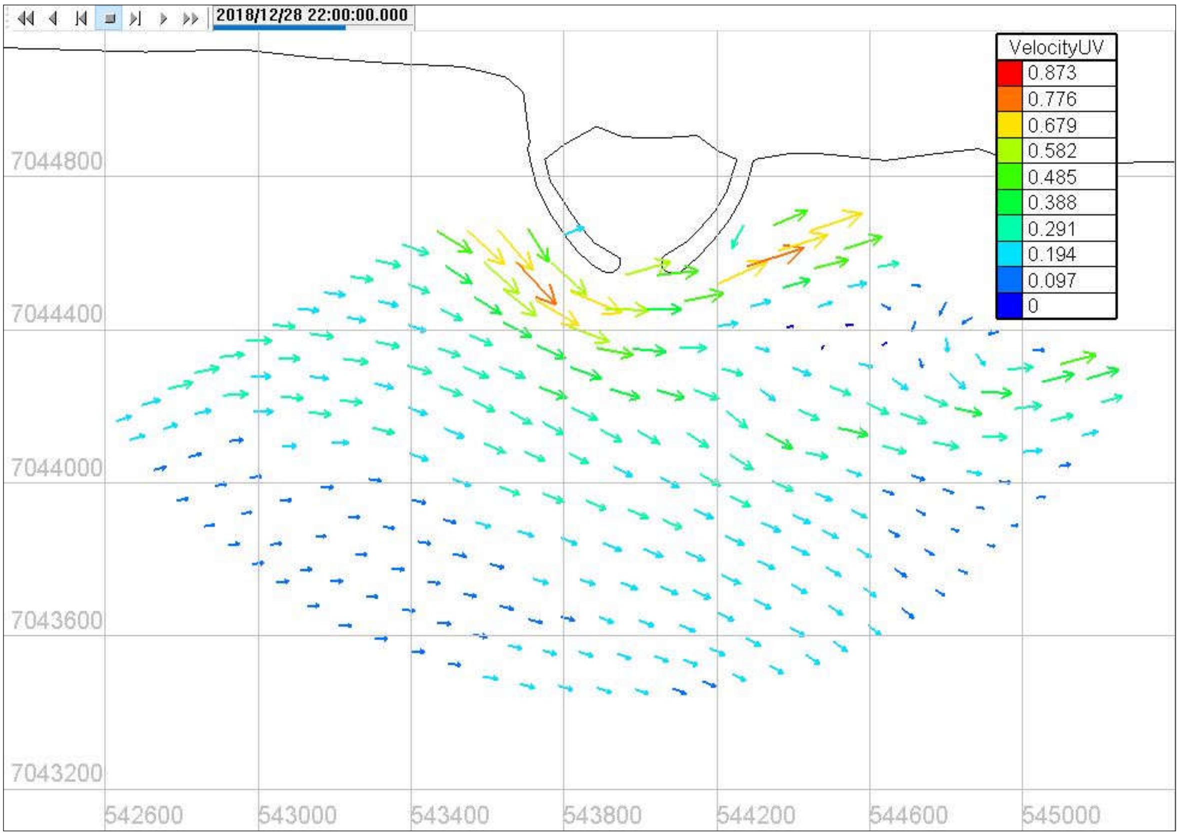

Figure A-17 Simulated current velocities at 22:00 on December 28th 2018. High tide

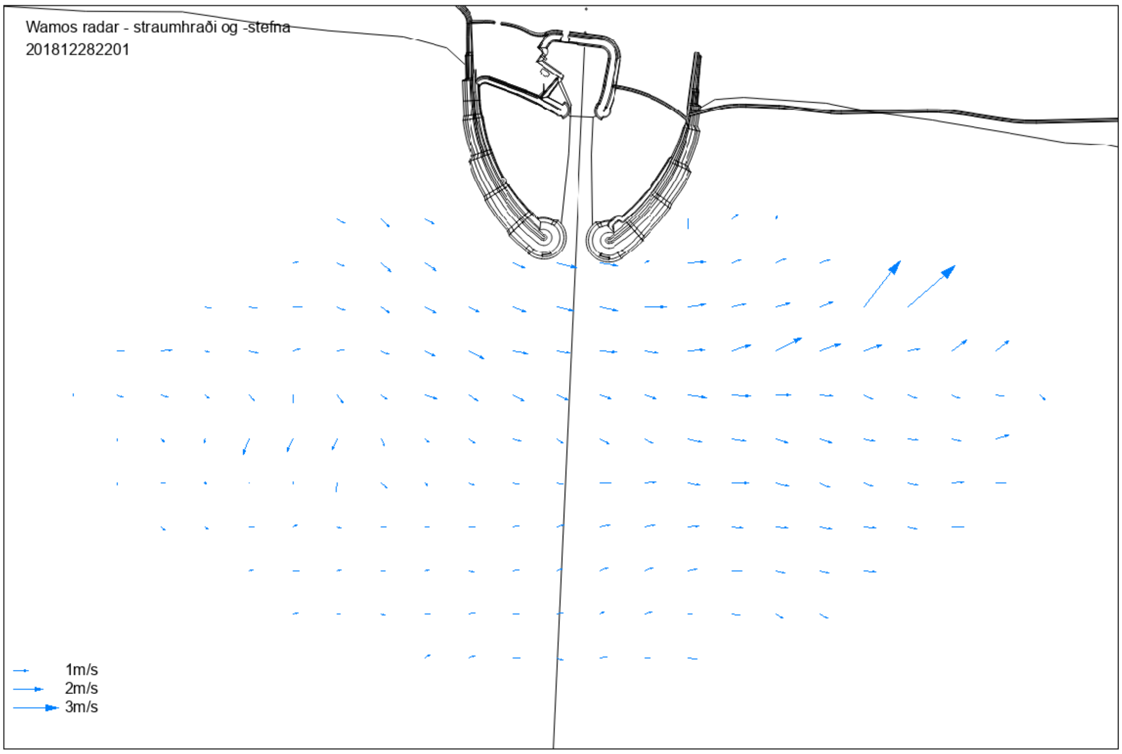

Figure A-18 Measured current velocities at 22:00 on December 28th 2018. High tide.

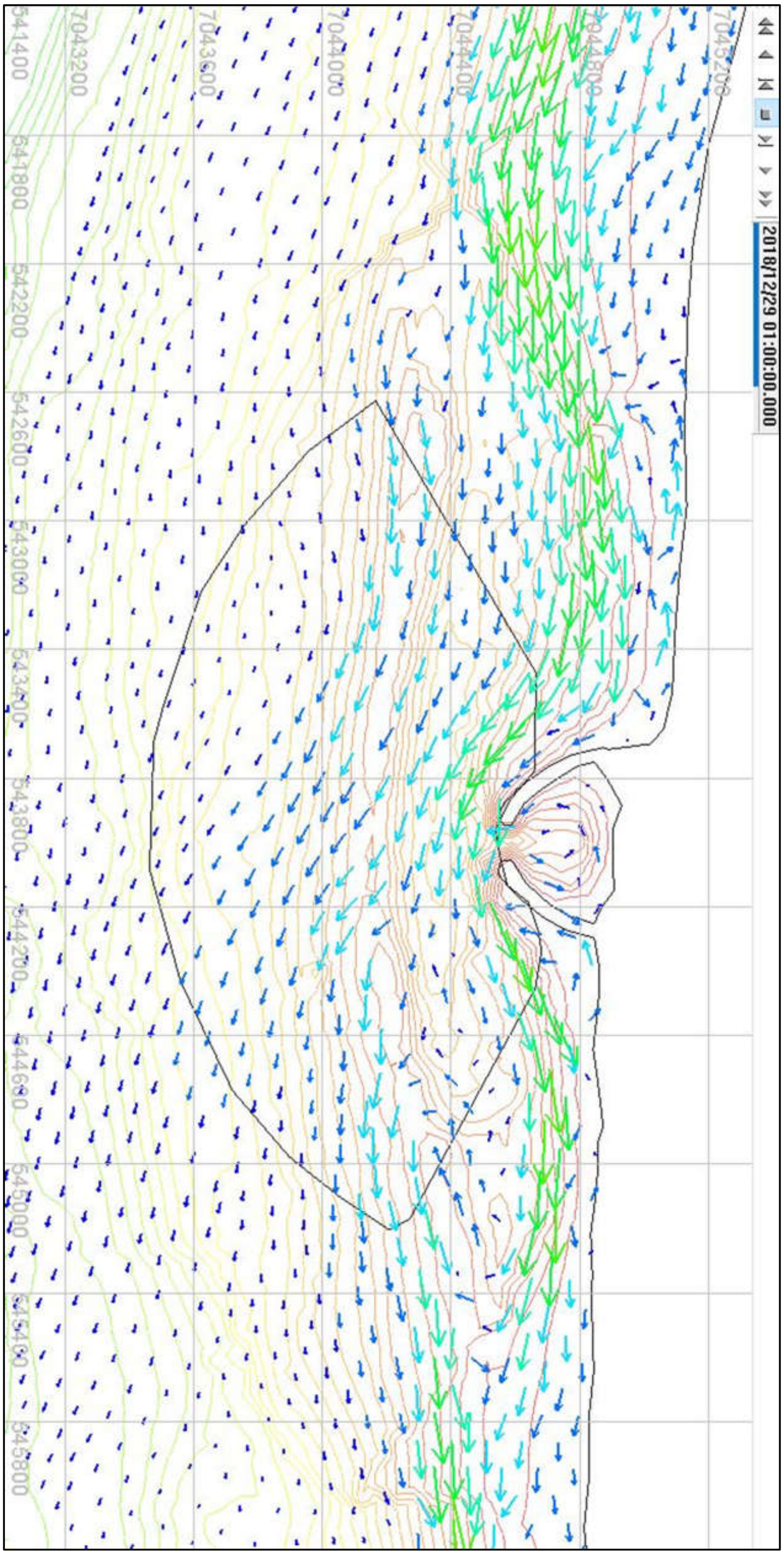

Figure A-19 Simulated current velocities at 01:00 on December 29th 2018. Ebb.

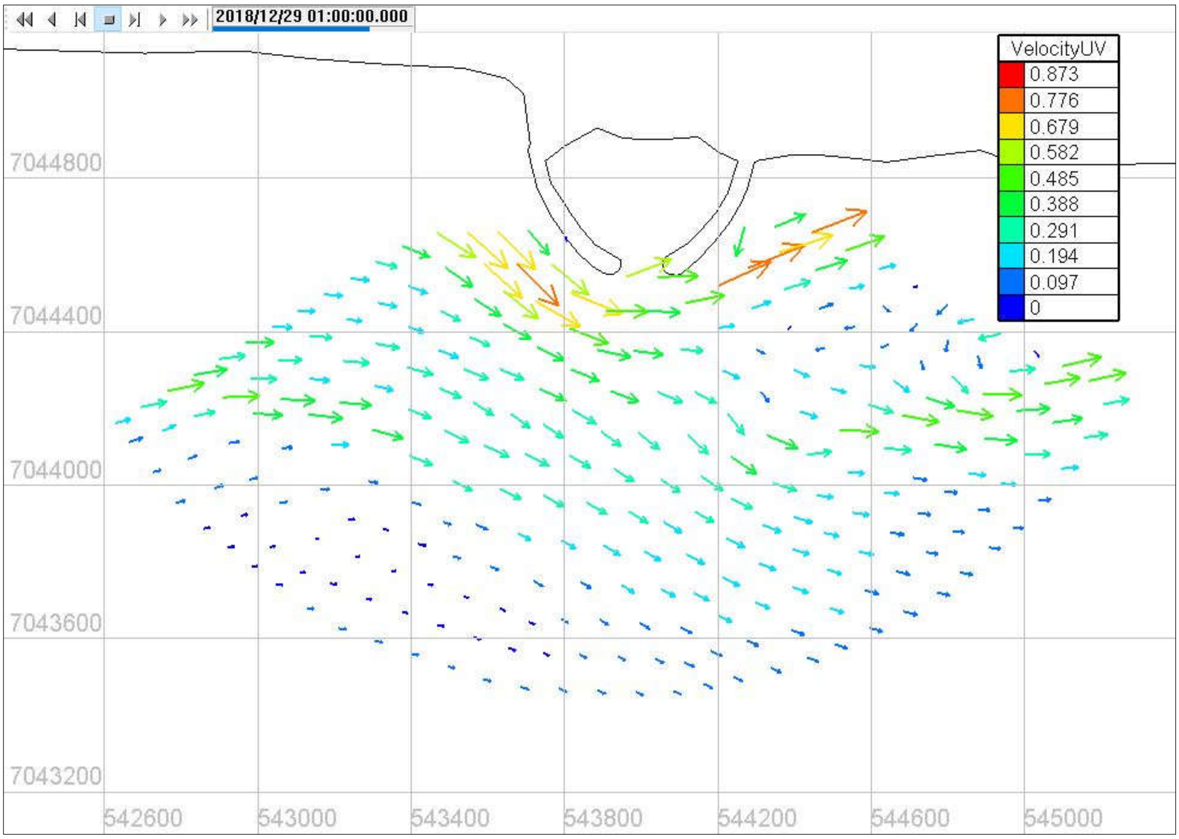

Figure A-20 Simulated current velocities at 01:00 on December 29th 2018. Ebb.

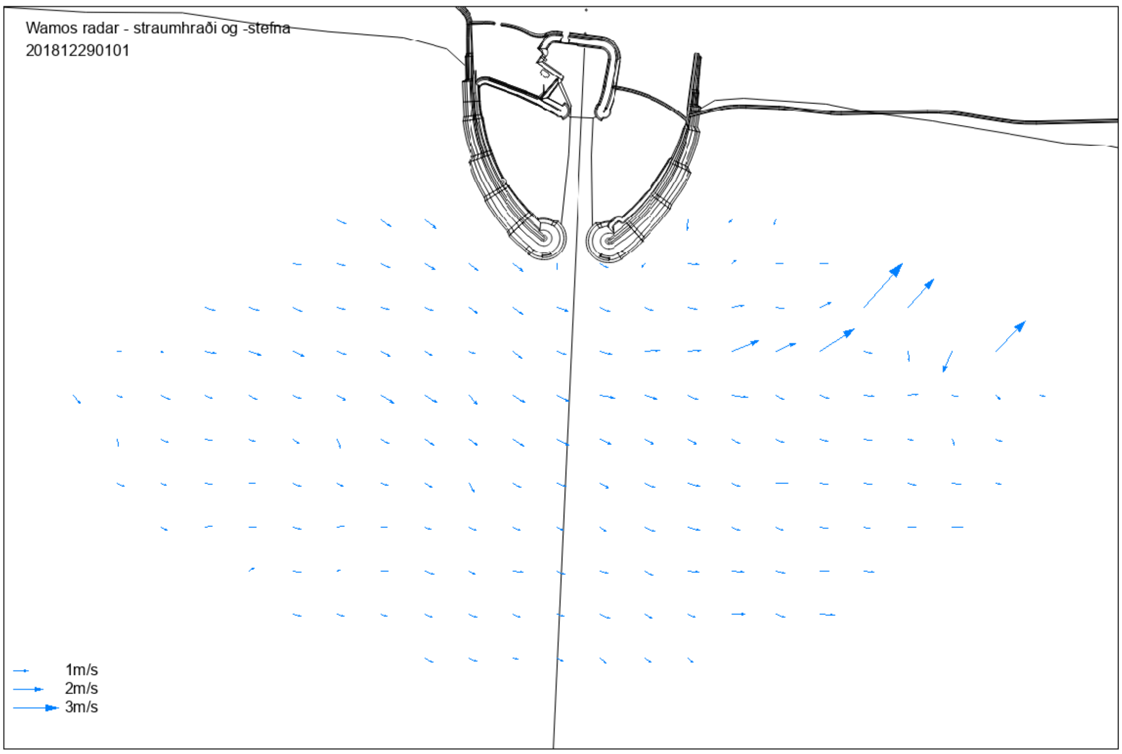

Figure A-21 Measured current velocities at 01:00 on December 29th 2018. Ebb.

Appendix B

Simulation results for south-eastern storm

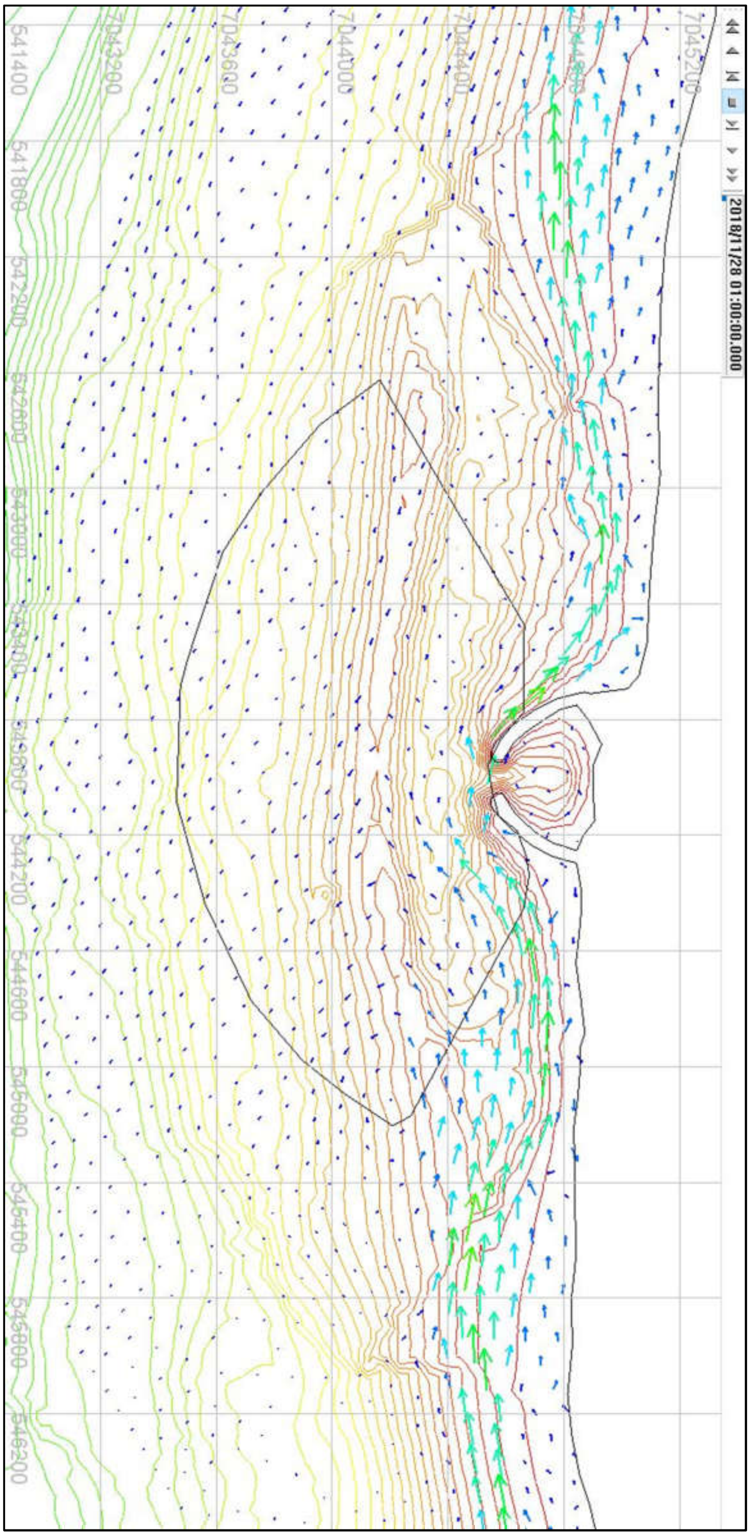

Figure B-1 Simulated current velocities at 01:00 November 28 2018. Ebb.

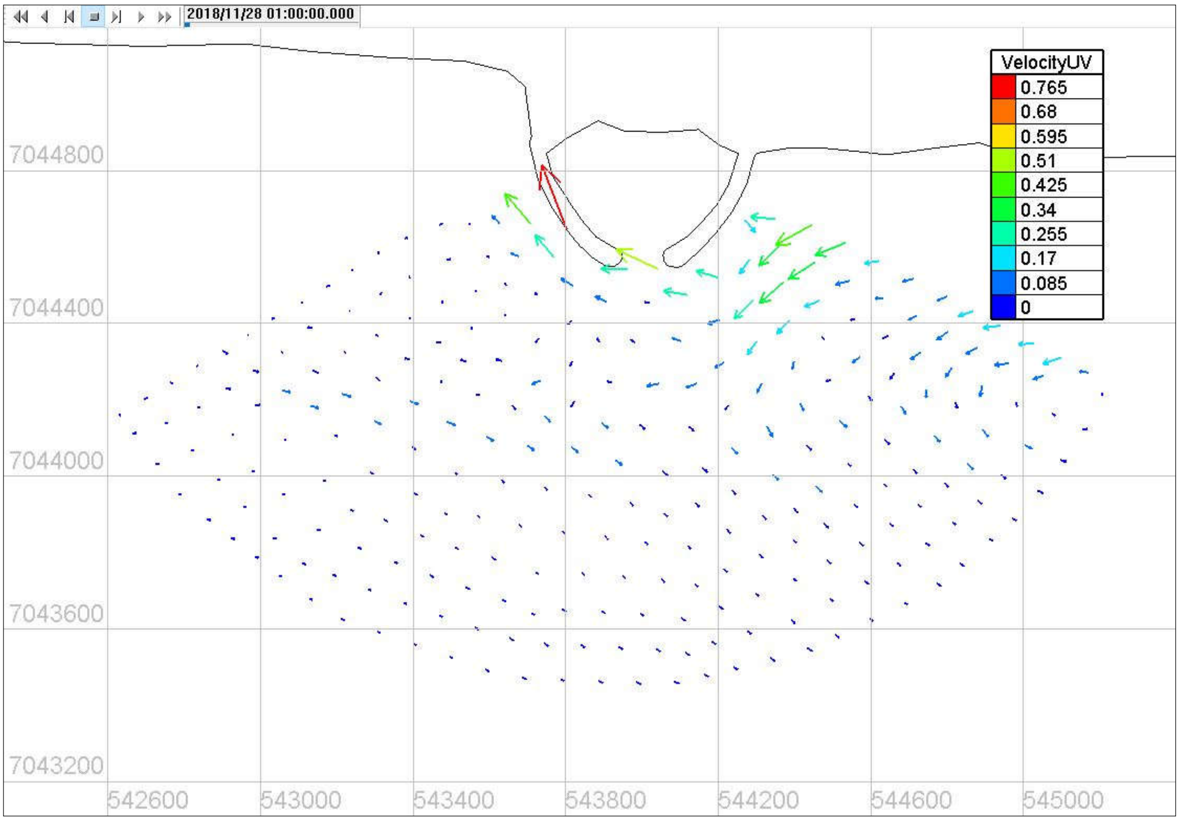

Figure B-2 Simulated current velocities at 01:00 November 28 2018. Ebb.

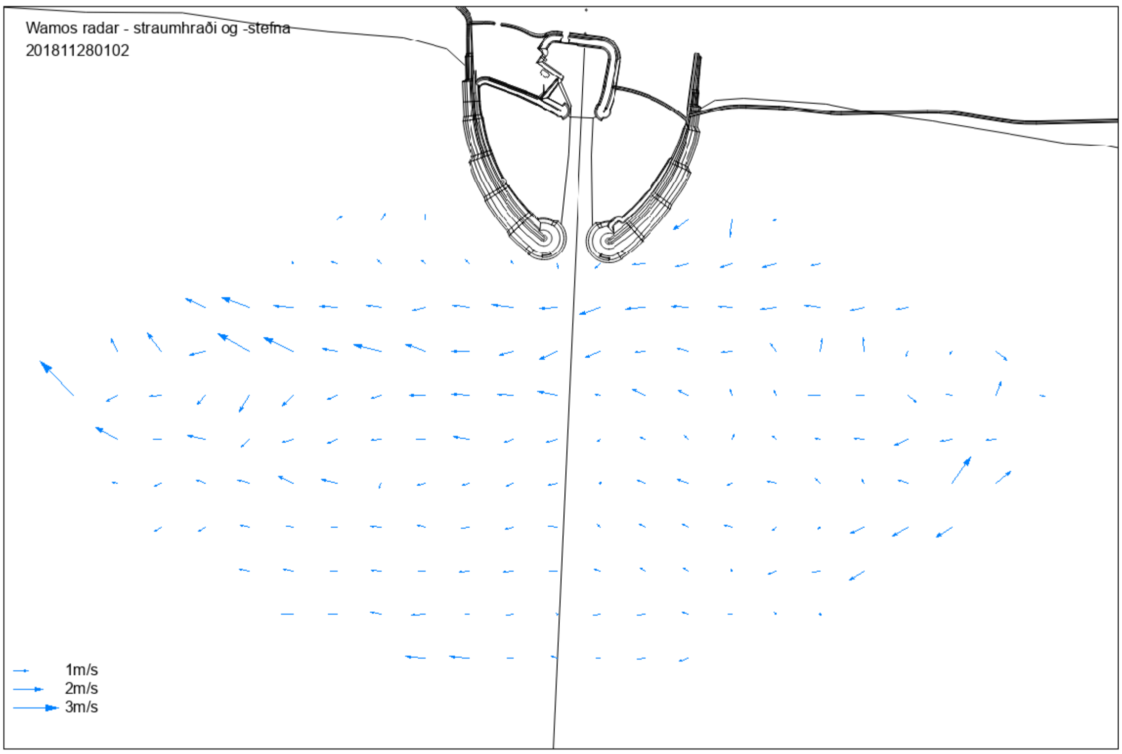

Figure B-3 Measured current velocities at 01:00 November 28 2018. Ebb.

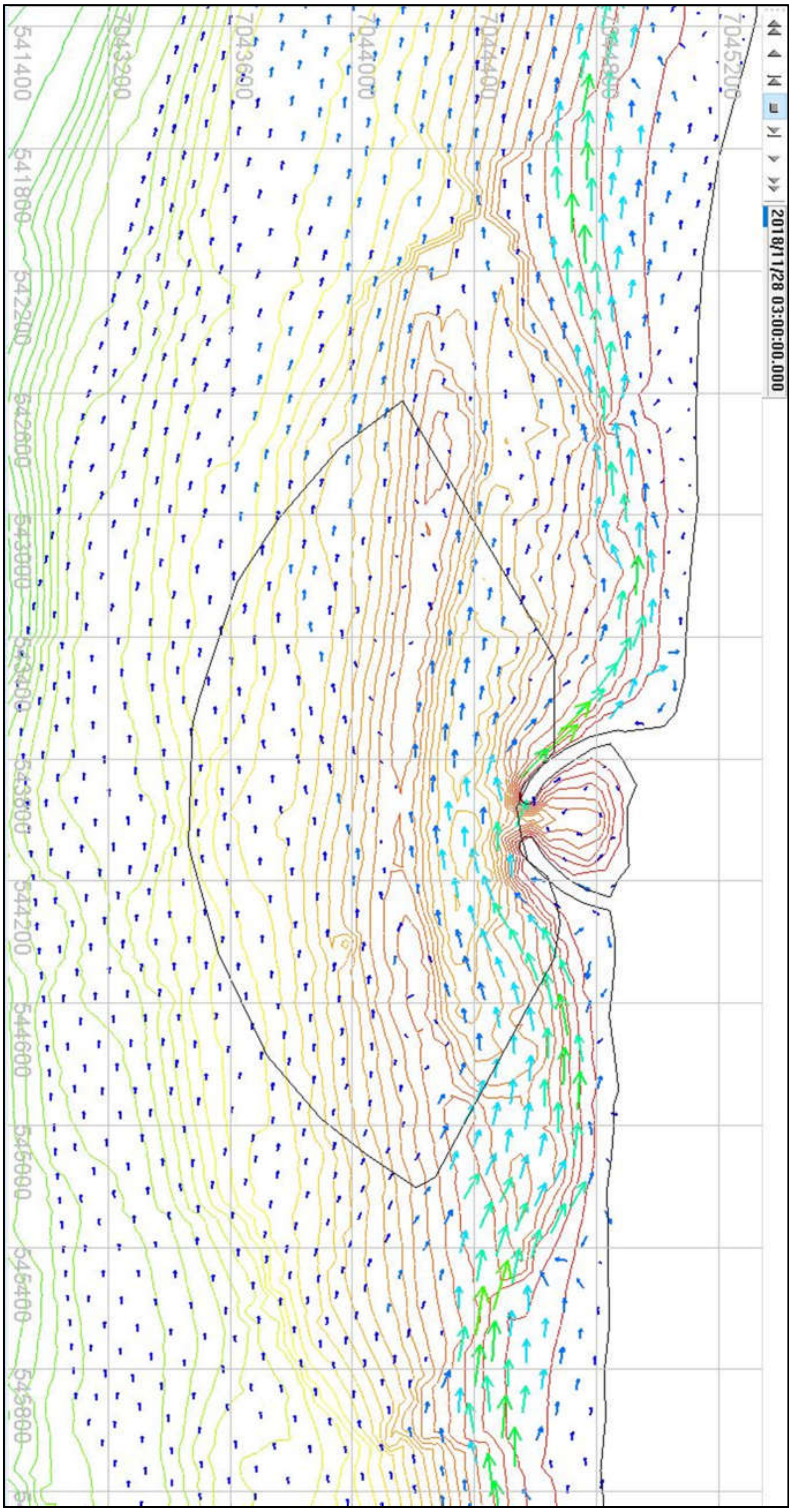

Figure B-4 Simulated current velocities at 03:00 November 28 2018. Low tide.

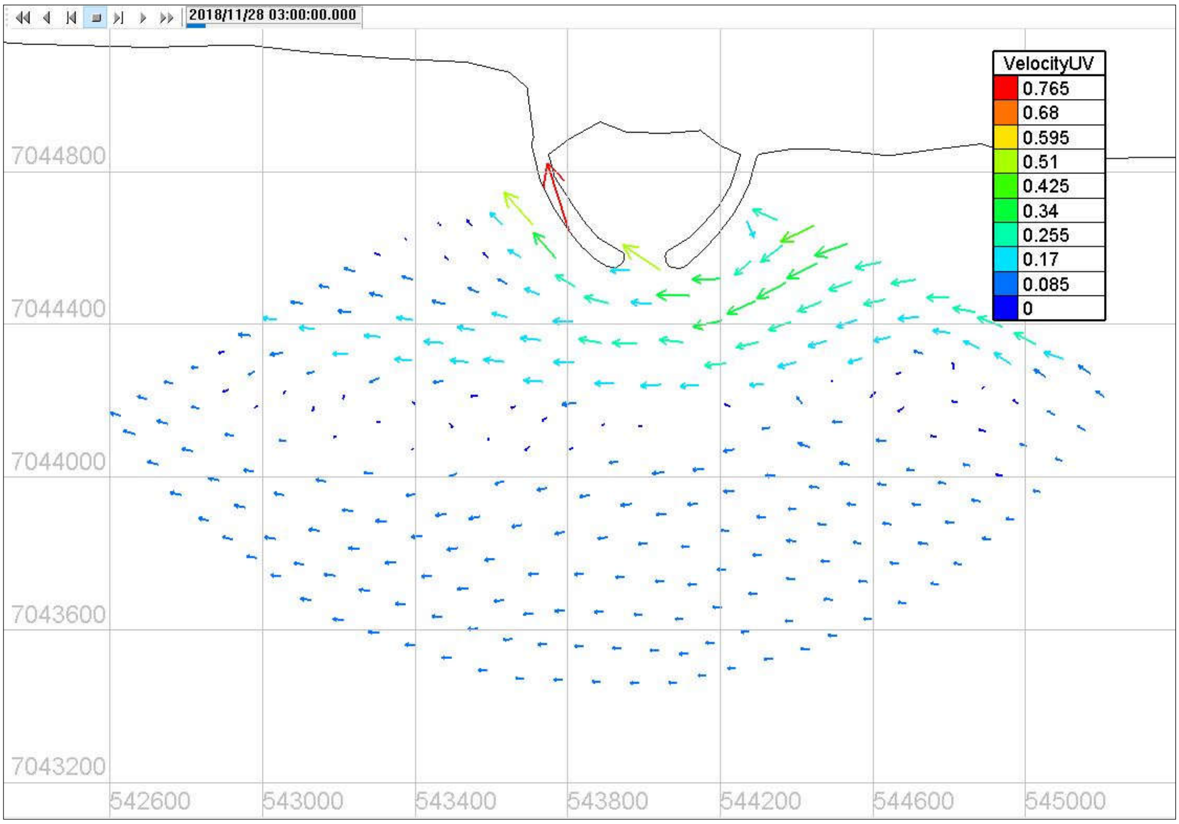

Figure B-5 Simulated current velocities at 03:00 November 28 2018. Low tide.

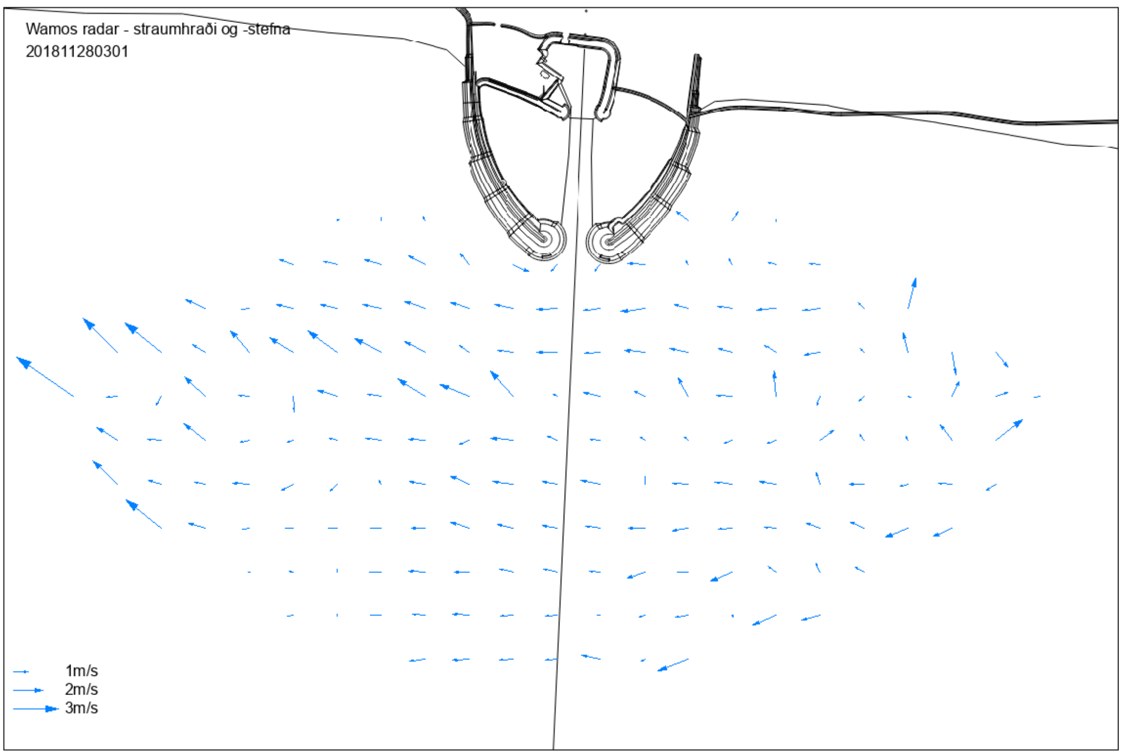

Figure B-6 Measured current velocities at 03:00 November 28 2018. Low tide.

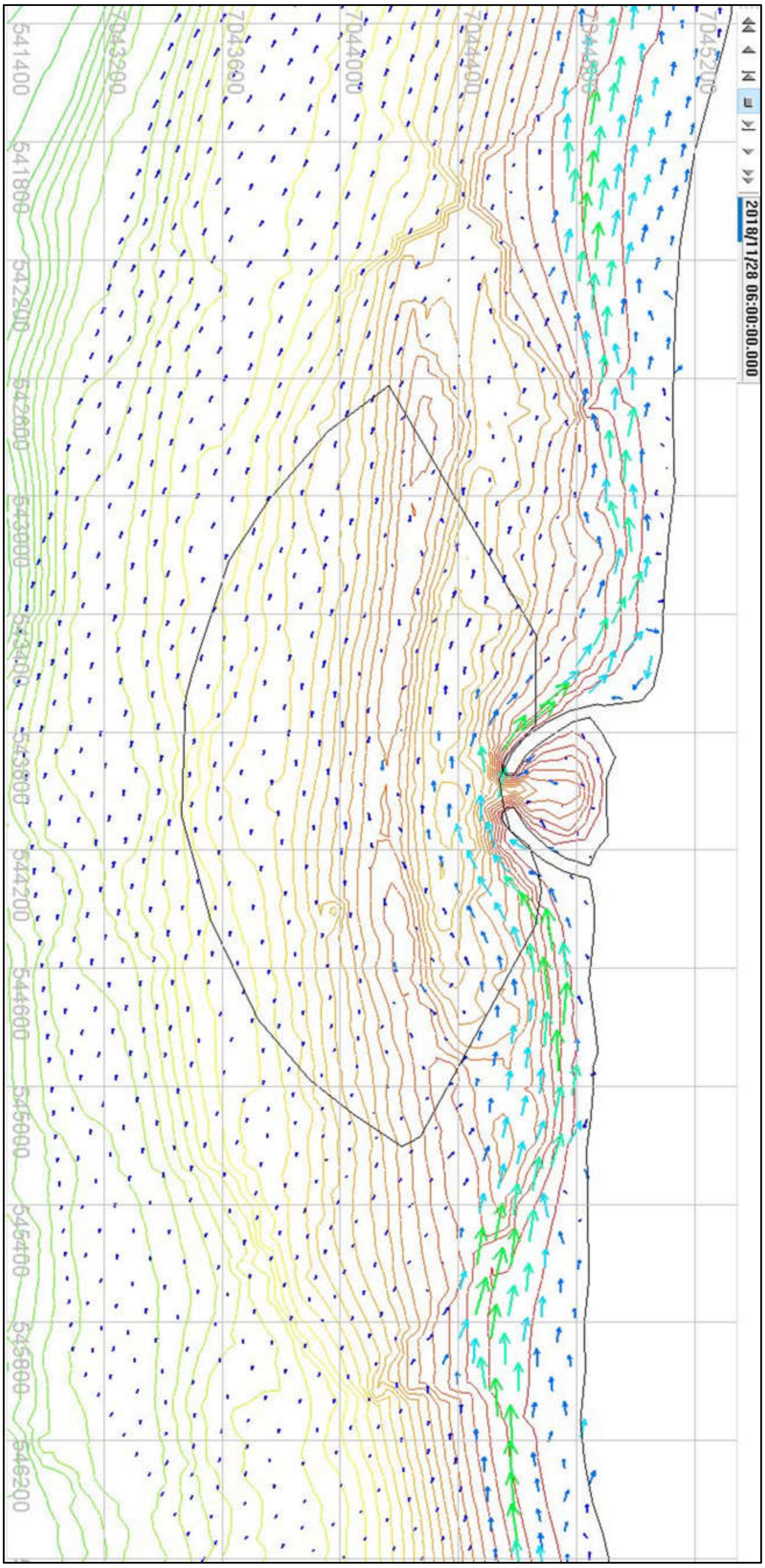

Figure B-7 Simulated current velocities at 06:00 November 28 2018. Flood.

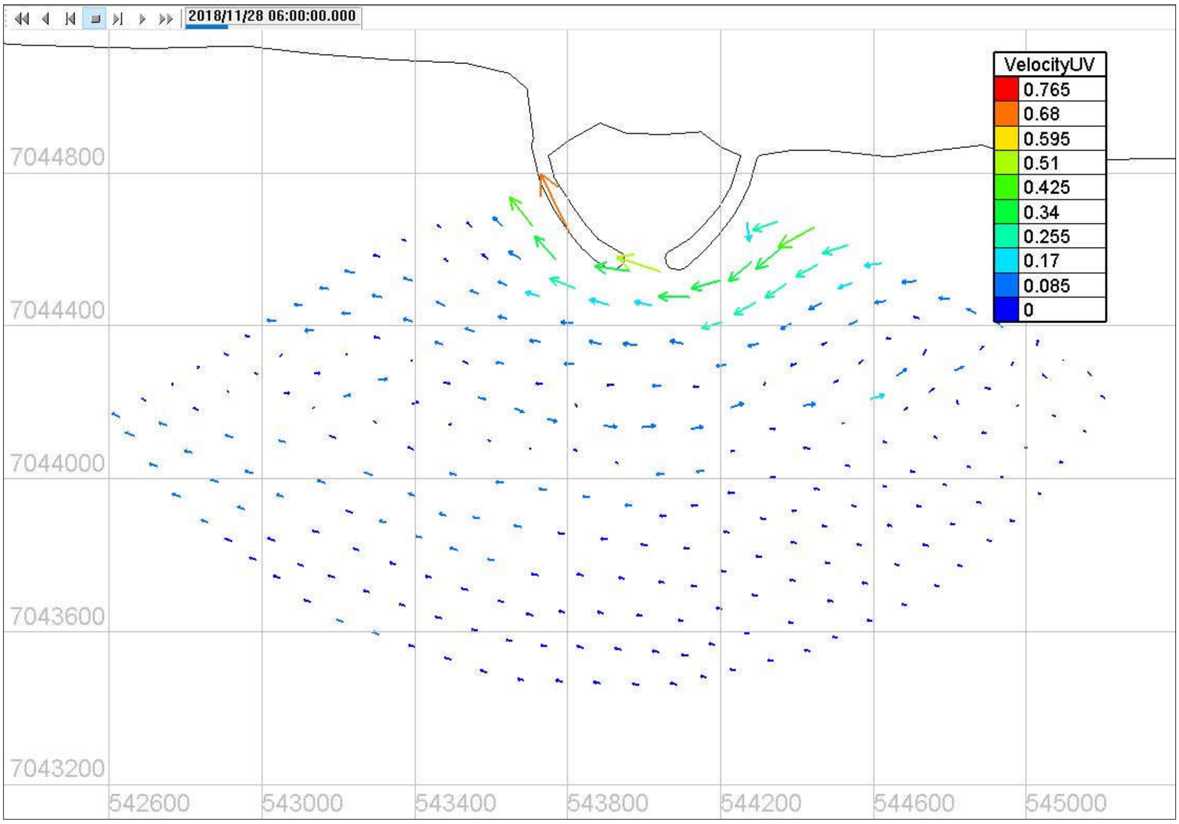

Figure B-8 Simulated current velocities at 06:00 November 28 2018. Flood.

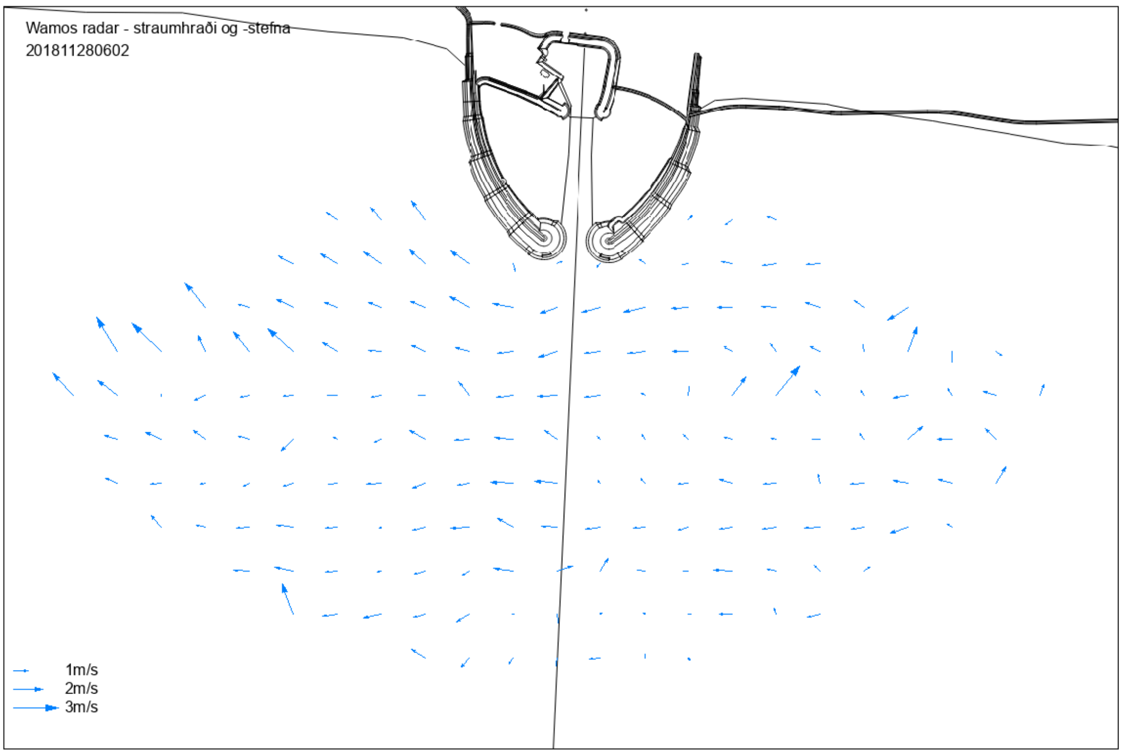

Figure B-9 Measured current velocities at 06:00 November 28 2018. Flood.

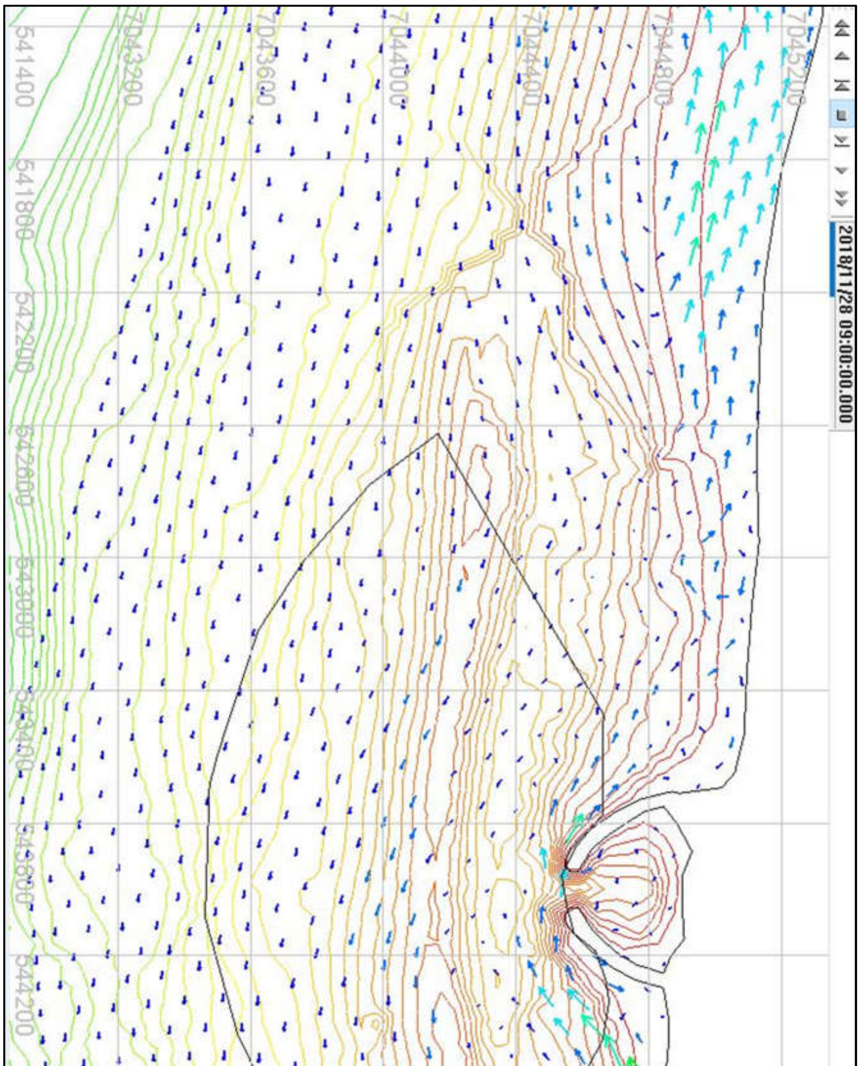

Figure B-10 Simulated current velocities at 09:00 November 28 2018. High tide.

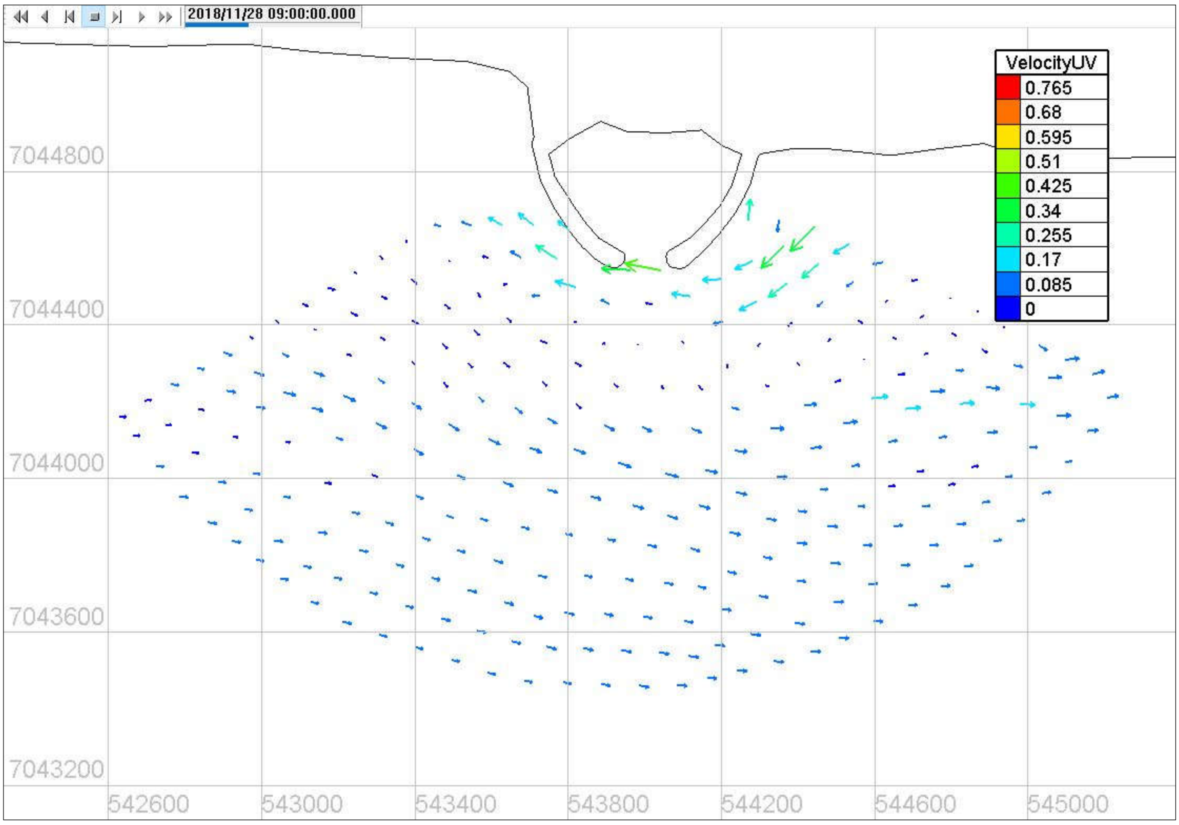

Figure B-11 Simulated current velocities at 09:00 November 28 2018. Hight tide

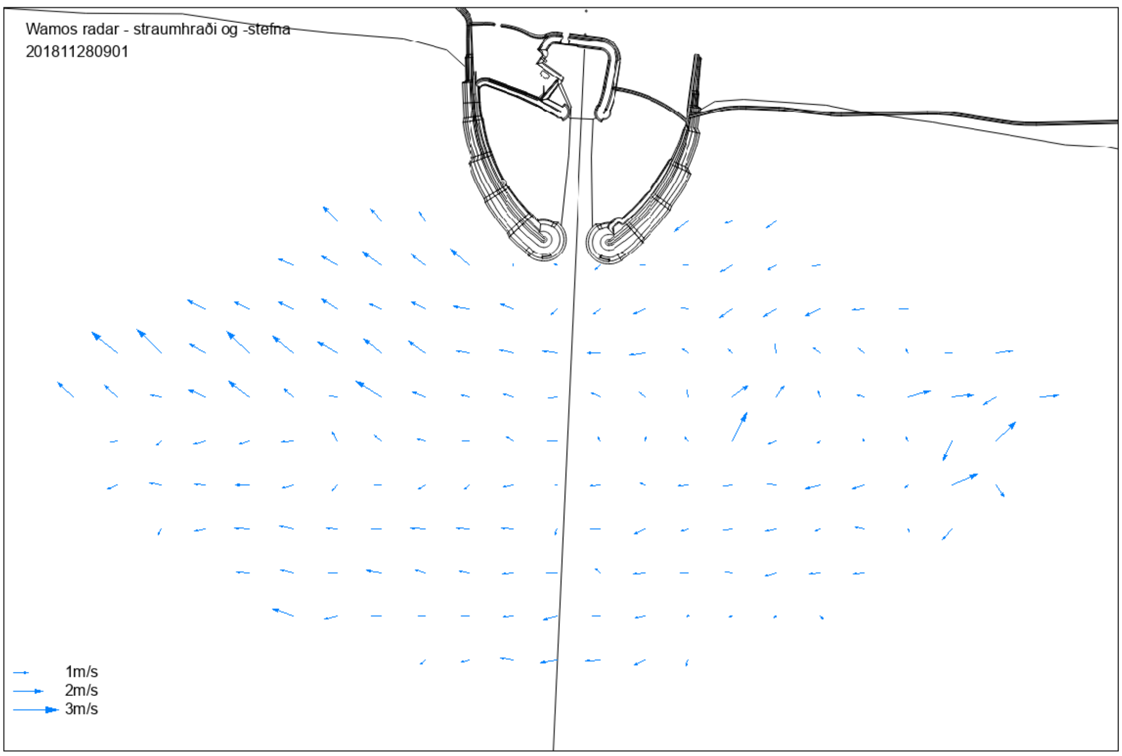

Figure B-12 Measured current velocities at 09:00 November 28 2018. High tide

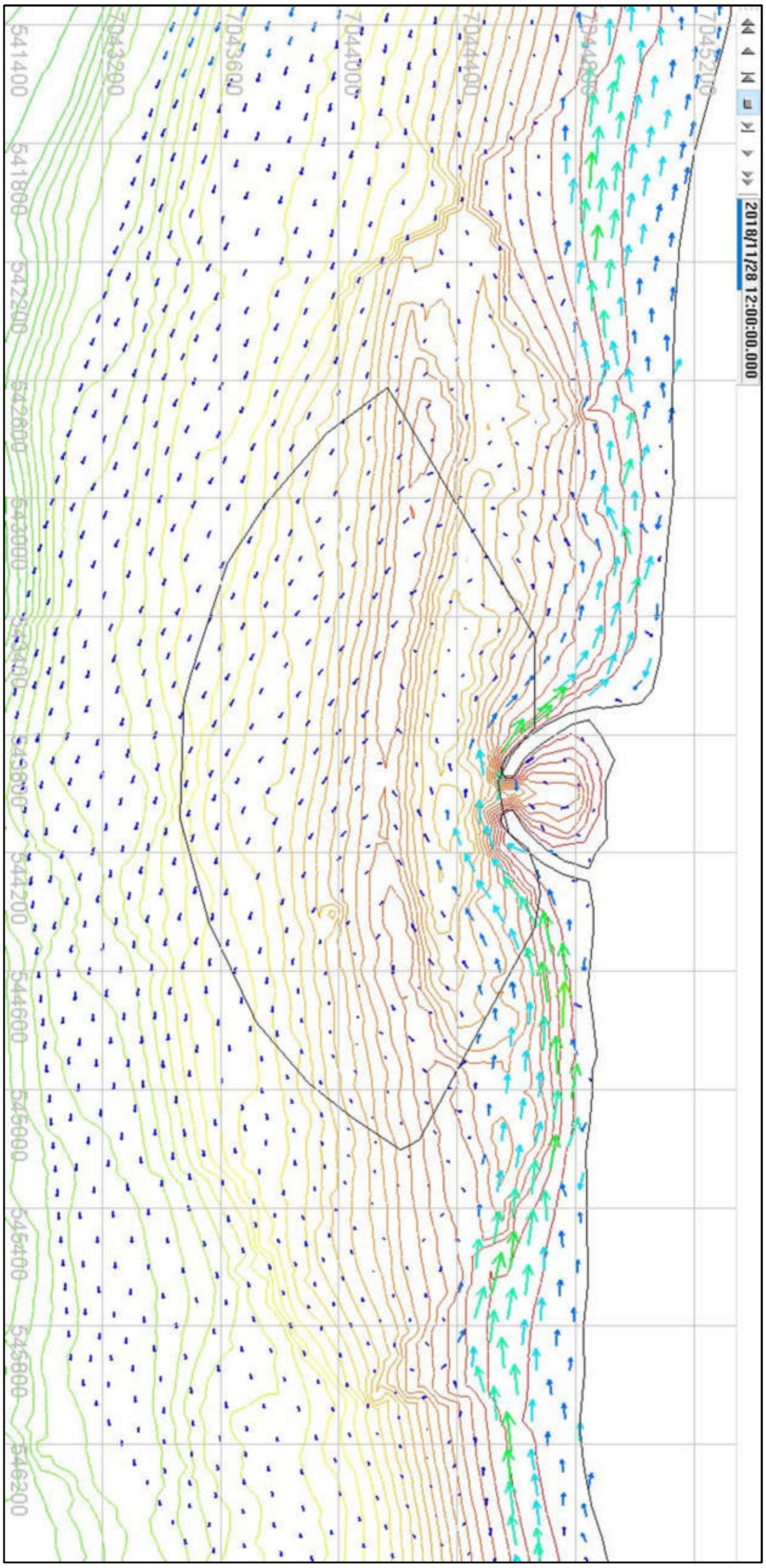

Figure B-13 Simulated current velocities at 12:00 November 28 2018. Ebb.

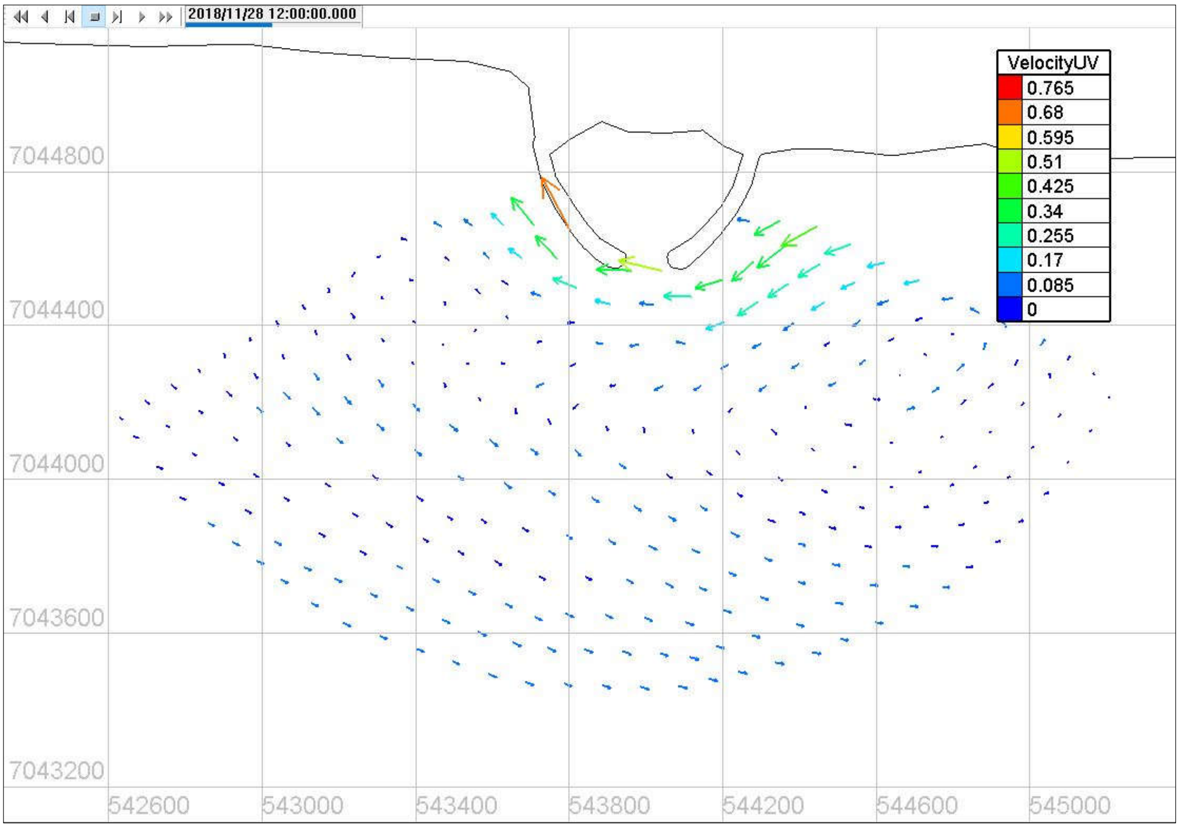

Figure B-14 Simulated current velocities at 12:00 November 28 2018. Ebb.

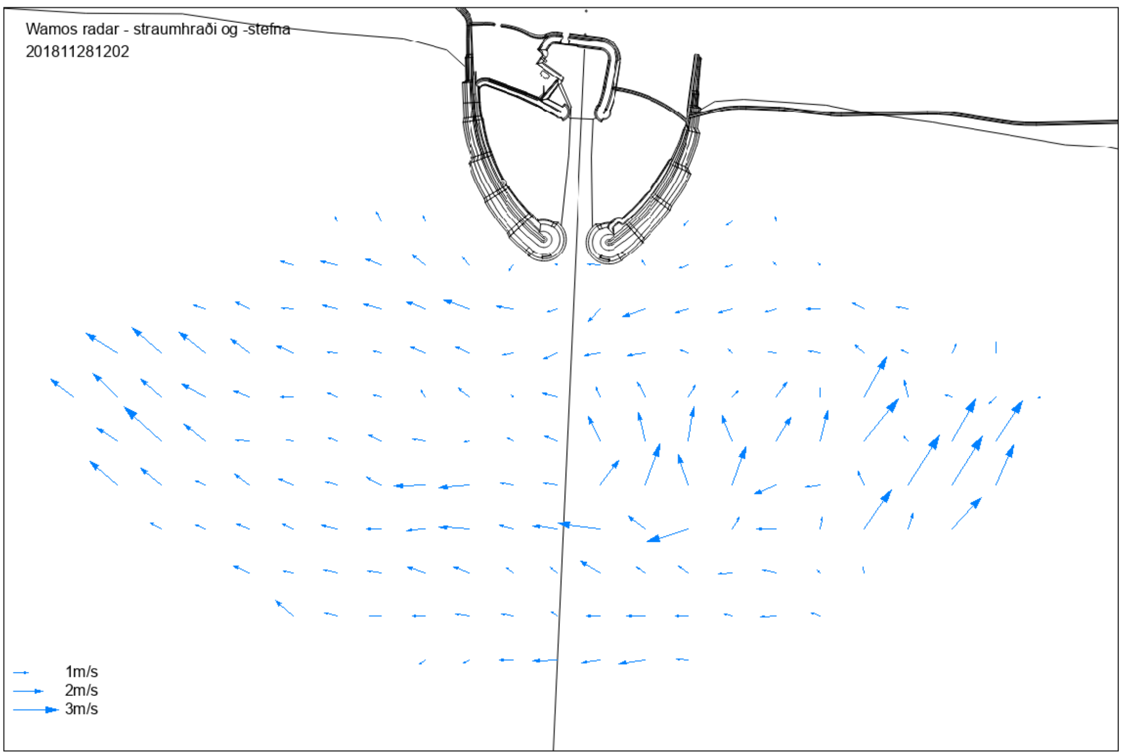

Figure B-15 Measured current velocities at 12:00 November 28 2018. Ebb.

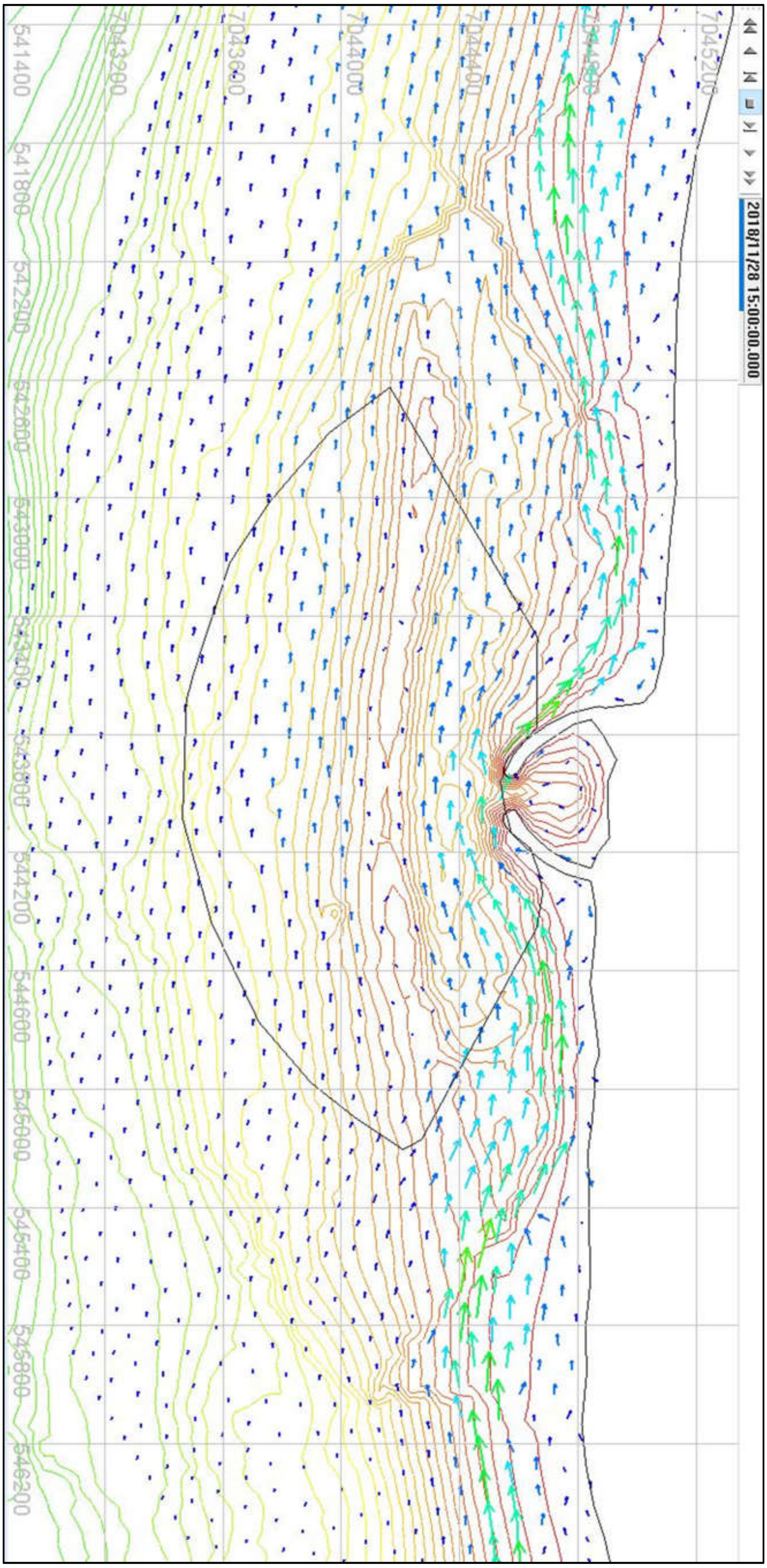

Figure B-16 Simulated current velocities at 15:00 November 28th 2018. Low tide.

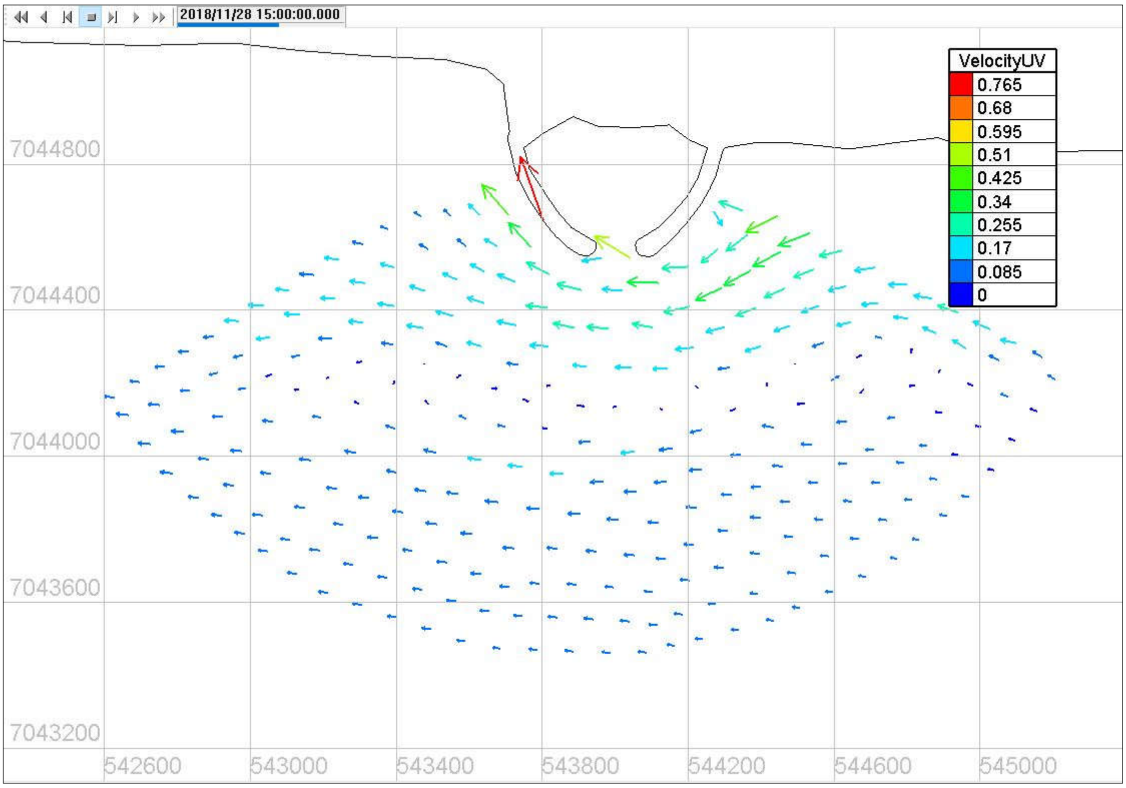

Figure B-17 Simulated current velocities at 15:00 November 28 2018. Low tide.

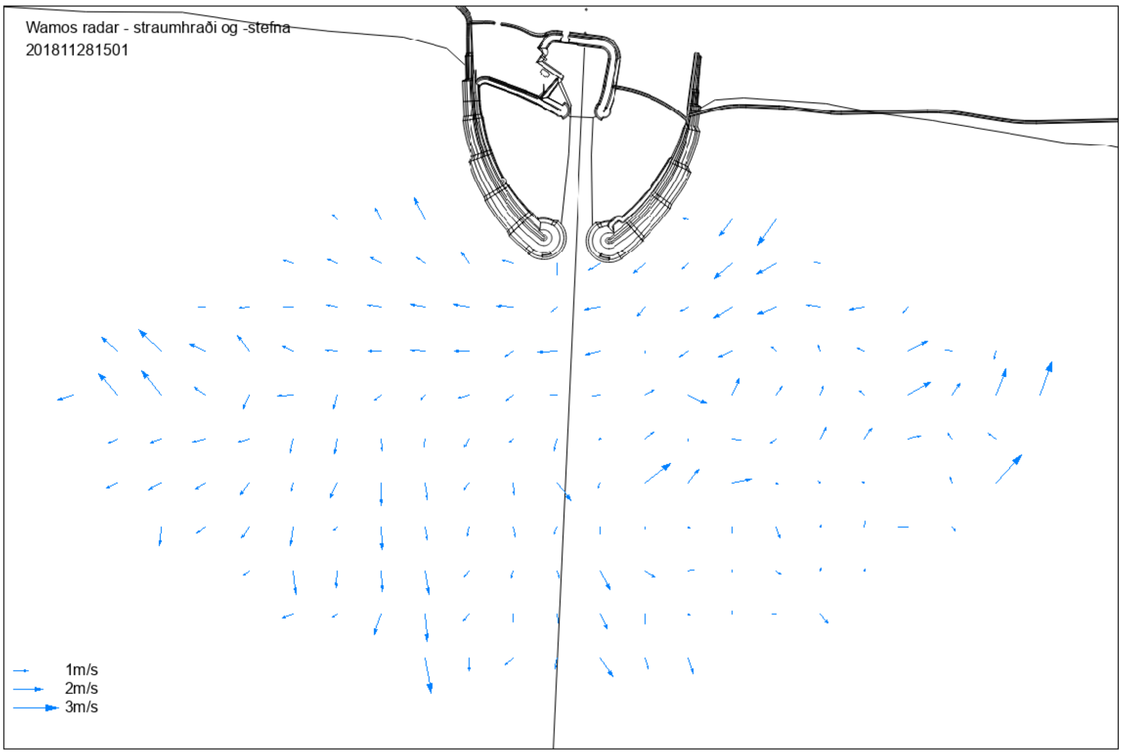

Figure B-18 Measured current velocities at 15:00 November 28th 2018. Low tide.

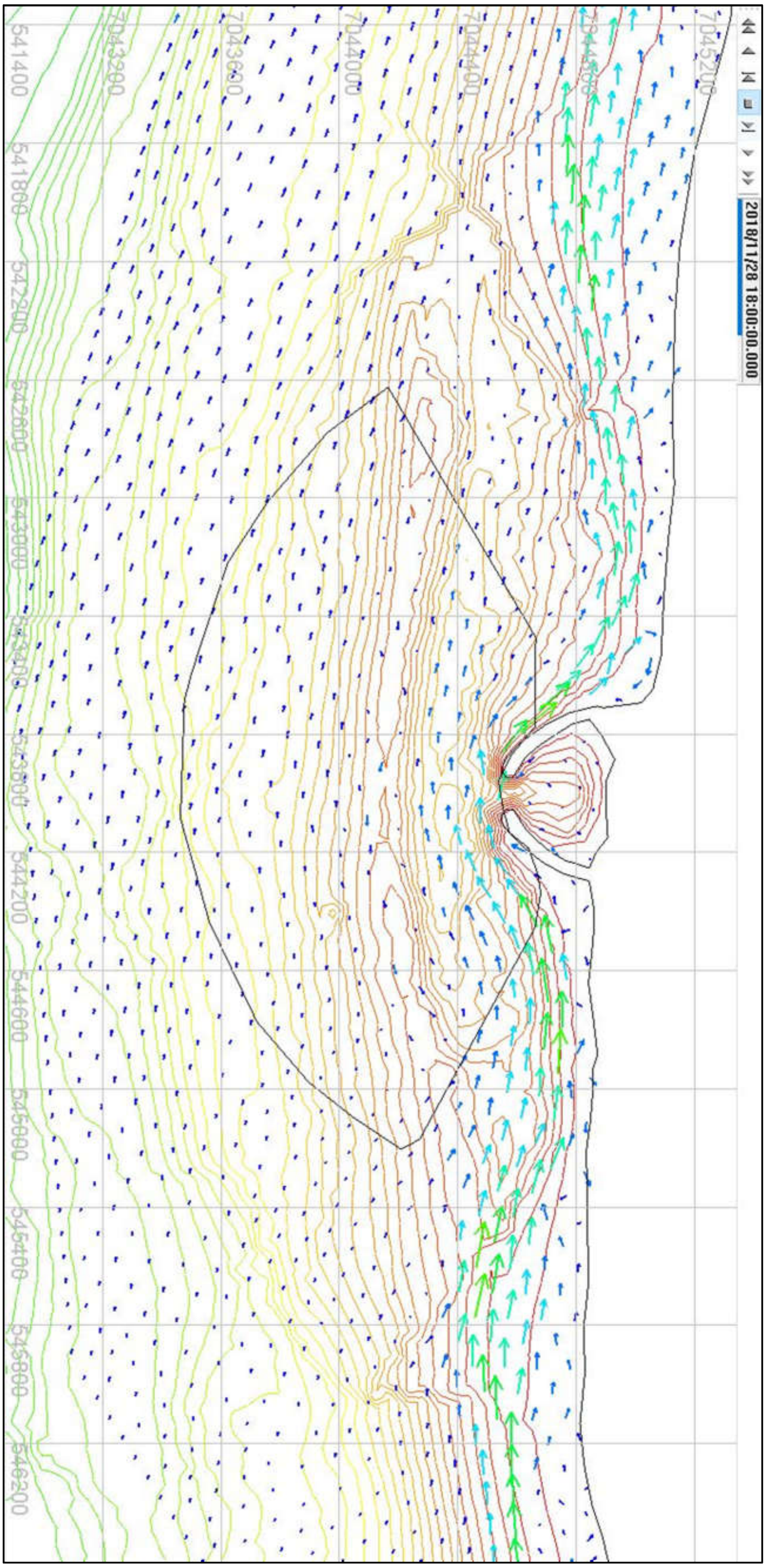

Figure B-19 Simulated current velocities at 18:00 on November 28th 2018. Flood.

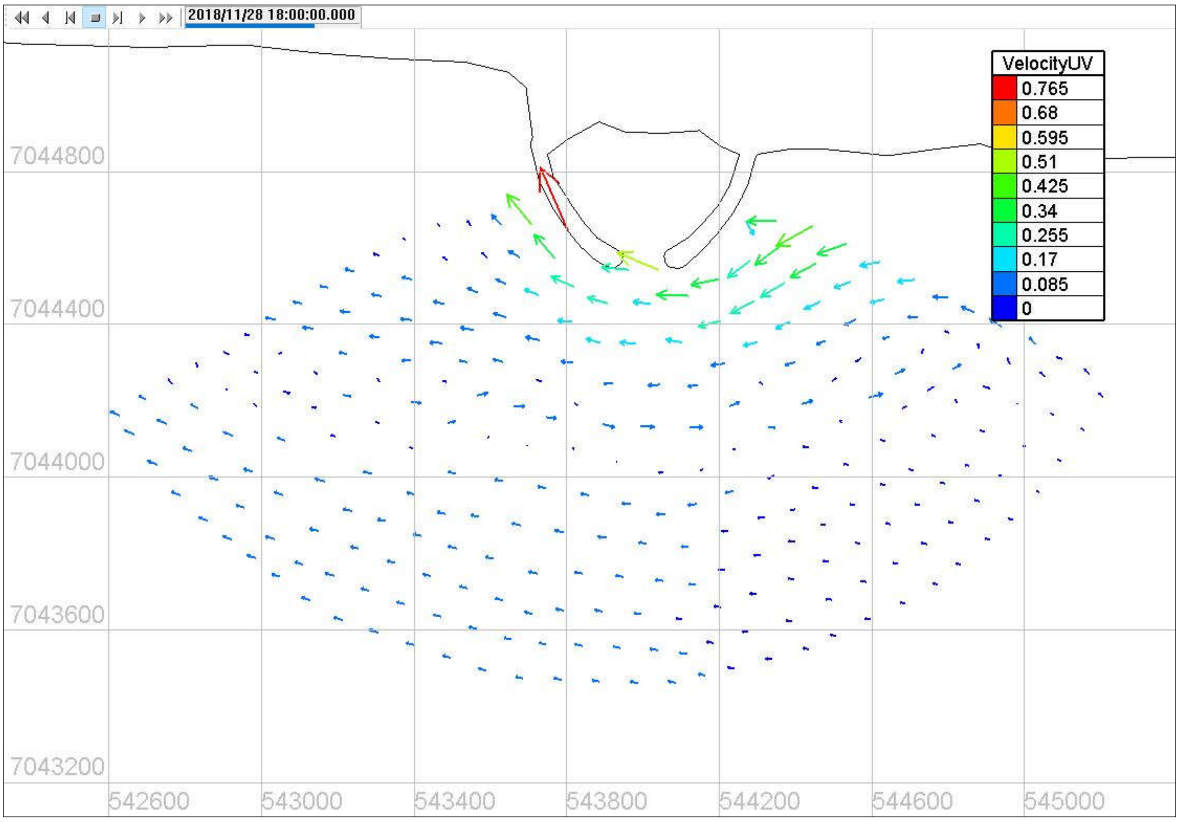

Figure B-20 Simulated current velocities at 18:00 on November 28th 2018. Flood.

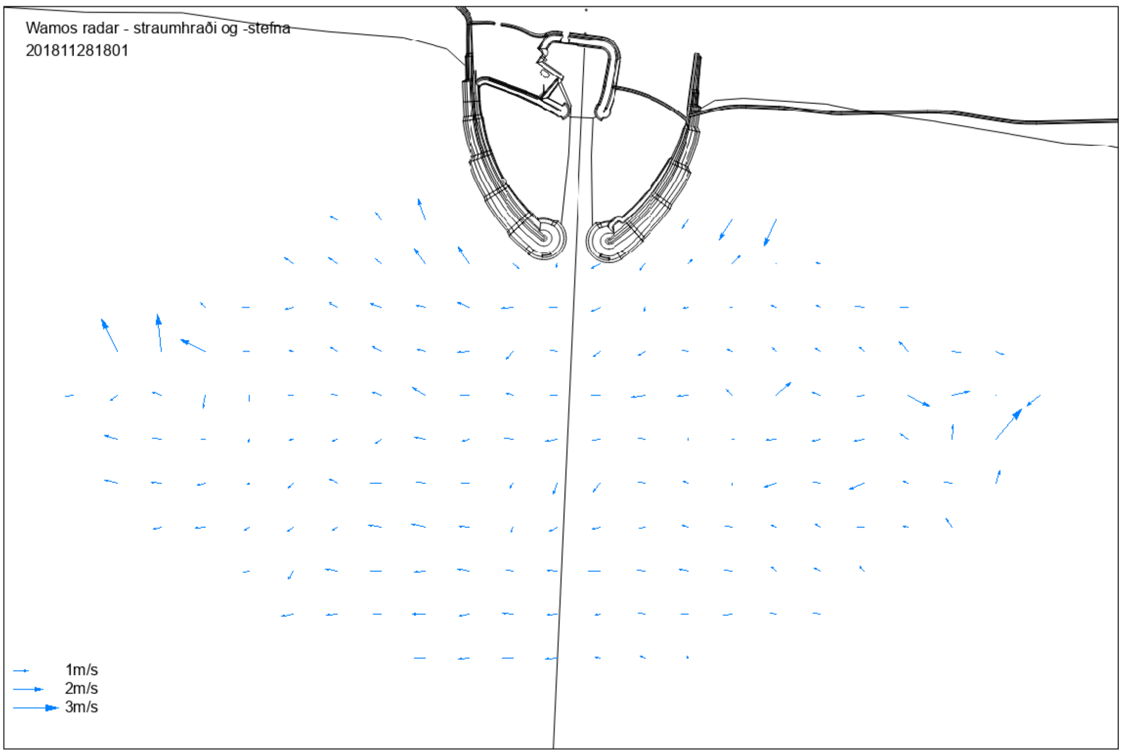

Figure B-21 Measured current velocities at 18:00 on November 28th 2018. Flood.

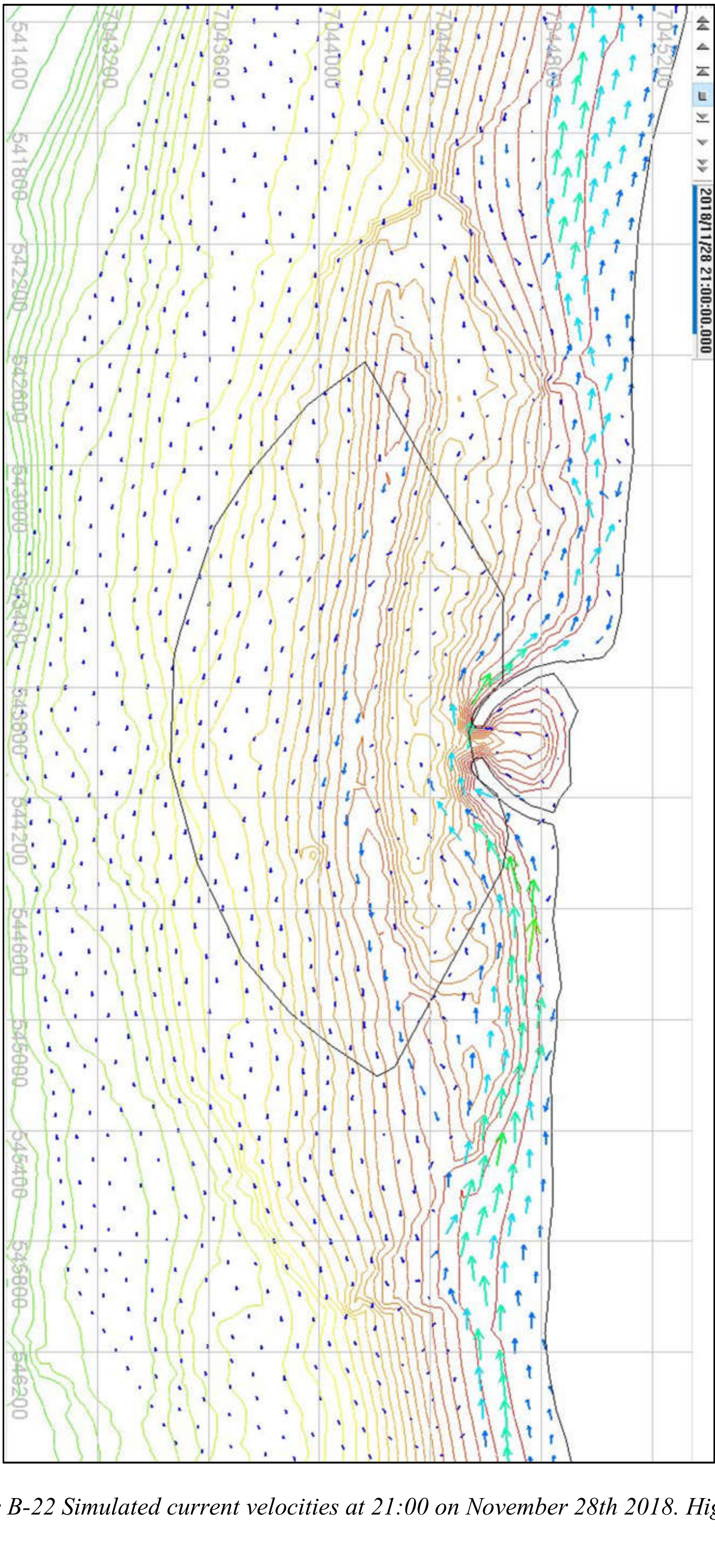

Figure B-22 Simulated current velocities at 21:00 on November 28th 2018. High tide.

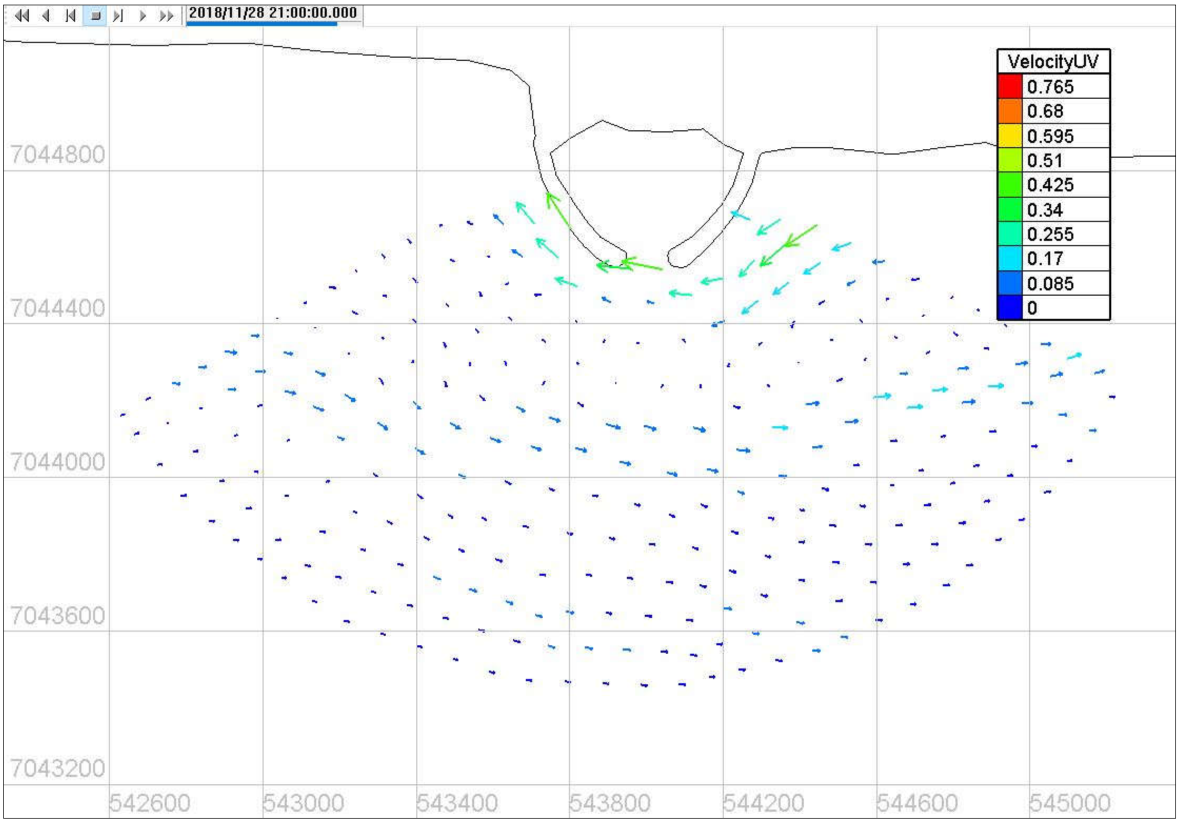

Figure B-23 Simulated current velocities at 21:00 on November 28th 2018. High tide.

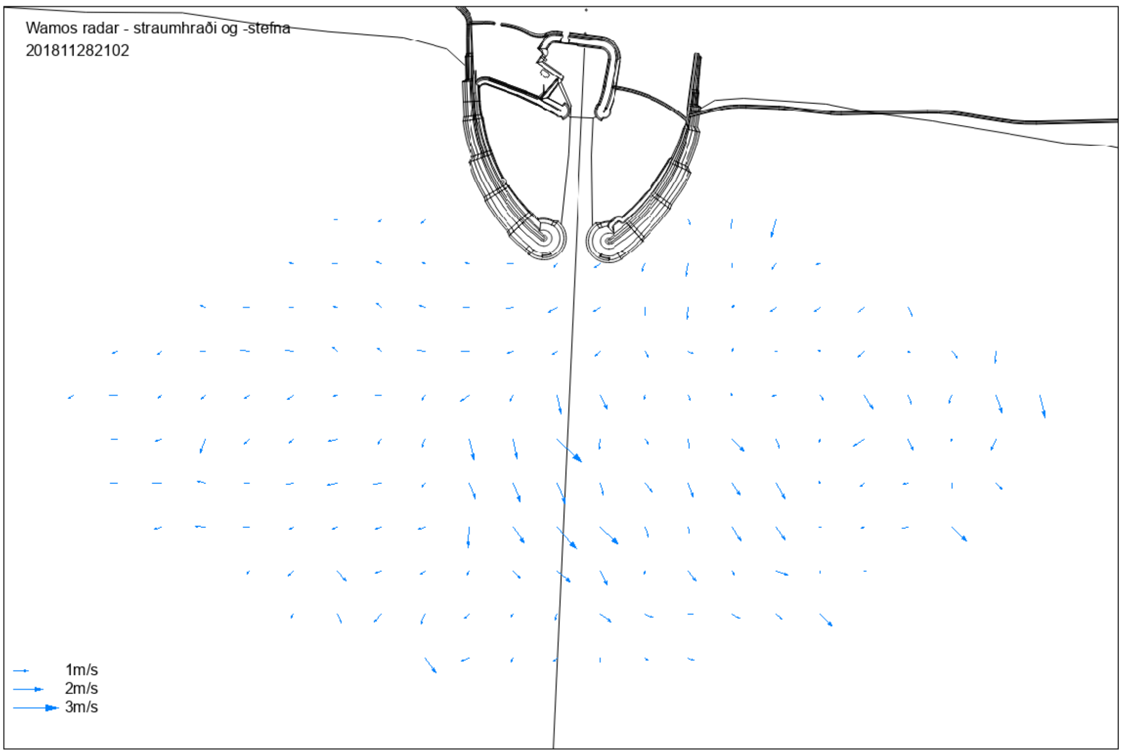

Figure B-24 Measured current velocities at 21:00 on November 28th 2018. High tide.

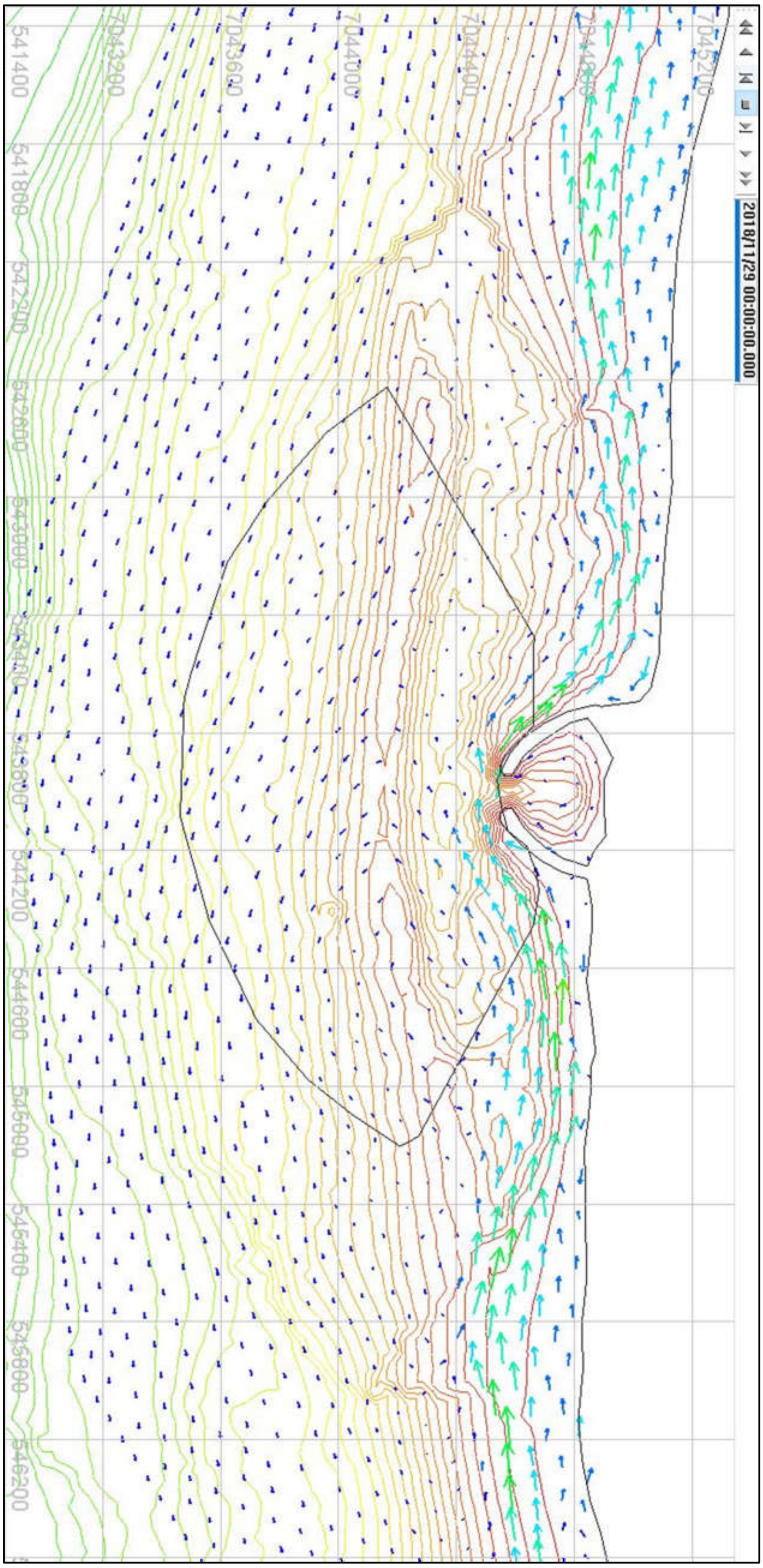

Figure B-25 Simulated current velocities at 24:00 on November 28th 2018. Ebb.

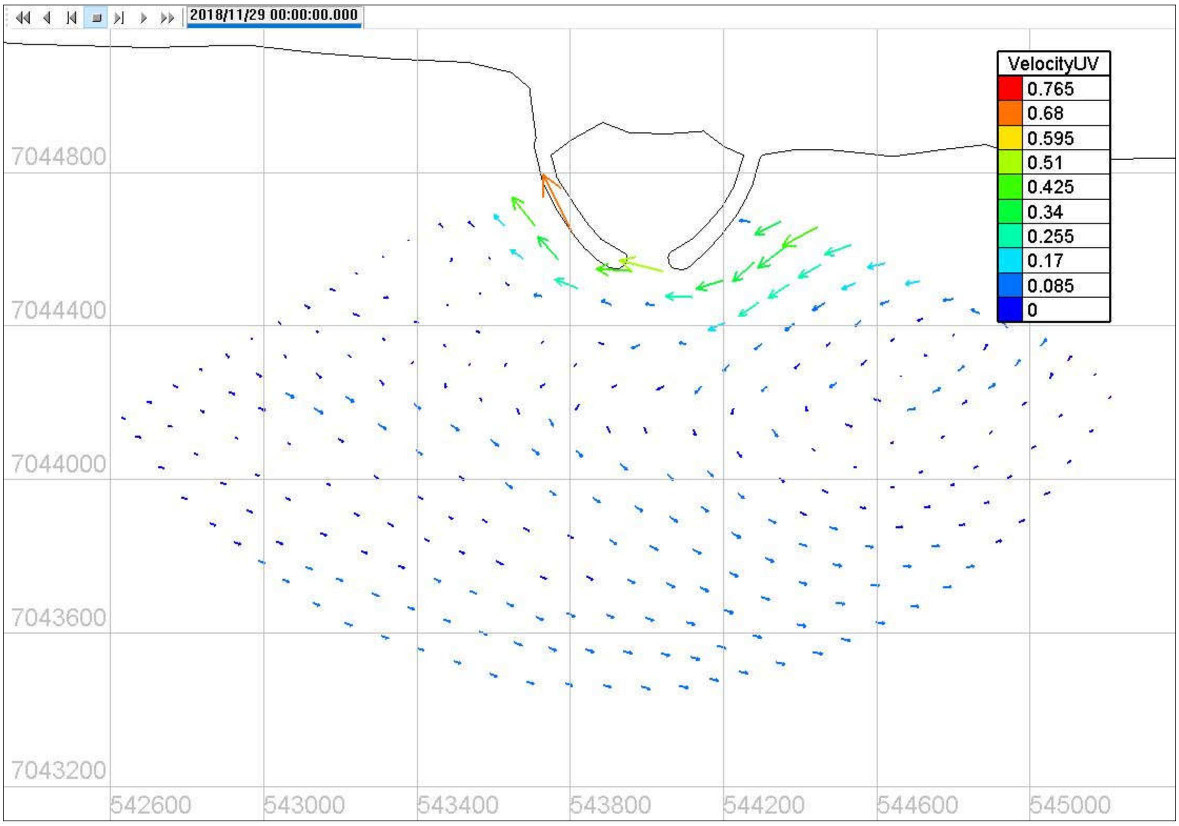

Figure B-26 Simulated current velocities at 24:00 on November 28th 2018. Ebb.

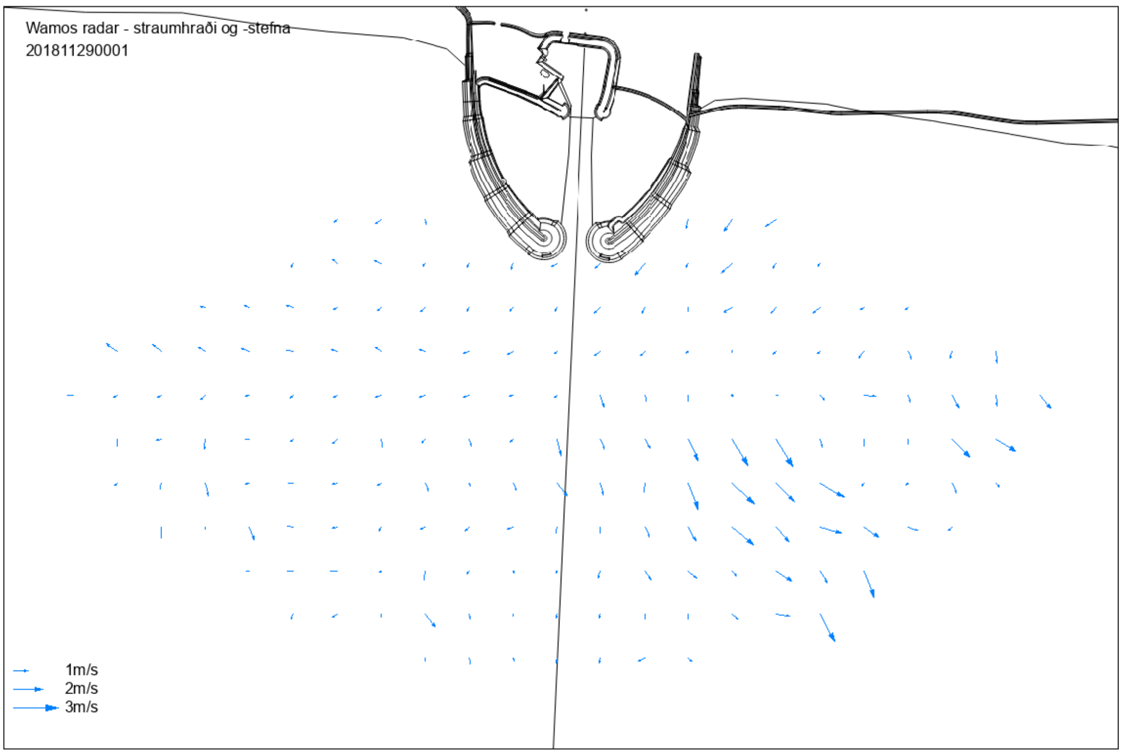

Figure B-27 Measured current velocities at 24:00 on November 28th 2018. Ebb.